

# NOTE TO USERS

This reproduction is the best copy available.

**UMI**<sup>®</sup>



**University of Alberta**

**Pseudoxazolones as Hepatitis A Virus 3C Proteinase Inhibitors and  
Bacterially Derived Antimicrobial Peptides**

by

*Nathaniel Isaac Martin*



A thesis submitted to the Faculty of Graduate Studies and Research in partial fulfillment  
of the requirements for the degree of  
Doctor of Philosophy

Department of Chemistry

Edmonton, Alberta

Spring 2004



Library and  
Archives Canada

Bibliothèque et  
Archives Canada

Published Heritage  
Branch

Direction du  
Patrimoine de l'édition

395 Wellington Street  
Ottawa ON K1A 0N4  
Canada

395, rue Wellington  
Ottawa ON K1A 0N4  
Canada

*Your file* *Votre référence*  
*ISBN: 0-612-96303-9*  
*Our file* *Notre référence*  
*ISBN: 0-612-96303-9*

The author has granted a non-exclusive license allowing the Library and Archives Canada to reproduce, loan, distribute or sell copies of this thesis in microform, paper or electronic formats.

L'auteur a accordé une licence non exclusive permettant à la Bibliothèque et Archives Canada de reproduire, prêter, distribuer ou vendre des copies de cette thèse sous la forme de microfiche/film, de reproduction sur papier ou sur format électronique.

The author retains ownership of the copyright in this thesis. Neither the thesis nor substantial extracts from it may be printed or otherwise reproduced without the author's permission.

L'auteur conserve la propriété du droit d'auteur qui protège cette thèse. Ni la thèse ni des extraits substantiels de celle-ci ne doivent être imprimés ou autrement reproduits sans son autorisation.

---

In compliance with the Canadian Privacy Act some supporting forms may have been removed from this thesis.

Conformément à la loi canadienne sur la protection de la vie privée, quelques formulaires secondaires ont été enlevés de cette thèse.

While these forms may be included in the document page count, their removal does not represent any loss of content from the thesis.

Bien que ces formulaires aient inclus dans la pagination, il n'y aura aucun contenu manquant.

# Canada

## ABSTRACT

A number of imino analogues of amino acids were synthesized and tested as inhibitors of the 3C proteinase enzyme of the Hepatitis A Virus (HAV 3C). The 3C proteinase is essential for viral replication and the conservation of its active site among a wide range of serotypes makes the enzyme an attractive target for chemotherapy. The most effective compounds tested were the monophenyl pseudoxazolones *E*-(**21a**) and *Z*-(**21b**)-2-benzylidene-2*H*-oxazol-5-one with IC<sub>50</sub> values of 6 and 4 μM, respectively.

Antibiotic peptides derived from bacterial sources were also studied. Mattacin (**52**) was originally identified as a peptide antibiotic isolated from *Paenibacillus kobensis* *M* with potent antimicrobial activity towards a variety of Gram-negative organisms. After performing a series of multidimensional NMR experiments and stereochemical analysis of the component amino acids, a full structural characterization of mattacin (**52**) was achieved, showing it to be a member of the polymyxin family of peptide antibiotics. Conformational analyses were undertaken using 2D NMR techniques (TNROESY and transferred NOE) to investigate the solution structure of mattacin, both in isolation and in the presence of lipid A (**51**). Lipid A is the endotoxic principle of the outer membrane of Gram-negative bacteria and is the putative receptor for polymyxin peptides. Isothermal titration calorimetry was used to compare the binding energy of mattacin and polymyxin B (**50**) (a common therapeutic agent) with lipid A. Results from these experiments indicate that mattacin behaves in a manner similar to polymyxin B, both in its preferred solution conformation and affinity for lipid A.

New methods for the characterization of lantibiotic peptides were also developed. Isolated from bacterial sources, lantibiotics exhibit antibacterial activity towards Gram-positive organisms, often several orders of magnitude more potent than traditional antibiotics such as penicillin. Lantibiotics contain a number of unique structural features including dehydro and lanthionine (thioether) residues. Introduced after ribosomal translation of the parent peptide, these moieties render conventional means of peptide analysis ineffective. A new analytical approach, successfully applied to the most common lantibiotic nisin (**53**), involved the use of nickel boride ( $\text{Ni}_2\text{B}$ ) in the presence of  $\text{D}_2$ , to reduce dehydro side chains and cleave lanthionine bridges with concomitant deuterium incorporation at the site of reduction or desulfurization. Using this method it was possible to identify and distinguish the original locations of dehydro side chains and lanthionine bridges by use of peptide sequencing (Edman degradation) coupled with mass spectrometry. This methodology was also successfully applied to a new two-component lantibiotic, lacticin 3147, produced by *Lactococcus lactis* subsp. *lactis* DPC3147. After acquiring a lactococcal strain with amplified production levels of lacticin 3147, and optimizing the isolation protocol, quantities of material suitable for NMR analysis were obtained. The primary structures, including the lanthionine bridging patterns of both peptides were determined by using multidimensional NMR. These results indicate that lacticin A1 (**68**) has a specific lanthionine bridging pattern similar to the known lantibiotic mersacidin (**66**) and that the A2 peptide **69** bears a resemblance to lactosin S (**67**).

*for Nigel*

## ACKNOWLEDGEMENTS

To simply acknowledge John Vederas as a superb research supervisor would be too little. John has been a source of motivation and encouragement when needed but he is also a person with whom many a story and laugh have been shared. I appreciate not only John's scholarly guidance but also the numerous opportunities (professional and extracurricular) that he has provided for me.

Many thanks are extended to Colin Hill and Paul Ross (University College Cork, Ireland) for their valuable collaboration on the lacticin project and the opportunity to work and learn in their laboratory. Tara Sprules, your help in the structure elucidation of the lacticin peptides has allowed me to realize a goal, which at times seemed unattainable, thank you. For their contribution to the biological testing in the mattacin project I thank Randy Worobo and Haijing Hu (Cornell). To Yeeman Ramtohol I am grateful for a productive collaboration on the pseudoxazolone project. Also to be acknowledged for their assistance throughout a variety of summer projects are Glen Armstrong (2003), Claire Ference (2002), and Lara Silkin (2000). For their extraordinary efforts and expert advice, I thank Michael Carpenter (peptide sequencing), Randy Whittal (mass spectrometry), Albin Otter (NMR), and Pavel Kitov (ITC).

The University of Alberta, Department of Chemistry, Natural Sciences and Engineering Research Council of Canada, and the Alberta Heritage Foundation for Medical Research, are gratefully acknowledged for providing financial support.

To all members of the Vederas group with whom I have had the pleasure of working, I offer thanks for your support and humour. Having a lab to go to in the



morning where one can be guaranteed a laugh, as well as a tremendous knowledge-base to draw from, has made my time in the group fly by. I am especially grateful to Rajendra Jain, Kamaljit Kaur, and Tara Sprules for proofreading this manuscript and providing suggestions for its improvement.

Personal thanks are extended to Andy Sutherland, John Sorensen, and Hanna Pettersson, for their valuable friendship during my time as a member of the Vederas group. Also to be thanked is Geoff, my brother-from-another-mother. You've always stood by me and your friendship and loyalty help me persevere.

Finally I must acknowledge my family. Dad; by example you have taught me to think critically without the exclusion of creativity. Mom; you show me what it is to be selfless and accepting. Together you two provide my model. Leah and Bronwyn; two sisters who each make me feel like a big brother but who also have provided me a shoulder when needed. Nigel; my brother, you consistently remind me to live in the moment. You all have always stood by me with unfailing support and faith. I love you guys.

## TABLE OF CONTENTS

	<b>Page</b>
<b>OVERVIEW</b>	1
<b>CHAPTER 1. Planar Derivatives of Amino acids and Pseudoxazolones as Inhibitors of Hepatitis A Virus 3C Proteinase</b>	
<b>INTRODUCTION</b>	3
1. Sulfenimines and Pseudoxazolones in Amino Acid Synthesis	3
2. Pseudoxazolones as Hepatitis A Virus and Human Rhinovirus 3C Proteinase Inhibitors	6
2.1 HAV and HRV 3C Activity in Viral Replication	7
2.2 Previous HAV and HRV 3C Inhibitors	9
3. Project Goals: Synthesis and Testing of Pseudoxazolones as HAV 3C Inhibitors	10
<b>RESULTS AND DISCUSSION</b>	11
1. Chemistry of Sulfenimines and Pseudoxazolones	11
1.1 Sulfenimines and Pseudoxazolones Preparation	11
1.2 Reactions Attempted	17
2. Pseudoxazolones as Inhibitors of HAV 3C Proteinase	22
3. Conclusions	24

**CHAPTER 2. Isolation and Study of Mattacin, a Cyclic Peptide Antibiotic of the Polymyxin Family**

<b>INTRODUCTION</b>	26
1. Mattacin, a Polymyxin Peptide	26
2. Non-ribosomal Biosynthesis and Unique Structural Features of Polymyxin Peptides	27
3. Background and Therapeutic Use of Polymyxins	28
4. Polymyxin Mode of Action	30
<b>RESULTS AND DISCUSSION</b>	32
1. Isolation and Characterization of Mattacin	32
1.1 Mass Spectrometry	32
1.2 NMR Spectroscopy	35
1.3 Stereochemical Analysis	39
2. Mattacin Spectrum of Activity and Comparison with Polymyxin B	40
3. Mode of Action	42
3.1 LPS Binding and Induced Conformation of Mattacin by tNOE NMR	42
3.2 LPS/Mattacin Association Energetics by ITC calorimetry	44
4. Conclusions	46

## **CHAPTER 3. Structural Investigations of Lacticin 3147; a Two-Component Lantibiotic**

<b>INTRODUCTION</b>	<b>48</b>
1. Bacterial Cell Wall Architecture and Traditional Antibiotics	48
2. Lantibiotic Two-Peptide Bacteriocins	50
2.1 Biosynthesis of Lantibiotics	51
2.2 Lantibiotic Structural Features	52
2.3 Secondary Structure and Mode of Action of Lantibiotics	55
2.4 Lacticin 3147 Spectrum of Activity and Therapeutic Use	59
3. Project Objectives: New Methods for the Structure Elucidation of Lantibiotic Peptides	60
<b>RESULTS AND DISCUSSION</b>	<b>63</b>
1. Isolation and Preliminary Characterization of Lacticin 3147	63
1.1 Mass Spectrometry and Preliminary Structural Features	65
2. Edman Chemistry and Lacticin 3147	68
2.1 Amino Acid Analysis	70
2.2 Compatibility of Lantibiotics with the Edman Degradation	71
3. Ni <sub>2</sub> B Modification of Lantibiotics	74
3.1 Model Studies	76
3.2 Ni <sub>2</sub> B Desulfurization and Reduction of Lacticin 3147 A1 and A2	78
3.3 Deuterating Desulfurization/Reduction of Lantibiotics with Ni <sub>2</sub> B	82

3.4	Proposed Structures	85
4.	Improved Isolation of Lacticin 3147	88
4.1	NMR Spectroscopy	89
4.2	Solved Structures of Lacticin A1 and A2	95
5.	Conclusions and Future Directions	96

## CHAPTER 4. Experimental Procedures

1.	General Procedures	98
1.1	Reagents, Solvents and Solutions	98
1.2	Purification Techniques	99
1.3	Instrumentation for Compound Characterization	99
2.	Sulfenimines and Pseudoxazolones	101
2.1	Experimental Data for Compounds	101
	Benzenesulfonyl Chloride (10)	101
	General Procedure for Preparation of Amino Acid Ester Sulfenimines (11-18)	101
	Methyl $\alpha$ -[[phenylthio]imino]benzenepropionate (11)	102
	<sup>1</sup> Propyl $\alpha$ -[[phenylthio]imino]benzenepropionate (12)	103
	Methyl 2-[[phenylthio]imino] propionate (13)	103
	Ethyl $\alpha$ -[[phenylthio]imino]benzenepropionate (14)	104
	<sup>1</sup> Butyl 2-[[phenylthio]imino] propionate (15)	104
	<sup>1</sup> Propyl 2-[[phenylthio]imino] propionate (16)	105
	Ethyl 2-[[phenylthio]imino] propionate (17)	106

Methyl $\alpha$ -[[[(phenyl)thio]imino]benzeneacetate ( <b>18</b> )	106
<b>21a</b> ( <i>E</i> )- and <b>21b</b> ( <i>Z</i> )-2-Benzylidene-2 <i>H</i> -oxazol-5-one	107
<b>22a</b> ( <i>E</i> )- and <b>22b</b> ( <i>Z</i> )-2-Benzylidene-4-methyl-2 <i>H</i> -oxazol-5-one	108
2-(Diphenylmethylene)-2 <i>H</i> -oxazol-5-one ( <b>24</b> )	109
2-(Diphenylmethylene)-4-methyl-2 <i>H</i> -oxazol-5-one ( <b>25</b> )	110
9-Chloro-9 <i>H</i> -fluorene-9-carbonyl chloride ( <b>27</b> )	111
2-Fluoren-9-ylidene-4-methyl-2 <i>H</i> -oxazol-5-one ( <b>28</b> )	111
( <i>R,S</i> )-(2,2-Diphenyl-acetylamino)-propionic acid methyl ester ( <b>29</b> )	112
(2 <i>S</i> )-Amino-3-methyl-1,1-diphenyl-butan-1-ol ( <b>32</b> )	113
(2 <i>S</i> ,3 <i>S</i> )-1,1-Diphenyl-butane-1,2,3-triol ( <b>40</b> )	114
( <i>R,S</i> )-(2,2-Diphenyl-acetylamino)-methoxy-acetic acid methyl ester ( <b>41</b> )	116
(3 <i>R</i> ,6 <i>RS</i> )-6-(2,2-Diphenyl-acetylamino)-5-oxo-thiomorpholine-3- carboxylic acid methyl ester ( <b>45</b> )	117
Crystallographic Data for <b>21b</b> and <b>22a</b>	118
<b>3. Mattacin and Polymyxin B Peptides</b>	119
3.1 Bacterial Strains and Culture Conditions	119
3.2 Antimicrobial Activity Monitoring During Purification	119
3.3 Isolation of Mattacin ( <b>52</b> )	119
3.4 Amino Acid Analysis	121
3.5 Acetylation of Mattacin	121
3.6 Mass Spectrometry	122
3.7 NMR Spectroscopy	123

3.8	Stereochemical Analysis of Mattacin	124
3.9	Isothermal Titration Calorimetry	125
<b>4.</b>	<b>Lacticin 3147 and Lantibiotic Peptides</b>	<b>127</b>
4.1	Bacterial Strains and Culture Conditions	127
4.2	Antimicrobial Activity Monitoring During Purification	127
4.3	Isolation of Lacticin (from Supernatant)	128
4.4	Mass Spectrometry	130
4.5	Experimental Data for Compounds	131
	(D,L)-Lanthionine bis-PTH ( <b>57</b> )	131
	2-Benzoylaminoacrylic acid Methyl Ester ( <b>58</b> )	132
	(2L)-Amino-(6D,L)-(benzoylamino)lanthionine Dimethyl Ester ( <b>59</b> )	132
	(2L)-Amino-(6D,L)-(benzoylamino)lanthionine Bis-methylamide ( <b>60</b> )	133
	(2L)-Amino-PTH-(6D,L)-(benzoylamino)lanthionine Mono- methylamide ( <b>61</b> )	134
	(2D,6L)-Bis-(benzoylamino)lanthionine Dimethyl Ester ( <b>62</b> )	135
	Isolation of Nisin ( <b>53</b> )	136
	General Procedure for Ni <sub>2</sub> B Desulfurization/Reduction of Model Compounds ( <b>58</b> ), ( <b>62</b> )	138
	(D,L)-Alanine Methyl Ester Benzamide ( <b>63</b> )	138
	α,β-Dideutero-(D,L)-alanine Methyl Ester Benzamide ( <b>64</b> )	139
	β-Deutero-(D,L)-alanine Methyl Ester Benzamide ( <b>65</b> )	139
4.6	Lacticin A2 N-terminal Deblocking	139
4.7	General Procedure for Ni <sub>2</sub> B Desulfurization/Reduction of	140

	Lantibiotic Peptides	
4.8	General Procedure for Deuterium Labeling Ni <sub>2</sub> B	141
	Desulfurization/Reduction of Lantibiotic Peptides	
4.9	Peptide Sequencing (Automated Edman Degradation)	141
4.10	LCMS Characterization of PTH Amino Acids from Edman Degradation	142
4.11	Lacticin 3147 Overproducer	148
4.12	Enhanced Isolation of Lacticin (from Cells)	148
4.13	NMR Spectroscopy	149
	<b>References</b>	<b>151</b>



## LIST OF TABLES

Table	Page
1. Sulfenimines prepared	13
2. Reductions attempted with alanine diphenyl pseudoxazolone	18
3. Inhibition data for HAV 3C, HRV 3C and half life of various pseudoxazolones in phosphate buffer at pH 7.5	24
4. Temperature coefficients of mattacin amide proton chemical shifts	38
5. Antimicrobial spectrum of live <i>P. kobensis</i> M and purified polymyxins	41
6. Some common antibiotics and their cellular targets	49
7. Amino acid analysis of A1 and A2 peptides	70
8. Lanthionine bis-PTH solubility	73
9. Mass analysis of standard PTH alanine and aminobutyric acid	144
10. Mass analysis of PTH residues derived from nisin treated with D <sub>2</sub> /Ni <sub>2</sub> B	145
11. Mass analysis of PTH residues derived from A1 peptide treated with D <sub>2</sub> /Ni <sub>2</sub> B	146
12. Mass analysis of PTH residues derived from A2 peptide treated with D <sub>2</sub> /Ni <sub>2</sub> B	147

## LIST OF FIGURES

Figure	Page
1. Sulfenimines and pseudoxazolones	6
2. Picornaviral polyprotein processing	8
3. HAV 3C proteinase hydrolysis	8
4. Known HAV 3C inhibitors	9
5. $^1\text{H}$ Chemical shift of the glycine pseudoxazolone olefinic proton in acetone- $d_6$ (300 MHz)	14
6. Crystal structures of <b>21b</b> and <b>22a</b>	15
7. General structure of polymyxins	28
8. Polymyxin B	29
9. Lipid A monomer	30
10. Schematic representation of a generic polymyxin molecule (oval with tail) bound to lipid A	31
11. MALDI-TOF mass spectrum of matttacin	33
12. MALDI-TOF mass spectrum of matttacin octa-acetate	34
13. 1D HNMR spectrum of matttacin with expansion of amide region	35
14. HH COSY identifying $\text{H}\alpha/\text{HN}$ correlations	36
15. TOCSY spectrum identifying spin system for all ten residues	36
16. Connectivities observed in ROESY and HH-COSY spectra leading to sequence assignment in matttacin	37
17. Matttacin	37

18.	Conformational model of mattacin and polymyxin B heptacycles based on tNOE data obtained from mattacin/LPS mixture	43
19.	Binding isotherms resulting from the titration of LPS with mattacin and polymyxin B	45
20.	Schematic representation of peptidoglycan layer in bacterial cell wall	48
21.	Nisin	51
22.	Model of cell killing by pore-forming bacteriocin	55
23.	Barrel-stave/wormhole mechanism of pore formation by cationic bacteriocin	57
24.	Lipid II	57
25.	Lipid II mediated pore formation by Nisin	58
26.	Irish kefir grain	63
27.	Structures of lanthionine and $\beta$ -methyllanthionine	64
28.	HPLC separation of lacticin 3147 A1 and A2 peptides	65
29.	Complementary activity of lacticin A1 and A2 against <i>Lactococcus lactis</i> subsp. <i>cremoris</i> HP	66
30.	MALDI-TOF mass spectrum of lacticin 3147 A1	67
31.	MALDI-TOF mass spectrum of lacticin 3147 A2	67
32.	Initial sequencing results and predicted genetic sequence of lacticin 3147	69
33.	Dehydroalanine and lanthionine analogues prepared	76
34.	MALDI-TOF mass spectrum of deblocked lacticin 3147 A2	81
35.	Dehydro residue / lanthionine bridge location in lacticin A1 and A2 peptides	85

36	Mersacidin structure and proposal for A1 peptide	86
37.	Lactocin S structure and proposal for A2 peptide	87
38.	HPLC separation of lacticin 3147 A1 and A2 peptides – improved isolation	89
39a.	TOCSY spectrum identifying spin systems for all residues in A1 peptide	90
39b.	TOCSY spectrum identifying spin systems for all residues in A2 peptide	91
40.	Intra-bridge NOE's used in Lan/MeLan bridging pattern assignment	92
41a.	Intra-bridge NOE's for lanthionine and $\beta$ -methyllanthionine linkages in A1 peptide	93
41b.	Intra-bridge NOE's for lanthionine and $\beta$ -methyllanthionine linkages in A2 peptide	94
42a.	Lacticin A1	95
42b.	Lacticin A2	95
43.	MALDI mass spectrum of nisin	137

## LIST OF SCHEMES

Scheme	Page
1. Enzymatic resolution of <i>N</i> -acyl amino acids	3
2. Examples of asymmetric amino acid synthesis on chiral templates	4
3. Aminotransferase action mediated by PLP	5
4. Amino acid de-racemization strategy	5
5. Reactivity pattern of pseudoxazolones toward oxygen and sulfur nucleophiles	7
6. Sulfenimine preparation	11
7. Mechanism of sulfenimine formation	12
8. Pseudoxazolone preparation	13
9. Diphenyl pseudoxazolone preparation	15
10. Preparation of 9-chloro-9H-fluorene-9-carbonyl chloride	16
11. Preparation of fluorenyl pseudoxazolones	16
12. NaBH <sub>4</sub> reduction of alanine diphenyl pseudoxazolone	17
13. Decomposition of pseudoxazolone <b>24</b> in methanol	21
14. Possible modes of nucleophilic attack on pseudoxazolones	22
15. Reaction of glycine diphenyl pseudoxazolone and L-Cys methyl ester	23
16. Two-peptide lantibiotic production mechanisms	52
17. Lantibiotic peptide modifications	53
18. $\alpha$ -Keto amide N-terminal blockage of lantibiotic peptides	54
19. C-terminal cysteine oxidative decarboxylation and ring formation	54

20. Thiol modification of lantibiotic peptide	62
21. The Edman degradation	68
22. Lanthionine bis-PTH preparation	72
23. Preparation of orthogonally protected lanthionine	72
24. Lanthionine mono-PTH preparation	73
25. Formation of nickel boride in protic solvent	75
26. Proposed mechanism for Ni <sub>2</sub> B desulfurization	76
27. Nickel boride reduction of lanthionine analogue <b>58</b>	77
28. Nickel boride desulfurization of dehydroalanine analogue <b>62</b>	77
29. Nickel boride modification of nisin	78
30. Nickel boride modification of the lactacin 3147 A1 peptide	79
31. N-terminal deblocking of lactacin A2	80
32. Nickel boride modification of the deblocked lactacin 3147 A2 peptide	82
33. Deuterating nickel boride reduction of lanthionine analogue <b>58</b>	83
34. Deuterating nickel boride desulfurization of dehydroalanine analogue <b>62</b>	83
35. Deuterating nickel boride modification of nisin	84

## LIST OF ABBREVIATIONS

$[\alpha]_D^{26}$	specific rotation
A or Ala	alanine
ABC	ATP-binding cassette
Abu	aminobutyric acid
Abu-S-Ala	$\beta$ -methyllanthionine
Ac	acetyl
Ac <sub>2</sub> O	acetic anhydride
AcOH	acetic acid
Anal.	analysis
Ala-S-Ala	lanthionine
APT	attached proton test
aq.	aqueous
Bn	benzyl
bp	boiling point
br	broad
<i>c</i>	concentration
C or Cys	cysteine
Calcd	calculated
CD	circular dichroism
COSY	correlation spectroscopy
$\delta$	chemical shift in parts per million downfield from tetramethylsilane
d	doublet

D or Asp	aspartic acid
Da	Dalton
DAB	$\alpha,\gamma$ -diaminobutyric acid
<i>m</i> -DAP	<i>meso</i> -diaminopimelic acid
DBU	1,8-diazabicyclo[5.4.0]undec-7-ene
Dha	dehydroalanine
Dhb	dehydrobutyrine
DMAP	4-(dimethylamino)pyridine
DMF	dimethylformamide
DMSO	dimethylsulfoxide
DTT	dithiothreitol
E or Glu	glutamic acid
EI	electron impact
eq	equivalent
ES	electrospray
Et	ethyl
Et <sub>2</sub> O	diethyl ether
EtOH	ethanol
F or Phe	phenylalanine
FAB	fast atom bombardment
G or Gly	glycine
Glc	glucose
H or His	histidine



HMQC	heteronuclear multiple quantum coherence
HPLC	high performance liquid chromatography
HRMS	high-resolution mass spectrum
IC <sub>50</sub>	concentration causing 50% inhibition
I or Ile	isoleucine
IPA	isopropyl alcohol
IR	infrared
ITC	isothermal titration calorimetry
<i>J</i>	coupling constant
K or Lys	lysine
L or Leu	leucine
LAB	lactic acid bacteria
LeuA	leucocin A
LHMDS	lithium hexamethyldisilazide
lit.	literature reference
LPS	lipopolysaccharide
m	multiplet
M or Met	methionine
<i>m/z</i>	mass to charge ratio
MALDI-TOF	matrix-assisted laser desorption ionization / time-of-flight
Me	methyl
MeCN	acetonitrile
MeOH	methanol

MIC	minimum inhibitory concentration
min	minute(s)
mp	melting point
MW	molecular weight
N or Asn	asparagine
NADPH	nicotinamide adenine dinucleotide phosphate (reduced form)
NaOAc	sodium acetate
NaOH	sodium hydroxide
NaOMe	sodium methoxide
Na <sub>2</sub> SO <sub>4</sub>	sodium sulfate
NBS	<i>N</i> -bromosuccinimide
<i>n</i> -BuOH	<i>n</i> -butanol
NMR	nuclear magnetic resonance
nm	nanometers
NOE	nuclear Overhauser effect
P or Pro	proline
ppm	parts per million
pyr	pyridine
q	quartet
Q or Gln	glutamine
quant.	quantitative yield
R or Arg	arginine
R <sub>f</sub>	retention factor

ROESY	rotating frame Overhauser effect spectroscopy
rt	room temperature
S or Ser	serine
t	triplet
T or Thr	threonine
Tf	trifluoromethanesulfonyl
TFA	trifluoroacetic acid
TFAA	trifluoroacetic anhydride
TFE	trifluoroethanol
THF	tetrahydrofuran
THP	tetrahydropyran
TLC	thin layer chromatography
TOCSY	total correlation spectroscopy
$t_R$	retention time
Ts	<i>p</i> -toluenesulfonyl
<i>p</i> -TsOH	<i>p</i> -toluenesulfonic acid
V or Val	valine
W or Trp	tryptophan
Y or Tyr	tyrosine

## OVERVIEW

This thesis is comprised of the results obtained from three distinct projects. While the projects are significantly different in their aims and approaches, all three have focused on the development and discovery of new agents for combating human disease.

The first project focused on the design and synthesis of inhibitors for the 3C proteinase enzyme utilized by the Hepatitis A Virus (HAV 3C). Because of the importance of the 3C proteinase in viral replication and the conservation of active site residues among a wide range of serotypes, this enzyme is an attractive target for chemotherapy. To this end a number of novel amino acid analogues bearing a reactive unsaturated moiety at the  $\alpha$ -position were synthesized. The most effective inhibitors of HAV 3C explored were the pseudoxazolones (Chapter 1).

Chapter 2 describes work with mattacin, a cyclic peptide with potent antimicrobial activity towards a number of Gram-negative bacteria. A full structure elucidation of this bacterially derived, non-ribosomal, antibiotic peptide was achieved. Following the structural characterization of mattacin, conformational analyses were also undertaken using 2D NMR techniques to investigate the solution structures of mattacin in isolation and in the presence of its cell surface target (lipid A). Also, using calorimetric methods, the binding properties of mattacin with lipid A were assessed.

The third project also involved antimicrobial peptides, specifically a unique pair of synergistic, antibiotic peptides termed lacticin 3147 A1 and A2. Isolated from bacterial sources, the lacticin 3147 peptides show impressive antibacterial activity towards Gram-positive organisms. Classified as lantibiotics, these peptides contain a number of unique structural modifications (lanthionine bridges and dehydro residues) rendering conventional means of peptide analysis ineffective. New chemical modifications relying on the use of nickel boride to desulfurize and reduce lantibiotic peptides have been developed. These new methods represent an advancement in the characterization of lantibiotic peptides and have been successfully applied to the lacticin 3147 peptides. Also, after optimizing the isolation of the lacticin 3147 peptides it was possible to employ multidimensional NMR to obtain their primary structures (Chapter 3).

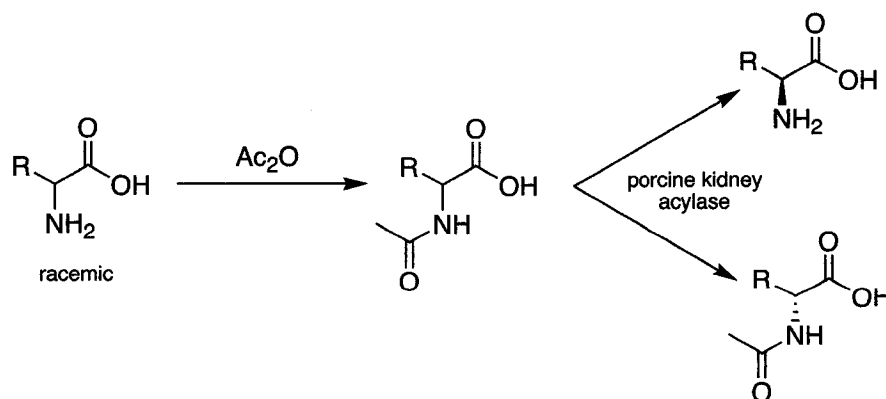
# CHAPTER 1. Planar Derivatives of Amino acids and Pseudoxazolones as Inhibitors of Hepatitis A Virus 3C Proteinase

## INTRODUCTION

### 1. Sulfenimines and Pseudoxazolones in Amino Acid Synthesis

Amino acids are important members of the chiral pool due to their abundance and natural occurrence in optically pure form. The approximately 20 natural L-amino acids, however, are insufficient to produce certain novel peptides and other compounds containing non-natural, stereochemically pure, D-amino acid building blocks. The desire to obtain new amino acids has led to many new methodologies. An early advancement in the area relied on the enzymatic resolution of racemic mixtures of *N*-acyl amino acids<sup>1,2</sup> (Scheme 1).

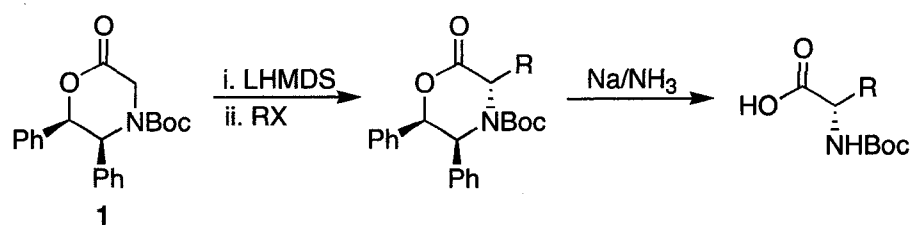
**Scheme 1.** Enzymatic resolution of *N*-acyl amino acids



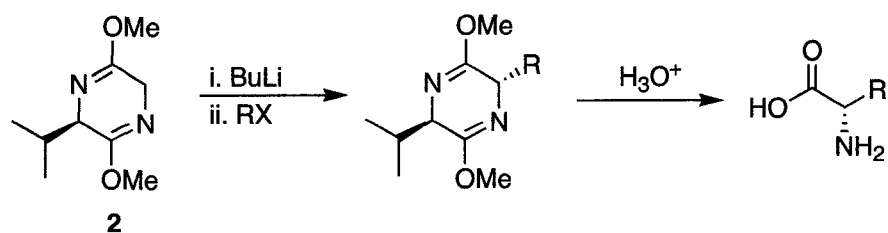
Advances in asymmetric synthesis have furthered the production of new amino acids<sup>3</sup> but generally rely on the use of a chiral catalyst or an equimolar amount of chiral auxiliary. Of the latter, the Williams chiral glycine synthon **1**<sup>4,5</sup> and the Schollkopf valine derived auxiliary **2**<sup>6,7</sup> are two of the most successful (Scheme 2).

**Scheme 2.** Examples of asymmetric amino acid synthesis on chiral templates

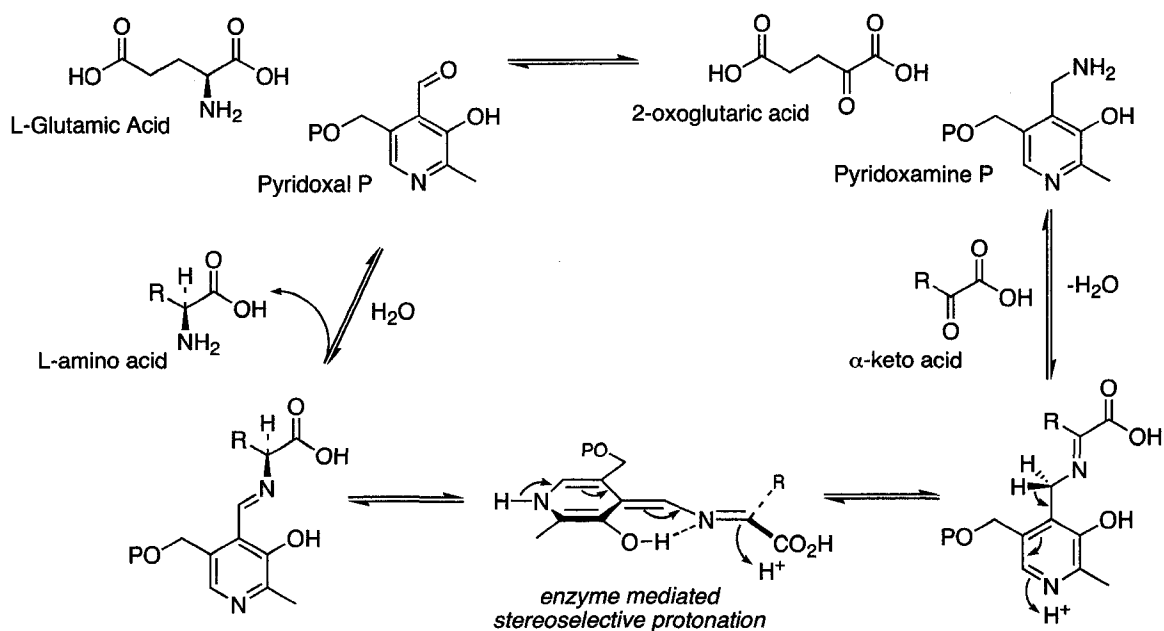
Williams Chiral Glycine Synthon



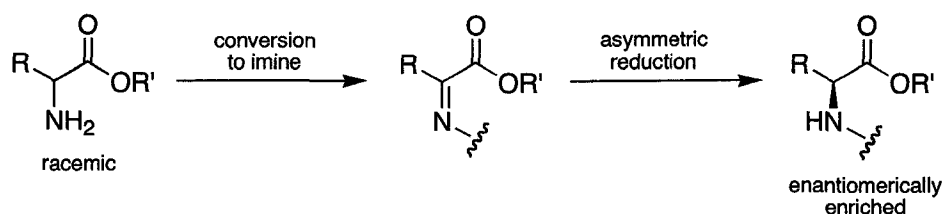
Schollkopf Chiral Glycine Synthon



The natural pathway by which many amino acids are generated involves the use of the coenzyme pyridoxal phosphate (PLP) and the prevalent amino group donor glutamic acid.<sup>8-10</sup> Transaminase enzymes (aminotransferases) use PLP-facilitated transamination whereby the amino group of glutamic acid is transferred to a suitable  $\alpha$ -keto acid to generate a new amino acid with defined stereochemistry at the  $\alpha$ -centre (Scheme 3).<sup>11-13</sup>

**Scheme 3.** Aminotransferase action mediated by PLP

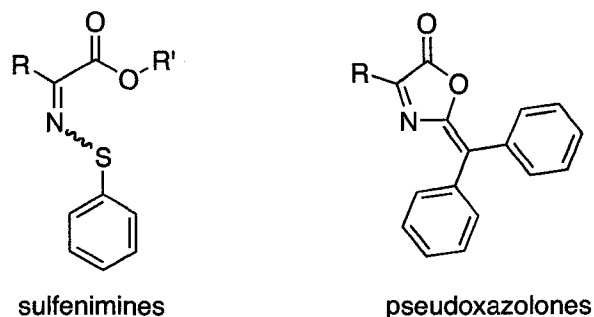
Our initial approach to optically pure amino acids is reminiscent of Nature's pathway to amino acids. Following conversion of racemic mixtures of amino acids to planar imine intermediates, we surmised that asymmetric reduction could be employed to yield the desired enantiomer, thereby de-racemizing the original mixture (Scheme 4).

**Scheme 4.** Amino acid de-racemization strategy



To this end, two classes of compounds were explored: the sulfenimines and pseudoxazolones (Figure 1) which are readily prepared in good yield from the simple amino acid precursors.

**Figure 1.** Sulfenimines and pseudoxazolones

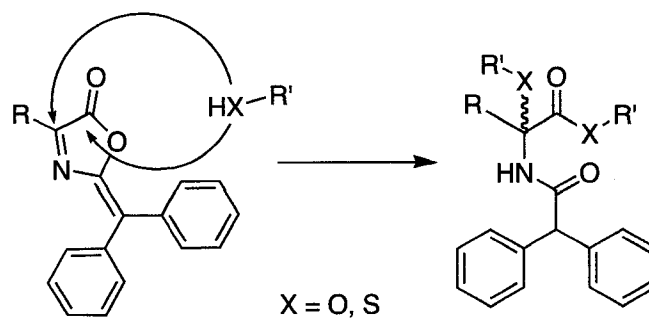


Both the sulfenimine<sup>14,15</sup> and pseudoxazolone<sup>16,17</sup> classes of amino acid derivatives had been explored earlier in the literature but not with the intent of generating new amino acids. Conditions for their preparation were optimized, their reductions under a variety of conditions studied, and their general reactivities explored.

## **2. Pseudoxazolones as Hepatitis A Virus and Human Rhinovirus 3C Proteinase Inhibitors**

In addition to serving as amino acid precursors, it was also proposed that pseudoxazolones might display unique patterns of reactivity with oxygen and sulfur nucleophiles. It became clear after a series of investigations that both the carbonyl and imine moieties of these species are susceptible to nucleophilic attack (Scheme 5).

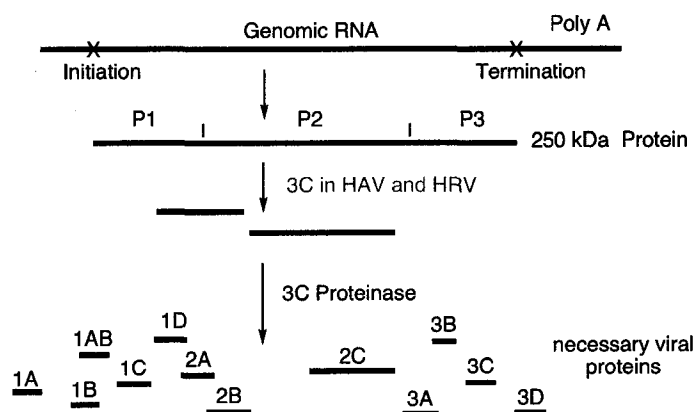
**Scheme 5.** Reactivity pattern of pseudoxazolones toward oxygen and sulfur nucleophiles



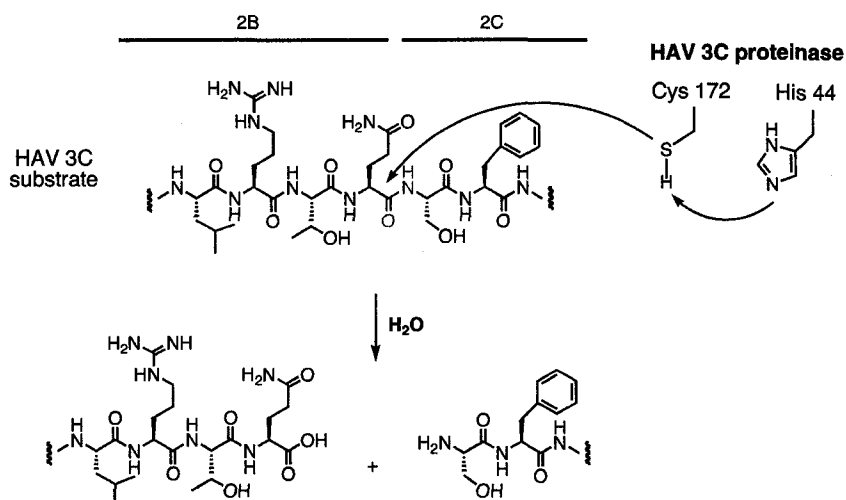
This unique pattern of nucleophilic addition by either sulfur or oxygen nucleophiles suggested the use of pseudoxazolones as small molecule, irreversible inhibitors of serine and cysteine proteinase enzymes.

### 2.1 HAV and HRV 3C Activity in Viral Replication

Cysteine proteinases have attracted much attention as therapeutic targets because of their implication in many diseases such as osteoporosis, Alzheimer's, and arthritis.<sup>18,19</sup> One of the major areas of study in our research group is the inhibition of hepatitis A virus (HAV) and human rhinovirus (HRV) 3C proteinases.<sup>20-22</sup> As in other picornaviruses, the HAV and HRV RNA genomes encode for a single large polyprotein (~250 kDa) precursor which is cleaved by the viral 3C proteinase to produce the structural and non-structural viral components (Figure 2).<sup>23,24</sup>

**Figure 2. Picornaviral polyprotein processing**

The proteinase enzyme mechanism involves a cysteine side-chain thiolate acting as a nucleophile in the cleavage of the polyprotein precursor (Figure 3).<sup>25</sup> It was reasoned that inhibitors of this process could be designed by placing an electrophilic site (for example, the imine moiety of the pseudoxazolones) within a peptide framework recognized by the enzyme.

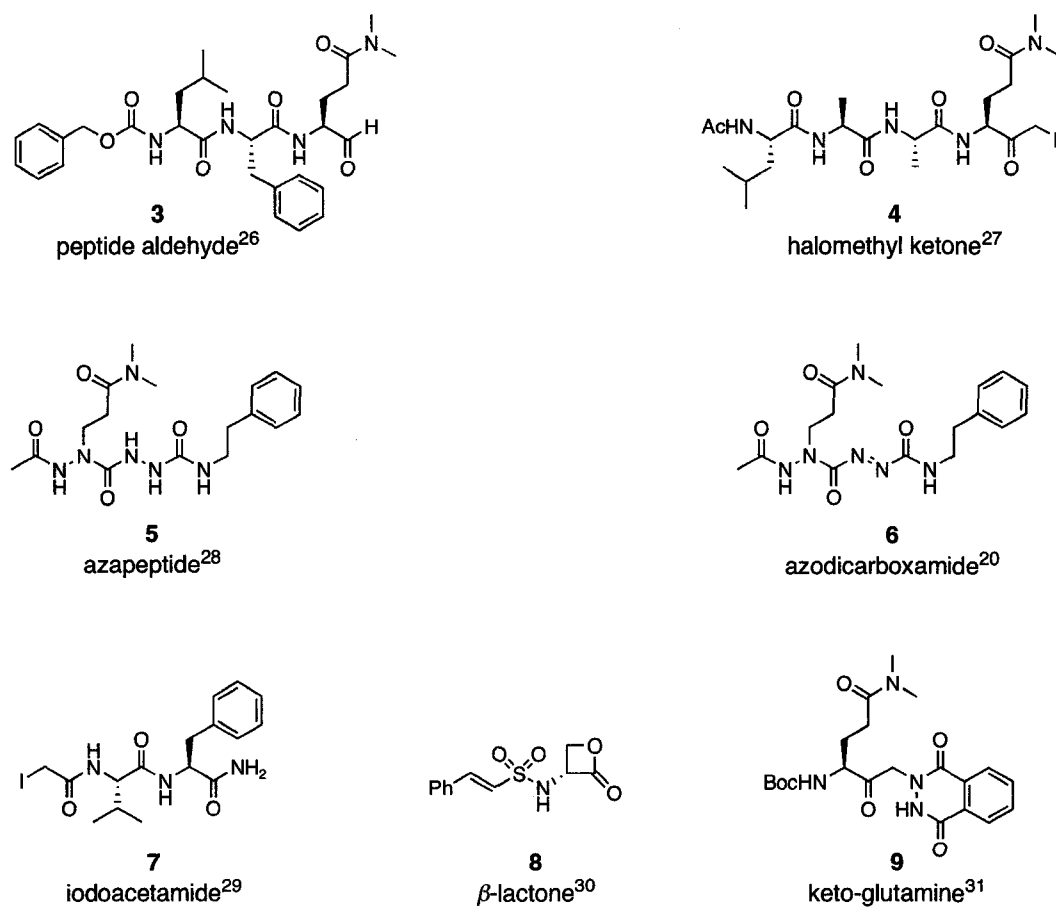
**Figure 3. HAV 3C proteinase hydrolysis**

*Peptide cleavage is initiated using the thiolate side chain of Cys 172 to form a thioester with concomitant departure of a peptide fragment containing a free amino terminus. In the second step, the thioester is hydrolyzed to release a carboxy terminal peptide and regenerate the active enzyme.*

## 2.2 Previous HAV and HRV 3C Inhibitors

A number of HAV 3C inhibitors have been reported to date with a focus on mimicking the cleavage region of the natural enzyme substrate. Representative compounds include peptide aldehyde **3**,<sup>26</sup> halomethyl ketone **4**,<sup>27</sup> azapeptide **5**,<sup>28</sup> azodicarboxamides **6**,<sup>20</sup> iodoacetamide **7**,<sup>29</sup>  $\beta$ -lactone **8**<sup>30</sup> and keto-glutamine **9**<sup>31</sup> (Figure 4).

**Figure 4.** Known HAV 3C inhibitors



### **3. Project Goals: Synthesis and Testing of Pseudoxazolones as HAV/HRV 3C**

#### **Inhibitors**

Pseudoxazolones contain an electrophilic site wherein the  $\alpha$ -carbon, present as an imine, may mimic the cleavage site of the enzyme's natural substrate and be susceptible to nucleophilic attack by the enzyme cysteine thiolate. A variety of pseudoxazolones were prepared and characterized. The ability of the pseudoxazolones to inhibit the HAV/HRV 3C proteinases as well as their mode of action towards the enzymes was investigated as described in subsequent sections.

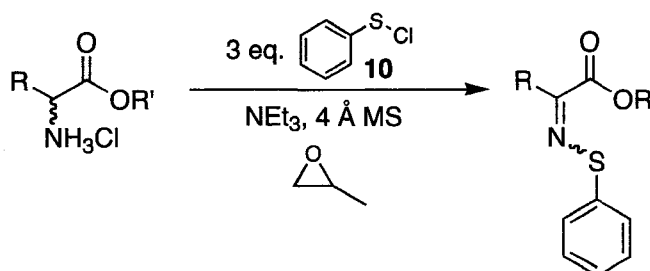
## RESULTS AND DISCUSSION

### 1. Chemistry of Sulfenimines and Pseudoxazolones

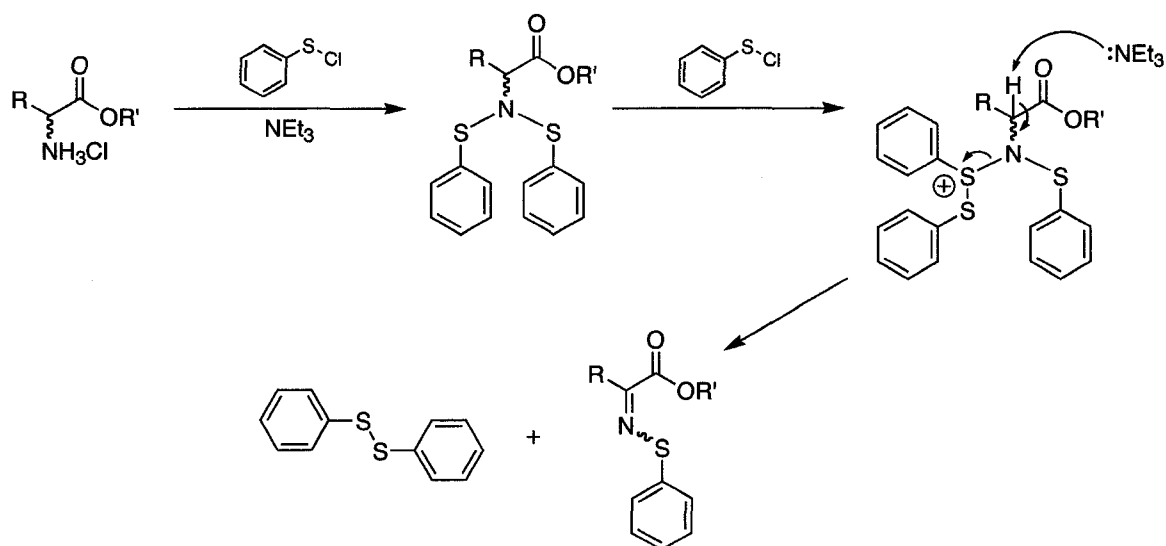
#### 1.1 Sulfenimine and Pseudoxazolone Preparation

The first planar amino acid precursors explored were the sulfenimines. Using a procedure based on the method of Gordon and coworkers,<sup>15</sup> sulfenimines are prepared in good to excellent yields. Briefly, by treating a racemic mixture of an amino acid ester with three equivalents of benzenesulfonyl chloride **10** and acid scavengers, sulfenimines are readily obtained (Scheme 6).

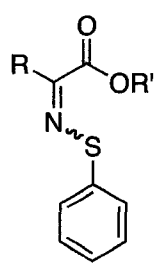
**Scheme 6.** Sulfenimine preparation



The mechanism proposed for this transformation by Gordon (Scheme 7) is also supported by our observations. Three equivalents of the sulfonyl chloride are necessary; if less than this quantity is used a significant amount of the *N*-bis-sulfonylated product is obtained. A molar equivalent of phenyl disulfide is isolated from the reaction mixture after completion, further supporting the proposed mechanism.

**Scheme 7.** Mechanism of sulfenimine formation

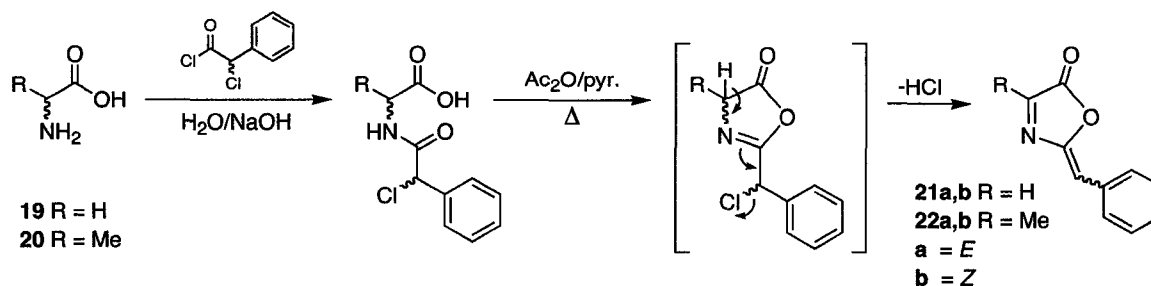
After synthesizing a number of sulfenimines, it became apparent that the *E/Z* isomerism consistently observed in the products was unavoidable. The two geometric isomers are not separable because they are in thermal equilibrium<sup>32</sup> as proven by variable temperature NMR investigations performed by ourselves and others.<sup>33,34</sup> When performing asymmetric manipulations on an imine it is generally accepted<sup>35,36</sup> that the geometry about the imine must be strictly defined. To this end the size of the ester was varied in the hope that increasing steric bulk might yield a single, non-equilibrating imine product (Table 1).

**Table 1.** Sulfenimines prepared


Compound Number	R	R'	% Yield	Isomer Ratio <sup>a</sup>
11	Bn	Me	91	3:1
12	Bn	<sup>i</sup> Pr	96	3:2
13	Me	Me	72	10:1
14	Bn	Et	89	2:1
15	Me	<sup>t</sup> Bu	87	4:1
16	Me	<sup>i</sup> Pr	93	6:1
17	Me	Et	82	8:1
18	Ph	Me	86	3:1

<sup>a</sup>ratios estimated by <sup>1</sup>H NMR spectroscopy in CDCl<sub>3</sub>

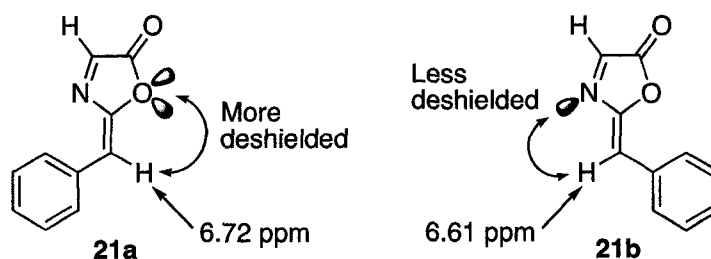
The inability to control the geometry about the sulfenimine prompted the search for other amino acid precursors with planarity at the  $\alpha$ -centre. This search resulted in the pseudoxazolones, a class of compounds briefly explored by Cornforth and coworkers in the 1950s.<sup>16,17</sup> These 3-oxazolin-5-one systems, termed pseudoxazolones, are readily prepared by acylation of a free amino acid with an  $\alpha$ -chloro acid chloride under Schotten-Baumann conditions, followed by cyclization and elimination of HCl to yield the conjugated imine species (Scheme 8).<sup>37</sup>

**Scheme 8.** Pseudoxazolone preparation



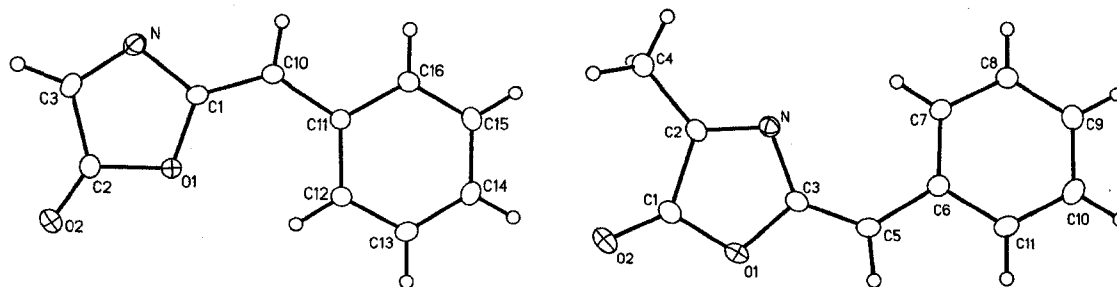
This preparation also yields mixtures of *E/Z* isomers, but unlike the sulfenimines, they are readily separable by flash column chromatography. Assignment of the *E* and *Z* isomers can be made based on the proton ( $^1\text{H}$ ) chemical shift of the olefinic hydrogen.<sup>38</sup> The less polar *E* isomer on TLC (e.g. **21a**, Figure 5) has its olefinic proton aligned with the oxazolone ring oxygen and is therefore more deshielded (6.72 ppm), whereas the more polar *Z* isomer (e.g. **21b**) has its olefinic proton aligned with the imine nitrogen and is consequently less deshielded (6.61 ppm). Although light induced isomerization and dimerization is known to occur for these compounds,<sup>39</sup> when stored in the dark no such effect was observed by  $^1\text{H}$  NMR.

**Figure 5.**  $^1\text{H}$  Chemical shift of the glycine pseudoxazolone olefinic proton in acetone- $d_6$  (300 MHz)



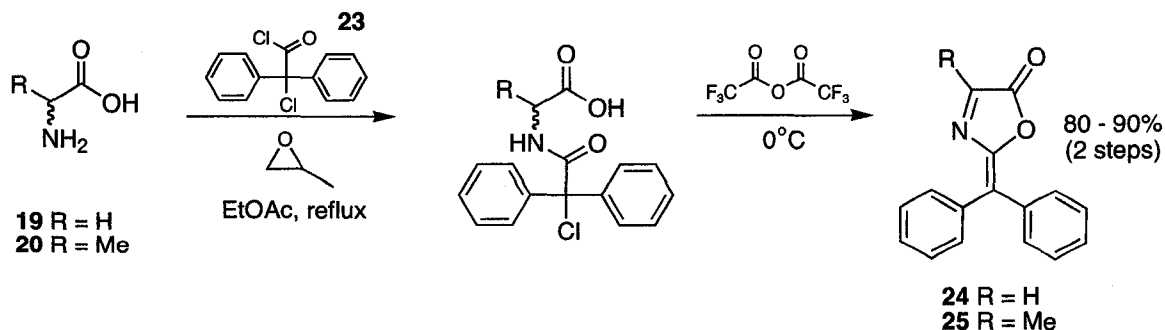
Additional support for the assignment of the *E/Z* isomers came from two X-ray crystal structures of **21b** and **22a**, which confirmed the geometry of the double bond (Figure 6). Analogous application of  $^1\text{H}$  NMR spectroscopy can be used to assign the *E* and *Z* configuration of other monophenyl pseudoxazolones.

**Figure 6.** Crystal structures of **21b** (left) and **22a** (right)



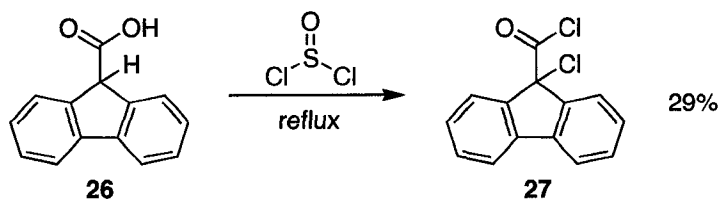
Rather than contend with the need to isolate each geometric isomer, methods and reagents were developed that yielded pseudoxazolones without the possibility of *E/Z* isomerism. One approach uses 2-chloro-2,2-diphenylacetyl chloride **23** as the initial acylating agent. The presence of the second aromatic ring at the  $\alpha$ -position, however, greatly destabilizes the acid chloride in aqueous media, thereby requiring the Schotten-Baumann conditions used for the preparation of the monophenyl species to be altered. A variety of conditions were explored to provide the high yielding protocol described in Scheme 9.

**Scheme 9.** Diphenyl pseudoxazolone preparation



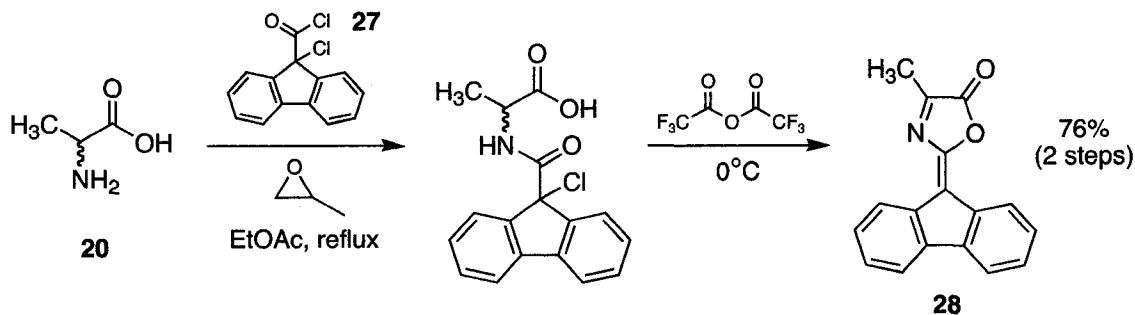
Another class of pseudoxazolones explored made use of a fluorenyl moiety in place of the two aromatic rings. The required  $\alpha$ -chloro acid chloride was prepared from 9H-fluorene-9-carboxylic acid **26** and thionyl chloride (Scheme 10).<sup>40</sup>

**Scheme 10.** Preparation of 9-chloro-9H-fluorene-9-carbonyl chloride



Once the desired  $\alpha$ -chloro acid chloride was obtained, racemic alanine was converted to the pseudoxazolone **28** following the same protocol used in the preparation of the diphenyl pseudoxazolones (Scheme 11).

**Scheme 11.** Preparation of fluorenyl pseudoxazolones

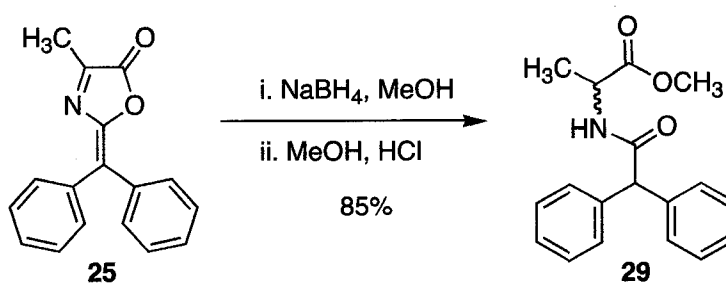


Using the three different alanine-derived pseudoxazolones, a variety of conditions and reagents were explored with the intention of reducing the imine bond.

## 1.2 Reactions Attempted

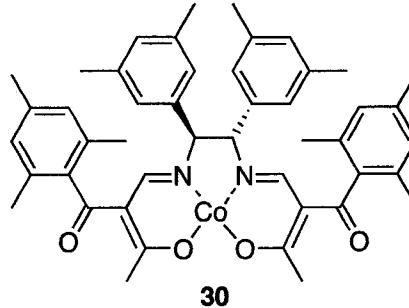
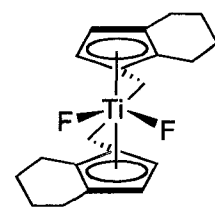
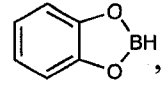
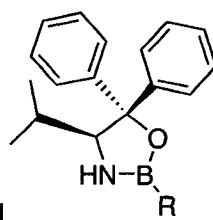
Early results with borohydride reducing agents on pseudoxazolones showed promise. In alcoholic solvent  $\text{NaBH}_4$  affords the expected acylated amino acid methyl ester **29** in good yield (Scheme 12).

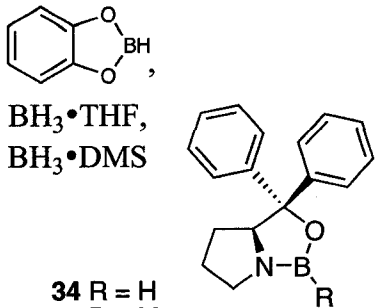
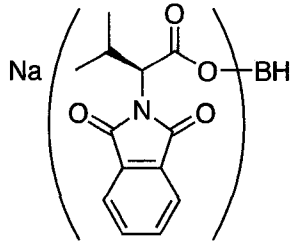
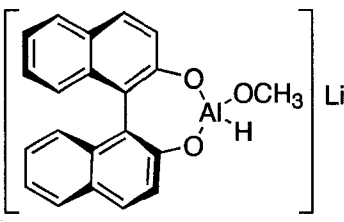
**Scheme 12.**  $\text{NaBH}_4$  reduction of alanine diphenyl pseudoxazolone

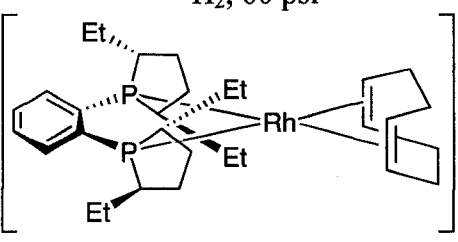
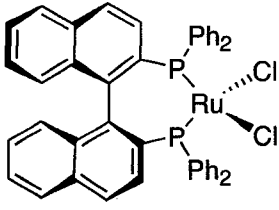
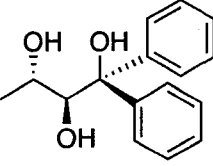


Based on these results a number of commercial chiral catalysts and reducing agents were screened (Table 2). In most cases there was little or no reduction. Where reduction did occur in the presence of a chiral reducing agent, there was no enantioselectivity.

**Table 2.** Reductions attempted with alanine diphenyl pseudoxazolone

Reducing System	Yield <sup>a</sup>	% ee <sup>b</sup>
NaBH <sub>4</sub> , MeOH, CHCl <sub>3</sub>  <b>30</b>	86	0
T. Mukaiyama - β-Oxoaldimine <sup>41</sup>		
PhSiH <sub>3</sub> , MeOH, Pyrrolidine  <b>31</b>	NR	-
S. Buchwald - Titanocene <sup>42</sup>		
 BH <sub>3</sub> •THF, BH <sub>3</sub> •DMS  <b>32</b> R = H <b>33</b> R = Me	NR	-
S. Itsuno - Oxazaborolidine <sup>43</sup>		

 <p> <math>\text{BH}_3 \cdot \text{THF}</math>,  <math>\text{BH}_3 \cdot \text{DMS}</math> </p> <p> <b>34</b> R = H  <b>35</b> R = Me         </p> <p>E.J. Corey - Oxazaborolidine<sup>44</sup></p>	NR	-
 <p><b>36</b></p> <p>A. Hajipour - <i>N</i>-phthalimido amino acid auxiliary<sup>45</sup></p>	NR	-
 <p><b>37</b></p> <p>P. Chan - BINAL-H<sup>46</sup></p>	NR	-

<p style="text-align: center;">H<sub>2</sub>, 60 psi</p>  <p style="text-align: center;"><b>38</b></p> <p style="text-align: center;">M.J. Burk - Et-DuPHOS<sup>47</sup></p>	NR	-
<p style="text-align: center;">H<sub>2</sub>, 1500 psi</p>  <p style="text-align: center;"><b>39</b></p> <p style="text-align: center;">R. Noyori - BINAP<sup>48</sup></p>	NR	-
<p>(NMe<sub>4</sub>)HB(OAc)<sub>3</sub>, MeCN LiBH<sub>4</sub>, THF</p>  <p style="text-align: center;"><b>40</b></p> <p style="text-align: center;">D. Evans - Triol Auxiliary<sup>49</sup></p>	74	0

<sup>a</sup> NR = no reaction, starting material recovered

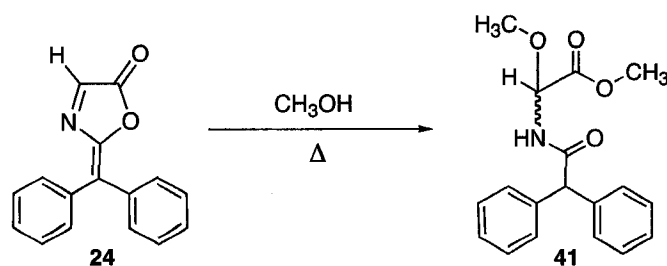
<sup>b</sup> %ee determination by <sup>1</sup>H NMR spectroscopy using Eu(hfc)<sub>3</sub> chiral shift reagent.

In light of these results it is clear that the pseudoxazolones are much less reactive than the ketone and imine species that are routinely transformed by these reducing agents. This stability is not surprising when considering the considerable conjugation in which the imine participates. It appears that in cases where reduction did occur it was likely not

via the catalyst but by direct reduction from the borohydride agent (accelerated during the acidic workup). This would explain the lack of enantioselectivity; protonation of the imine nitrogen increases the reactivity of the imine to reduction while decreasing selectivity.

Fortunately, the pseudoxazolones were not without promise in other areas. Early in the investigation, while preparing the glycine-derived diphenyl pseudoxazolone **24**, an important observation was made. After purification of the pseudoxazolone by flash column chromatography, a small sample of pure material was crystallized from methanol to prepare a high-purity sample for elemental analysis. However, during the crystallization process, the pure pseudoxazolone (bright yellow crystals) began to grow a large number of white crystals in the mixture. Upon TLC analysis of the mother liquor a large spot at lower  $R_f$  than the desired pseudoxazolone was observed and identified as the di-methoxy adduct **41** (Scheme 13).

**Scheme 13.** Decomposition of pseudoxazolone **24** in methanol



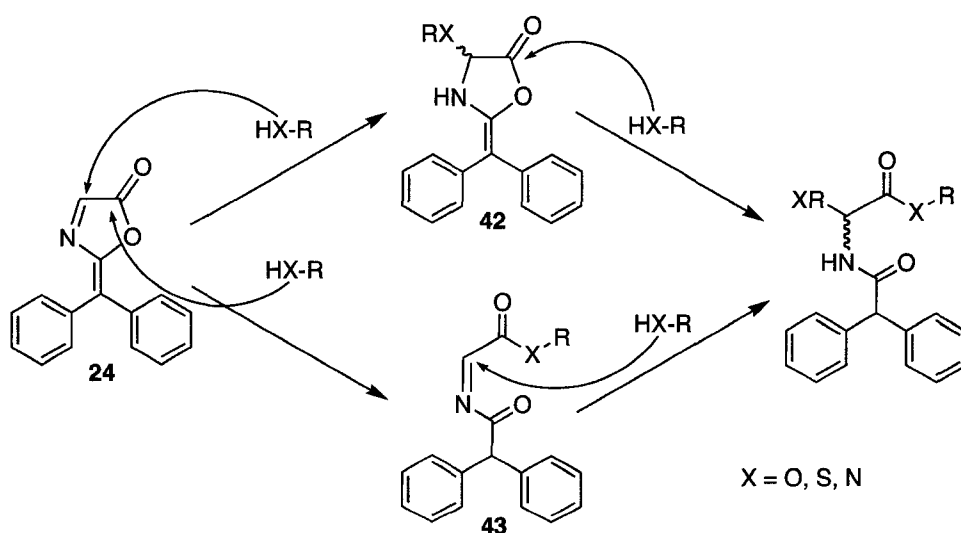
Although initially frustrating to have had the desired product decompose, isolation of the addition product proved fruitful.



## 2. Pseudoxazolones as Inhibitors of HAV 3C Proteinase

The ability of alcohols to form adducts with pseudoxazolones prompted an exploration of the general reactivity of various nucleophiles towards these compounds. One of the questions to be addressed was the precise order in which nucleophiles added into the imine and lactone moieties (Scheme 14). One possible mode of reactivity would first see nucleophilic addition at the imine yielding a highly reactive 5-membered lactone containing an exocyclic double bond **42**, that would then rapidly open by addition of a second nucleophile.<sup>50</sup> In the alternative reaction pathway, the lactone ring is first opened forming an extremely reactive N-acyl imine **43**,<sup>51</sup> that would then rapidly react with a second equivalent of nucleophile.

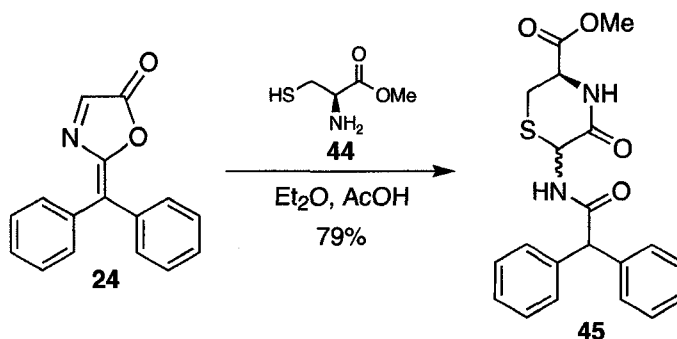
**Scheme 14.** Possible modes of nucleophilic attack on pseudoxazolones



To explore the addition mechanism, Lara Silkin (*Summer Student 2000*) studied the reactivity of the simple pseudoxazolone **24**, derived from glycine, towards di-

nucleophiles. A sample of the pseudoxazolone was treated with L-cysteine methyl ester **44** under acidic conditions to yield the adduct **45** as a 4:1 mixture of diastereomers (Scheme 15).

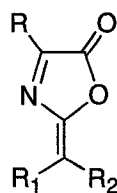
**Scheme 15.** Reaction of glycine diphenyl pseudoxazolone and L-Cys methyl ester



Formation of the adduct **45** suggests nucleophilic attack by the thiol at the imine moiety first followed by addition of the amino group to the carbonyl centre of the transient lactone. These results are in agreement with earlier results obtained by Kaneda and others who examined the behaviour of similar pseudoxazolones.<sup>52</sup>

With evidence for the ability of sulfur nucleophiles to attack pseudoxazolones in protic solvent, it was reasoned that the active site thiolate of a cysteine proteinase enzyme might also be affected by these compounds. A variety of pseudoxazolones were prepared and tested as inhibitors of the 3C cysteine proteinase enzymes from hepatitis A virus and human rhinovirus-14 (Table 3).<sup>53</sup>

**Table 3<sup>a</sup>.** Inhibition data for HAV 3C, HRV 3C and half-life of various pseudoxazolones in phosphate buffer at pH 7.5



Compounds	Substituents	HAV 3C IC <sub>50</sub> (μM)	HRV 3C IC <sub>50</sub> (μM) <sup>b</sup>	Aqueous Hydrolysis t <sub>1/2</sub> (min)
<b>24</b>	R = H, R <sub>1</sub> = R <sub>2</sub> = Ph	33	38	40
<b>25</b>	R = Me, R <sub>1</sub> = R <sub>2</sub> = Ph	>100	>100	15
<b>28</b>	R = Me, R <sub>1</sub> = R <sub>2</sub> = Fluorenone	68	>100	68
<b>21a</b>	R = H, R <sub>1</sub> = Ph, R <sub>2</sub> = H	6	16	28
<b>21b</b>	R = H, R <sub>1</sub> = H, R <sub>2</sub> = Ph	4	17	16
<b>22a</b>	R = Me, R <sub>1</sub> = Ph, R <sub>2</sub> = H	26	43	17
<b>22b</b>	R = Me, R <sub>1</sub> = H, R <sub>2</sub> = Ph	>100	>100	14
<b>46a</b>	R = (CH <sub>2</sub> ) <sub>3</sub> CONH <sub>2</sub> , R <sub>1</sub> = Ph, R <sub>2</sub> = H	43	>100	29
<b>46b</b>	R = (CH <sub>2</sub> ) <sub>3</sub> CONH <sub>2</sub> , R <sub>1</sub> = H, R <sub>2</sub> = Ph	>100	>100	13
<b>47a</b>	R = (CH <sub>2</sub> ) <sub>2</sub> CONH <sub>2</sub> , R <sub>1</sub> = Ph, R <sub>2</sub> = H	47	>100	24
<b>47b</b>	R = (CH <sub>2</sub> ) <sub>2</sub> CONH <sub>2</sub> , R <sub>1</sub> = H, R <sub>2</sub> = Ph	>100	>100	12
<b>48a</b>	R = H, R <sub>1</sub> = <i>p</i> -F-C <sub>6</sub> H <sub>4</sub> , R <sub>2</sub> = H	3	11	17
<b>48b</b>	R = H, R <sub>1</sub> = H, R <sub>2</sub> = <i>p</i> -F-C <sub>6</sub> H <sub>4</sub>	4	13	19
<b>49a</b>	R = H, R <sub>1</sub> = <i>p</i> -MeO-C <sub>6</sub> H <sub>4</sub> , R <sub>2</sub> = H	20	n.d.	21
<b>49b</b>	R = H, R <sub>1</sub> = H, R <sub>2</sub> = <i>p</i> -MeO-C <sub>6</sub> H <sub>4</sub>	10	n.d.	39

<sup>a</sup> All enzyme testing and synthesis of compounds **46-49** by Yeeman Ramtohul, Vederas group graduate student 1997-2002. <sup>b</sup> ND = not determined.

### 3. Conclusions

These results indicate that the glycine-derived pseudoxazolones (**24**, **21a**, **21b**) are better inhibitors than the pseudoxazolones with substitution at the imine carbon (**25**, **22a**, **22b**, **46a**, **46b**, **47a**, **47b**). The monophenyl pseudoxazolones (**21a**, **21b**, **22a**, **22b**, **46a**,

**46b, 47a, 47b**) are more potent than the diphenyl pseudoxazolones (**24, 25**). The *E* monophenyl derivatives are generally better inhibitors than the *Z* monophenyl pseudoxazolones when there is substitution at the imine carbon. Although no significant increase in stability is observed for compounds **48a, 48b** and **49a, 49b**, these results demonstrate that additional functionality on the phenyl ring can be tolerated with no drastic loss of inhibition. Such systems with appropriate functional groups as recognition sites can potentially be applied to other cysteine proteinases.

A drawback to the development of pseudoxazolones as therapeutic drugs is their propensity to react indiscriminantly with primary thiols (i.e. dithiothreitol). Hence, further structural modifications will probably be necessary to tune the reactivity of such inhibitors to prevent condensation with other thiol-containing proteins in living mammalian cells.

## **CHAPTER 2. Isolation and Study of Mattacin, a Cyclic Peptide Antibiotic of the Polymyxin Family**

### **INTRODUCTION**

#### **1. Mattacin, a Polymyxin Peptide**

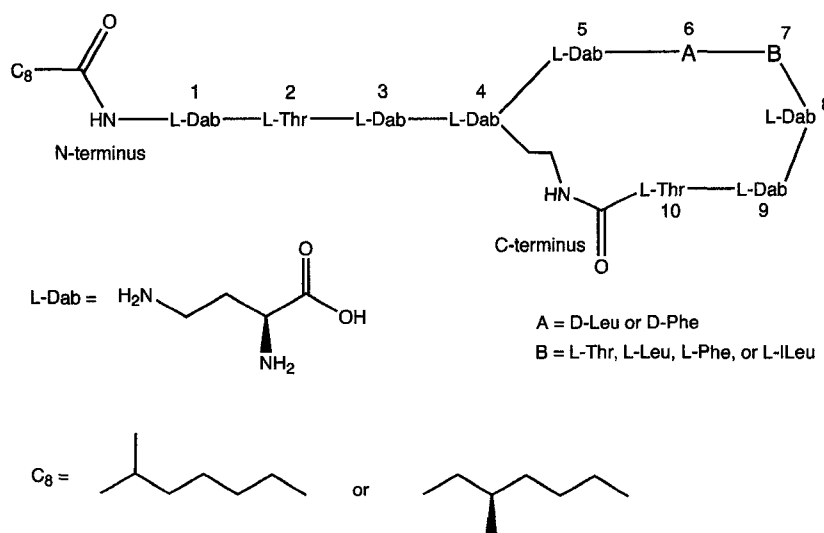
To survive in the natural environment and compete with other microorganisms for resources, many bacteria produce antimicrobial peptides (bacteriocins) to inhibit or kill other competing strains, including human and animal pathogens. Growing interest in bacteriocins from lactic acid bacteria, both unmodified<sup>54,55</sup> and multi-component, post-translationally modified lantibiotics,<sup>56</sup> has led to the examination of other species of Gram-positive bacteria, such as *Bacillus*,<sup>57</sup> for novel peptidic antimicrobial agents.

During a screening program, our collaborators (Randy Worobo and coworkers at Cornell University) found that a *Paenibacillus kobensis* strain isolated from a soil/manure sample produced a biologically active peptide which they named mattacin. Mattacin was shown to have antibiotic activity against a variety of Gram-negative organisms, including a number of human and animal pathogens.

## **2. Non-Ribosomal Peptide Biosynthesis and Unique Structural Features of Polymyxin Peptide Antibiotics**

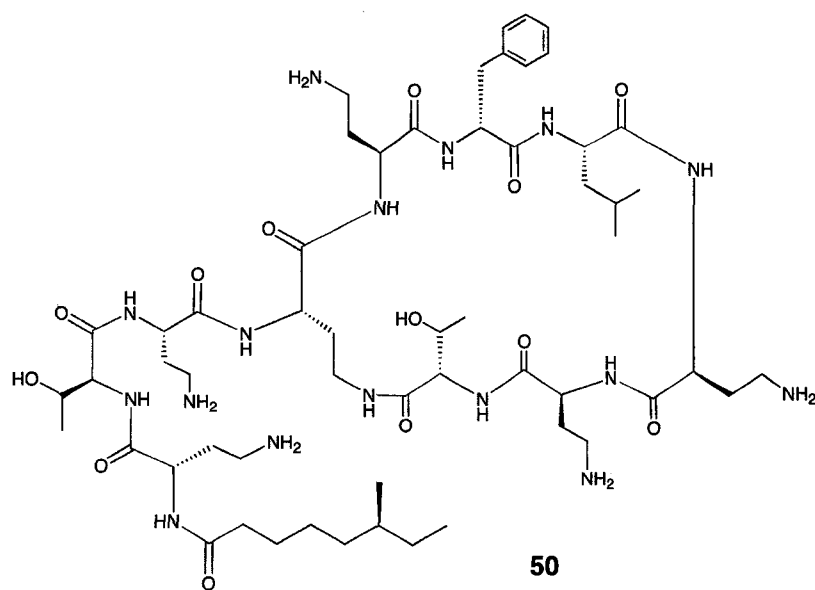
Antibacterial peptides can be divided into two categories based on the biosynthetic pathways by which they are generated. One group consists of gene-encoded, ribosomally synthesized peptides (bacteriocins) that typically have 30 to 60 residues, which may be either unmodified or extensively post-translationally altered (i.e. lantibiotics), and are active against closely related bacteria.<sup>58-60</sup> Peptides in the second class, including the polymyxin group (Figure 7), are non-ribosomal in origin and are produced by a series of condensations catalyzed by specific non-ribosomal peptide synthetases (NRPSs) using a templated multienzyme mechanism.<sup>61,62</sup> These NRPSs are large, multi-functional proteins composed of different modules, each of which has different domains capable of performing one step in the condensation of an amino acid onto a growing peptide chain.<sup>63</sup> The resulting peptidic compounds often contain non-proteinaceous amino acids, including D-amino acids, hydroxy acids, or other unusual constituents.<sup>64</sup> The peptide portion of antibiotics produced in this fashion is generally smaller than in ribosomal bacteriocins and usually has fewer than 20 amino acids.<sup>65</sup>

**Figure 7.** General structure of polymyxins



### 3. Background and Therapeutic Use of Polymyxins

In recent years a large number of antimicrobial peptides from Gram-positive bacteria have been discovered, including ribosomally produced bacteriocins.<sup>66-68</sup> The non-ribosomally generated polymyxins represent one of the earliest classes of structurally unique peptide antibiotics to be identified.<sup>69</sup> *Paenibacillus* spp. are Gram-positive, spore-forming bacteria from which polymyxins have been isolated and their *in vitro* biosynthesis by cell-free enzyme systems successfully demonstrated.<sup>70</sup> The first member of the polymyxin family, polymyxin B **50** (Figure 8), was discovered in 1947<sup>69</sup> and is currently sold in a variety of formulations under the name Polysporin®.

**Figure 8. Polymyxin B**

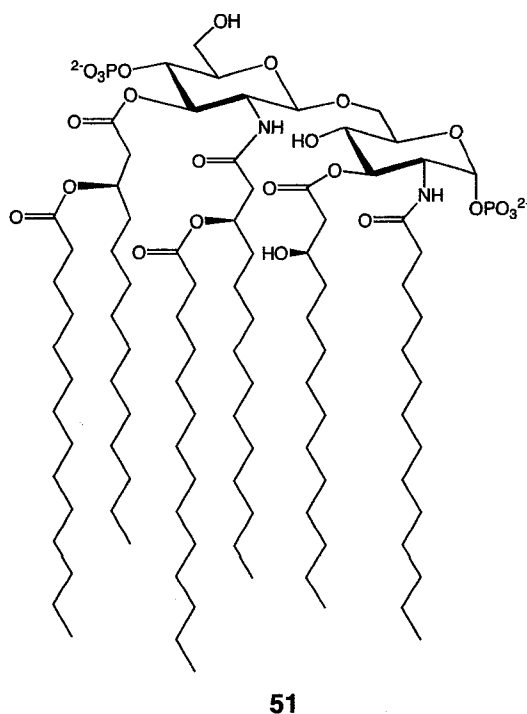
Although the polymyxins were one of the first classes of therapeutically important antibiotics to be identified, and at least 15 unique polymyxins have been described,<sup>71</sup> only polymyxin B is currently widely prescribed and studied.



#### 4. Polymyxin Mode of Action

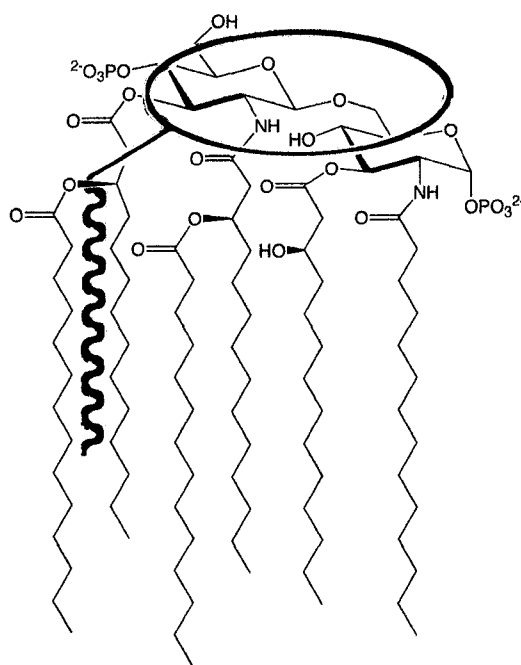
It has long been believed that polymyxins elicit their bactericidal effects by binding to and disrupting the action of lipopolysaccharide (LPS), the major antigen of the outer membrane of Gram-negative bacteria.<sup>72</sup> LPS contains three major structural components: Lipid A, a core oligosaccharide, and an outer polysaccharide composed of repeating hetero-oligosaccharide subunits. Lipid A (**51**) is a hydrophobic, lipid-rich moiety that harbors the endotoxic principle of LPS and is the most highly conserved part of the structure, containing two glucosamines, two phosphate esters, and six fatty acid chains (Figure 9).<sup>73</sup>

**Figure 9.** Lipid A monomer



The proposed binding model for the polymyxin-LPS conjugate involves ionic interactions between the side chain amino groups of the polymyxin peptide ring (positively charged at physiological pH) and the negatively charged phosphate groups of the lipid A disaccharide.<sup>74</sup> Also proposed to contribute to binding is the hydrophobic interaction between the nine carbon fatty acid side chain of the polymyxin and the fatty acid portion of lipid A (Figure 10).

**Figure 10.** Schematic representation of a generic polymyxin molecule (oval with tail) bound to lipid A



## RESULTS AND DISCUSSION

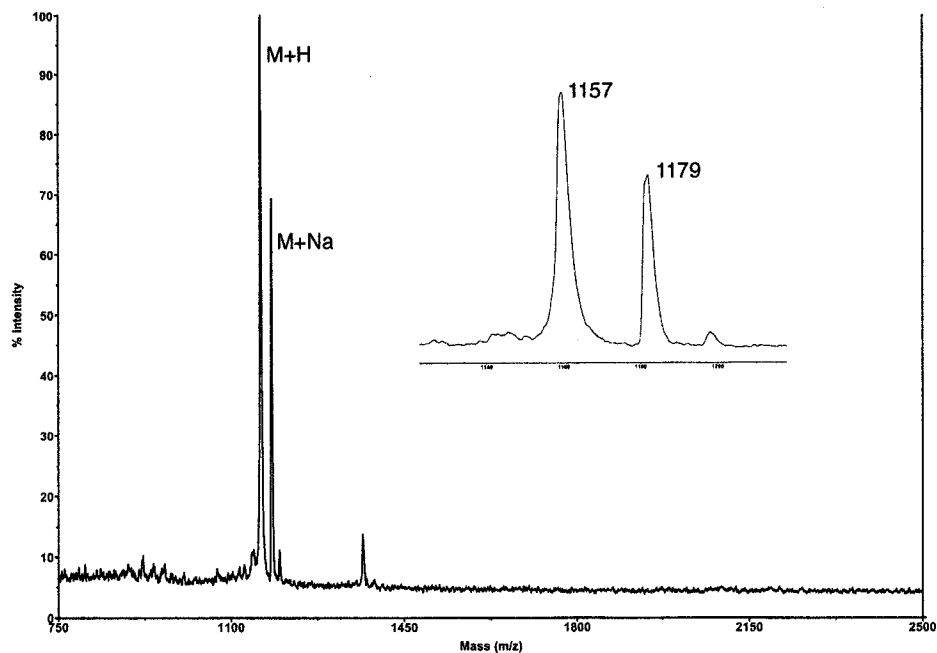
### 1. Isolation and Characterization of Mattacin

Initial investigations into the structure of mattacin did not immediately lead to the polymyxin family of peptide antibiotics. Standard peptide analyses, consisting of Edman degradation and amino acid analysis after HCl hydrolysis, were first performed.

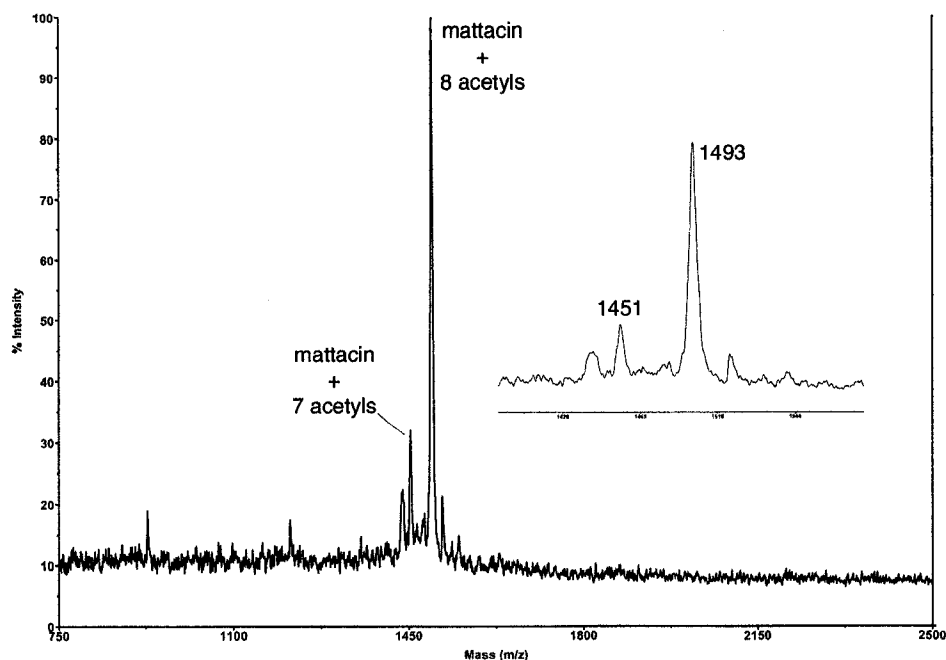
Attempts at Edman sequencing of the peptide failed, indicating the presence of an N-terminal blocking moiety. Upon strong acid hydrolysis of the peptide, however, detectable amounts of Leu, Thr, and a third non-proteinaceous amino acid (later identified as  $\alpha,\gamma$ -diaminobutyric acid) were observed. Attempts at partial hydrolysis of the peptide with either mild base or acid failed to yield fragments amenable to Edman sequencing.

#### 1.1 Mass Spectrometry

MALDI-TOF mass spectrometric analysis suggested a molecular weight of 1157  $\pm$  1 Da (Figure 11) for the native peptide.

**Figure 11.** MALDI-TOF mass spectrum of mattacin

With the knowledge that the peptide contained threonine residues, an acylation experiment was performed with acetic anhydride in the hope that the derivatized peptide might yield crystalline material suitable for X-ray crystallographic analysis. Although the acylated peptide was not crystalline, it was clear by mass spectrometry that 8 acylations had occurred, indicating eight nucleophilic moieties in the structure (Figure 12).

**Figure 12.** MALDI-TOF mass spectrum of mattacin octa-acetate

Extensive mass spectrometric analysis was then performed on the native peptide using MALDI-TOF tandem MS/MS techniques in an attempt to gain sequence information. This mass spectrometry work showed the presence of a number of amino acid residues with an experimental mass of 100.064 Da supporting a molecular formula of  $C_4H_8N_2O$ , thereby suggesting the presence of  $\alpha,\gamma$ -diaminobutyric acid moieties in the peptide. A high-resolution molecular ion  $MH^+$  value of 1157.7370 (monoisotopic) indicated a molecular formula of  $C_{51}H_{97}N_{16}O_{14}$ . Thus it became apparent that mattacin was likely a member of the polymyxin class of antibiotics.

## 1.2 NMR Spectroscopy

Complete structure elucidation of mactacin was achieved by use of NMR spectroscopy. Initial 1D and HH-COSY experiments confirmed that mactacin belonged to the polymyxin group of peptide antibiotics by revealing the presence of eleven amide protons and ten alpha protons (Figures 13 and 14) as well as the fatty acid side chain.

**Figure 13.** 1D  $^1\text{H}$  NMR spectrum of mactacin with expansion of amide region<sup>a</sup>

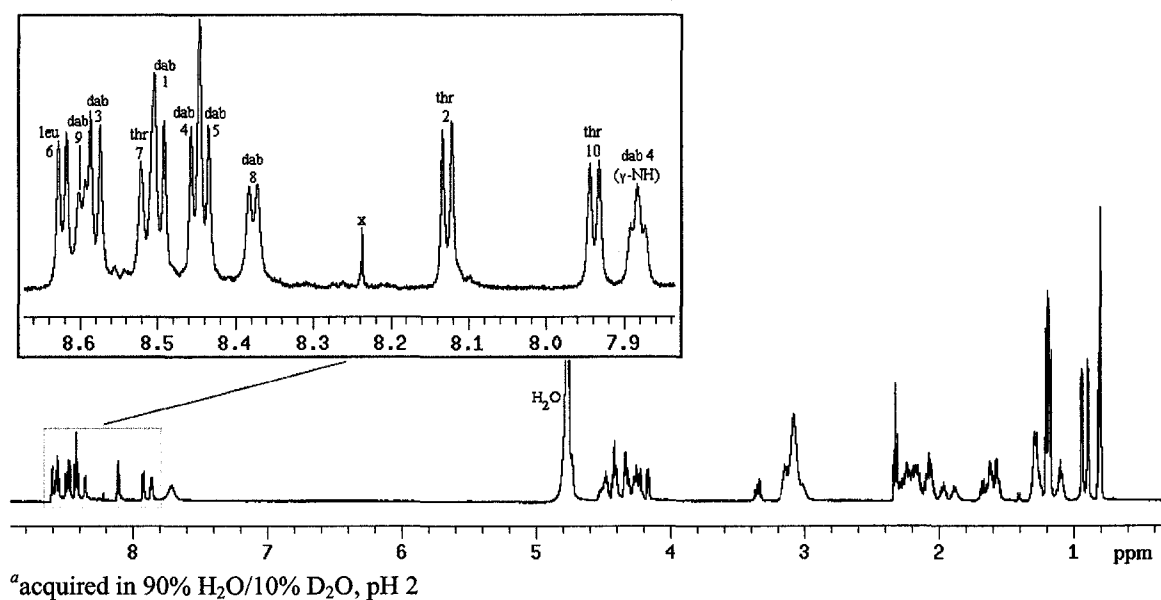
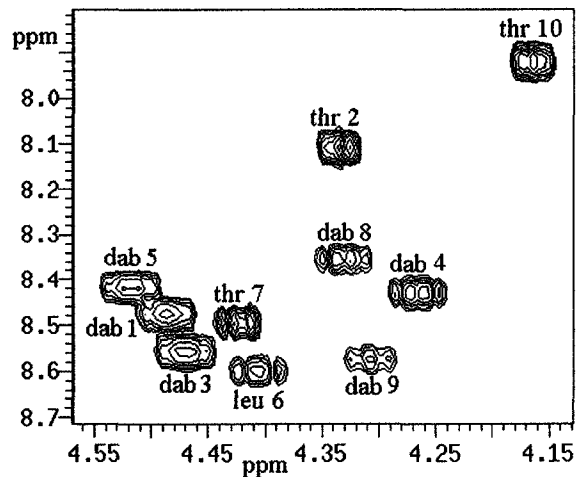
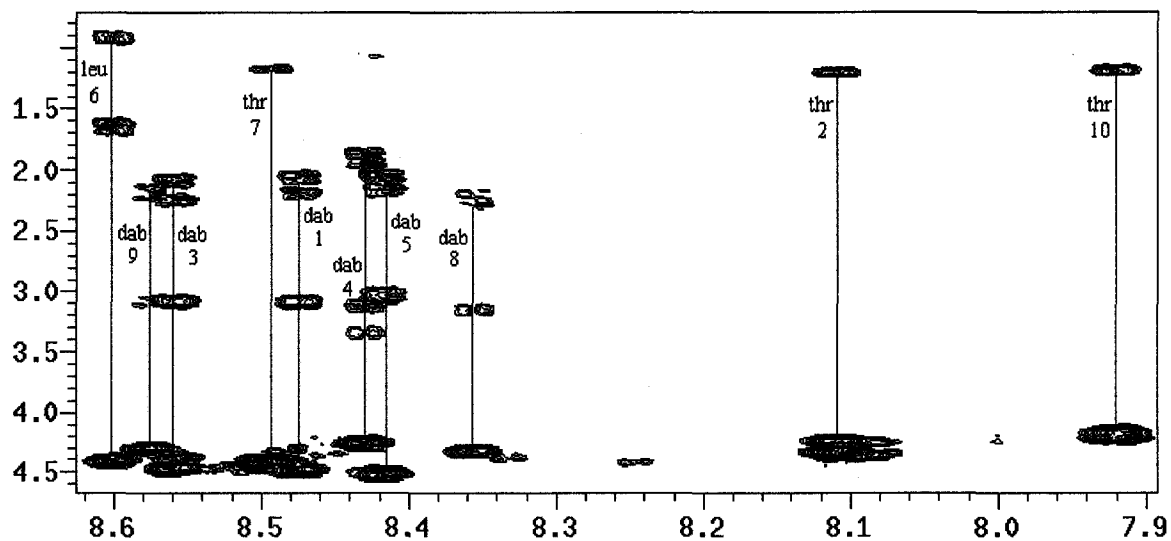


**Figure 14.** HH COSY identifying H $\alpha$ /HN correlations



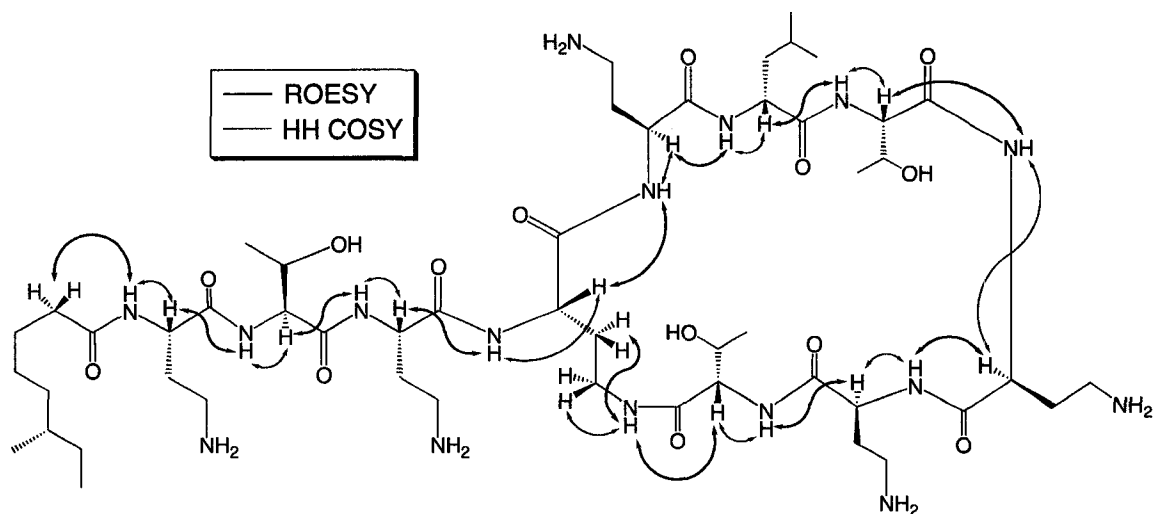
The spin systems in the TOCSY spectrum of mattacin were assigned to the respective residues by taking into consideration the characteristic frequencies and numbers of resonances (Figure 15).

**Figure 15.** TOCSY spectrum identifying spin system for all ten residues



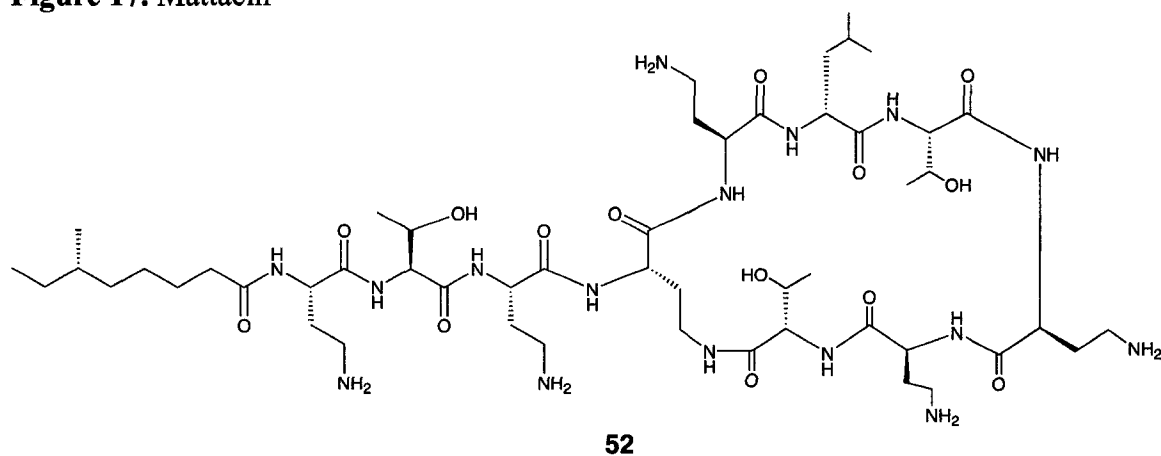
Sequential assignment of the peptide was achieved using  $d_{\alpha M}(i, i+1)$  connectivities in the ROESY spectrum and connectivities suggested by the HH-COSY spectrum (Figure 16).

**Figure 16.** Connectivities observed in ROESY and HH-COSY spectra leading to sequence assignment in mattacin



It was then shown that mattacin **52** is identical to polymyxin M, an uncommon polymyxin antibiotic previously reported in the Russian literature (Figure 17).<sup>75-78</sup>

**Figure 17.** Mattacin





Preliminary information regarding the solution conformation of mattacin was obtained by performing a series of 1D NMR experiments at various temperatures (ranging from 27 to 42 °C). This standard peptide NMR technique is used to assess the temperature dependencies of amide proton chemical shifts. Specifically, amide protons that are least affected by temperature change are likely shielded from solvent by participation in intramolecular hydrogen bonding. The results indicate that two of the ring-amide protons (Dab 4 $\gamma$  and Dab 8) in the mattacin heptacycle are shielded in this manner (Table 4).

**Table 4.** Temperature coefficients of mattacin amide proton chemical shifts

Residue*	Temperature coefficient (10 <sup>-3</sup> ppm/K)
Dab 1	-7.8
Thr 2	-5.3
Dab 3	-6.5
Dab 4	-5.6
Dab 4 $\gamma$	<b>-3.9</b>
Dab 5	-4.8
Leu 6	-5.6
Thr 7	-7.1
Dab 8	<b>-2.6</b>
Dab 9	-4.7
Thr 10	-5.5

*\*Coefficients marked in bold indicate amides protected from solvent.*

As is common for small peptides, mattacin exhibits considerable conformational flexibility when pure in solution, as shown by the absence of extensive long range NOE

interactions. Recent NMR investigations by Kidric and Pristovsek<sup>79</sup> have shown that two of the amide protons in the polymyxin B heptacycle participate in intramolecular hydrogen bonding as well. In mattacin it was observed that the amide protons of Dab 8 and the side chain of Dab 4 are both shielded, as in polymyxin B (Table 4). These results suggest that mattacin and polymyxin B, while containing some structural differences, are both expected to be highly flexible and adopt similar conformations in solution.

### 1.3 Stereochemical Analysis

To verify the stereochemistry of each residue present in mattacin, a sample of the peptide was hydrolyzed and the resulting free amino acids were derivatized to their corresponding *N*-pentafluoropropanamide - isopropyl esters for analysis using chiral phase GC-MS. From the analysis it was clear that all three threonines were of the L configuration (D-isomer  $R_t = 10.8$  min, L-isomer  $R_t = 11.2$  min) as were all six  $\alpha,\gamma$ -diaminobutyric acid residues (D-isomer  $R_t = 30.6$  min, L-isomer  $R_t = 31.1$  min). The sole leucine residue had the D configuration (D-isomer  $R_t = 15.5$  min, L-isomer  $R_t = 16.3$  min). A sample of polymyxin B, derivatized and analyzed in the same manner (to serve as a secondary standard), gave results in complete agreement with the known stereochemistry for each residue. Thus the sequence, constituent amino acids, lipid portion, and connectivity of mattacin were identical to the structure proposed earlier by Russian workers for polymyxin M,<sup>75-78</sup> although no conformational information or detailed comparison to polymyxin B were reported.

## 2. Mattacin Spectrum of Activity and Comparison with Polymyxin B

After isolating suitable quantities of mattacin from fermentation and polymyxin B from commercial sources, our collaborators (Randy Worobo and Haijing Hu) performed a series of inhibition assays against a variety of organisms. Live-cell deferred inhibition assays show that the mattacin producer *P. kobensis* M inhibits numerous Gram-positive and Gram-negative species including, among others, *E. coli* ATCC 33150, *Salmonella* Rubislaw, and *Listeria monocytogenes*, but fails to inhibit *Pediococcus acidilactici*. Purified mattacin and polymyxin B show the same inhibition spectrum as live cells of *P. kobensis* with the exception that they both failed to inhibit the strains of *Listeria* and *Bacillus* tested (Table 5).

**Table 5.** Antimicrobial spectrum of live *P. kobensis* M and purified polymyxins

Indicator Strain	Live <i>P. kobensis</i> M	MIC ( $\mu$ M)	
		Mattacin	Polymyxin B
<i>E. coli</i> BF2	+	3	25
<i>E. coli</i> O157:H7 380-94	+	6	25
<i>E. coli</i> O157:H7 933	+	12.5	12.5
<i>E. coli</i> O157:H7 3081	+	12.5	50
<i>E. coli</i> O157:H7 ATCC 33150	+	12.5	25
<i>E. coli</i> O157:H7 ATCC 25922	+	6	12.5
<i>Yersinia enterocolitica</i>	+	3	6
<i>Klebsiella pneumonia</i>	+	12.5	50
<i>Shigella sonnei</i>	+	3	12.5
<i>Alcaligenes faecalis</i> ATCC 8750	+	12.5	50
<i>Pseudomonas putida</i> D3375	+	12.5	25
<i>Pseudomonas fluorescens</i>	+	12.5	25
<i>Pseudomonas aeruginosa</i>	+	100	100
<i>Salmonella enterica</i> serovar Typhimurium 14028	+	12.5	25
<i>Salmonella enterica</i> serovar Rubislaw F2833	+	25	25
<i>Salmonella enterica</i> serovar Gaminara 140665	+	25	50
<i>Acinetobacter baumannii</i>	+	12.5	25
<i>Vibrio parahaemolyticus</i> G1-166	+	12.5	-
<i>Vibrio parahaemolyticus</i> G1-172	+	12.5	25
<i>Alicyclobacillus acidoterrestris</i> VF	+	50	100
<i>Listeria monocytogenes</i> 2289	+	-	-
<i>Listeria innocua</i>	+	-	-
<i>Listeria ivanovii</i>	+	-	-
<i>Bacillus subtilis</i> ATCC 6633	+	-	-
<i>Bacillus cereus</i>	+	-	-
<i>Pediococcus acidilactici</i>	-	NT	NT

+, inhibition; -, no inhibition; NI, no inhibition up to 100  $\mu$ M; NT, not tested

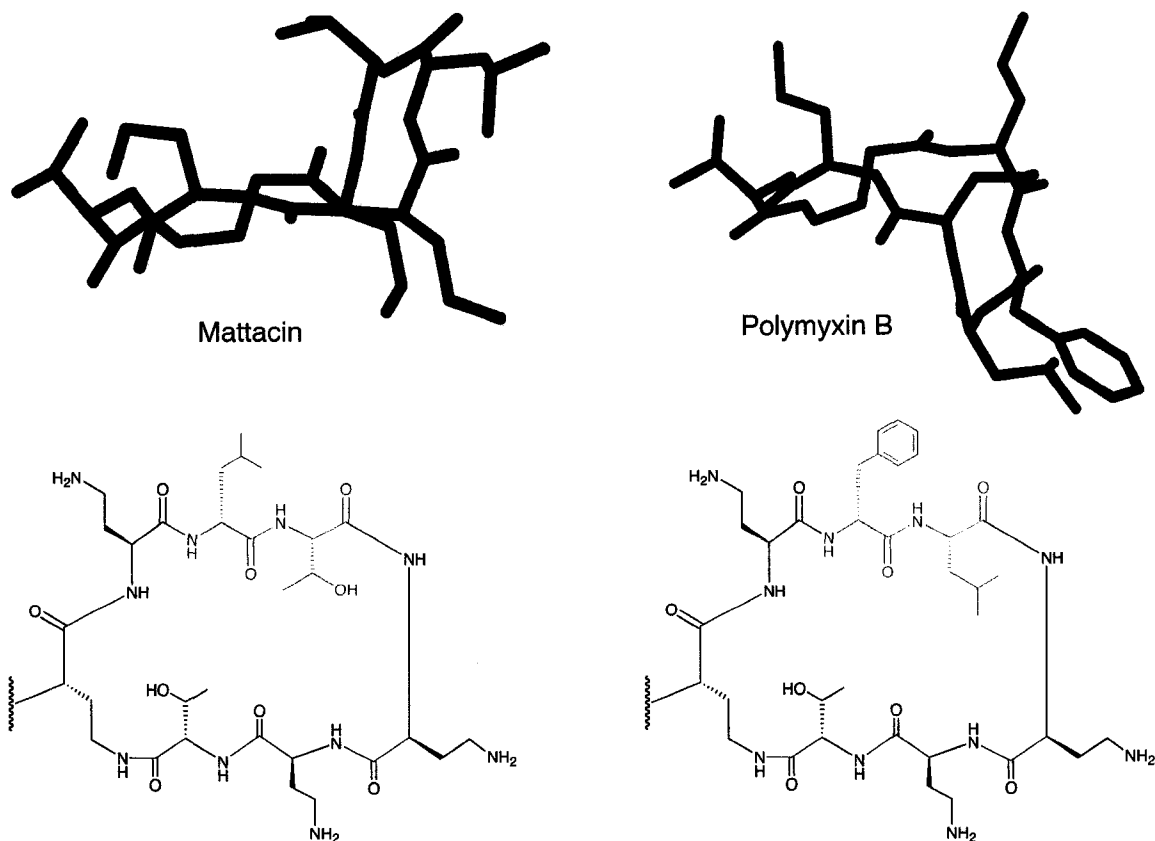
Results from the activity assays for both mattacin and polymyxin B show that the two peptides have virtually indistinguishable spectra of activity. Mattacin does appear to be slightly more active in most cases, but these differences are not very significant (less than an order of magnitude).

### **3. Mode of Action**

#### **3.1 LPS Binding and Induced Conformation of Mattacin by tNOE NMR**

Using 2D transferred NOE NMR techniques, Kidric and Pristovsek<sup>79</sup> recently investigated the preferred conformation(s) induced in polymyxin B when in solution with LPS isolated from *E. coli*. Their results indicate that although the peptide is highly flexible, the side chains of Dab 4 and 8 are in close proximity while bound to LPS. The same transferred NOE experiments described by Kidric and Pristovsek were performed with a mattacin/LPS mixture also revealing a number of NOEs for the heptacyclic region of the peptide that were not visible prior to the addition of LPS. These NOEs (62 total) were used to produce a conformational model for comparison to that of polymyxin B.<sup>79</sup> Upon interaction with LPS, mattacin adopts a chair-like conformation with the side chains of all three Dab residues pointing downwards from those of Thr 6 and Leu 7 (Figure 18).

**Figure 18.** Conformational model of mattacin and polymyxin B heptacycles based on tNOE data obtained from mattacin/LPS mixture



*Residues in red are different for the two peptides.*

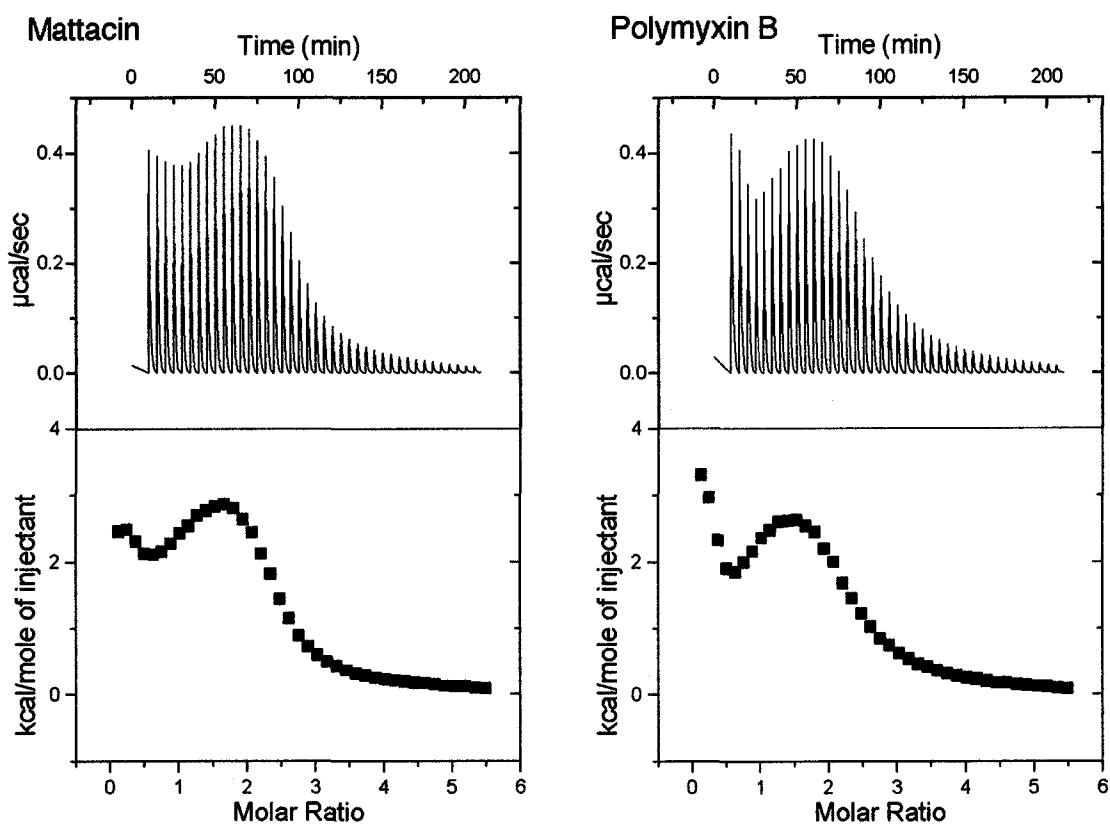
However, these experiments with mattacin and the same LPS preparation used by Kidric and Pristovsek, did not display the same correlations. The conformational model suggested by the results is in fact somewhat different than that of polymyxin B (Figure 18). While the side chains of all three Dab residues contained in the heptacycle are on the opposite side of the molecule from the hydrophobic Phe and Leu side chains in the polymyxin B structure, the bend in the mattacin heptacycle is in the opposite direction. This results in a less dramatic separation of hydrophobic and hydrophilic sidechains.

Whether this result is due to our experiment not detecting the critical NOEs seen for polymyxin B, or whether the conformational differences have an explanation owing to the structural differences is not clear. Mattacin is significantly different at residues 6 and 7 (D-Leu, L-Thr) compared with the corresponding residues in polymyxin B (D-Phe, L-Leu). It is in this region of the heptacycle that the greatest conformational variation in the two models is observed, and it seems reasonable to suggest that the significantly different hydrophobic/hydrophilic residues present in the two peptides contribute to these deviations.

### **3.2 LPS/Mattacin Association Energetics by Isothermal Titration Calorimetry**

To ascertain whether mattacin behaves in a manner similar to polymyxin B in its interaction with LPS,<sup>80</sup> isothermal titration calorimetry (ITC) was also employed. In separate experiments, the peptides were titrated into a solution of LPS and the heats of binding were monitored. The results of these binding assays are complex. However, it is evident that both peptides bind LPS in almost identical fashion. The binding isotherms are virtually indistinguishable (Figure 19) and suggest that both peptides are interacting with the same receptor site(s) present in LPS. The results do not support a simple 1:1 interaction, but rather a model with a high probability of identical stoichiometry and a series of sequential binding events.

**Figure 19.** Binding isotherms resulting from the titration of LPS with mattacin and polymyxin B



The thermodynamics of polymyxin B binding to LPS have been previously investigated using ITC by the group of Surolia.<sup>80</sup> In those studies, a highly processed LPS preparation from *E. coli* was used (extensive treatments with proteases, chelating agents, and purifications via dialysis and size exclusion chromatography). Using such conditions, which lead to smaller fragments of LPS, Surolia obtained results supporting a simple 1:1 binding between polymyxin B and LPS. For the mattacin study a LPS preparation isolated from the same *E. coli* strain was used, but without extensive processing because the primary interest was a comparison of mattacin with polymyxin B and their respective



binding to unmodified LPS. The same stock LPS solution and concentrations were used for the ITC experiments with both mattacin and polymyxin B. As seen in Figure 19, the binding isotherms for both peptides are almost indistinguishable. The data sets do not lend themselves to simple binding models and the ORIGIN software<sup>81</sup> used in the analysis could only fit the data by employing a complex sequential binding model. Initial interaction of the polymyxins with unprocessed LPS appears to lead to disruption of tertiary structural arrangements, thereby exposing additional lipid A binding sites. The simple 1:1 binding of polymyxin B seen in previous experiments<sup>80</sup> with highly processed lipid A may be due to the predominance of smaller unglomerated units. Whether this form provides a more accurate model of what occurs with living bacterial cells remains uncertain. However, our results clearly suggest that mattacin binds to LPS in a similar manner as polymyxin B. Very recent ITC investigations into lipid A derivatives and their interactions with polymyxin B by Savage and coworkers<sup>82</sup> also suggest a more complex mode of binding.

#### **4. Conclusions**

Results from the various comparative studies of both mattacin and polymyxin B show that the mode of action of the two peptides is virtually indistinguishable.<sup>83</sup> An interesting observation in the activity assays is that all strains of *Listeria* and *Bacillus* are inhibited by the live cells of *P. kobensis* M, but purified polymyxins B and mattacin have no effect. This suggests that another compound(s) is produced by this organism which is either lethal to *Listeria* and *Bacillus* on its own, or acts in synergy with another substance,

possibly the polymyxin peptide, to elicit its killing effects. Many multiple-component bacteriocin systems are known to be produced by Gram-positive organisms, have been recently reviewed,<sup>56,84</sup> and are the focus of the next chapter. Future investigations aimed at determining whether *P. kobensis* M produces other novel antimicrobial compounds may help to more fully understand the organism's bacterial defense strategy. As a therapeutic agent, mattacin could likely be used in the same fashion as polymyxin B (primarily a topical antibiotic), which currently sells in excess of \$91 million (US) per year.<sup>85</sup>

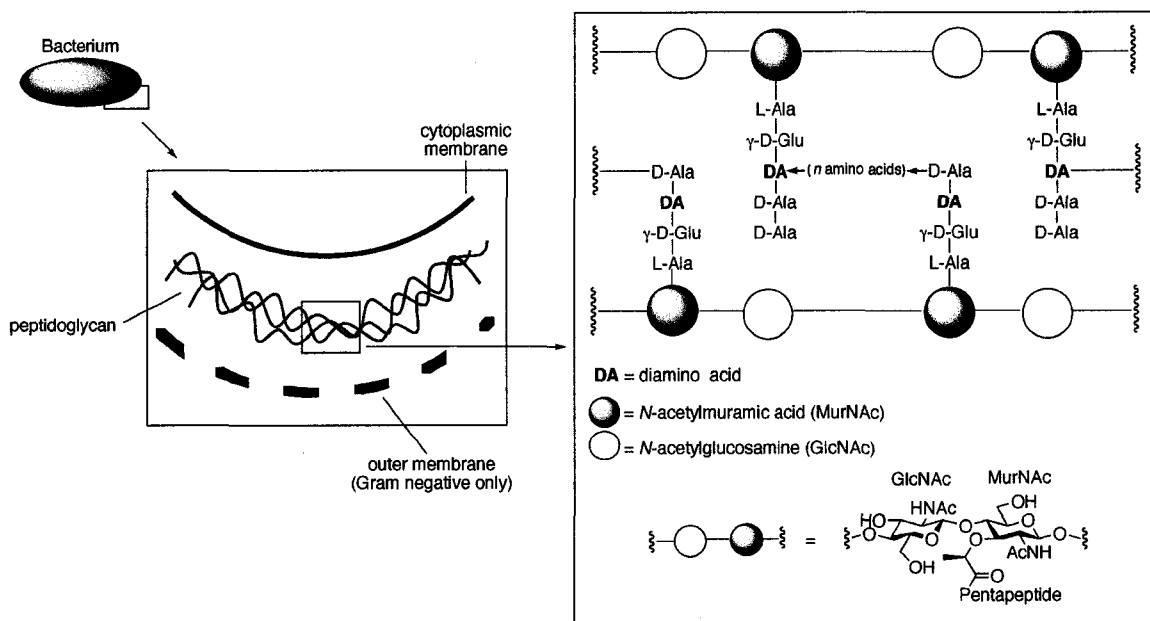
## CHAPTER 3. Structural Investigations of Lacticin 3147, a Two-Component Lantibiotic

### INTRODUCTION

#### 1. Bacterial Cell Wall Architecture and Traditional Antibiotics

Peptidoglycan (or murein) is a continuous covalent macromolecular structure which provides the strength and rigidity of the cell walls of both Gram-positive and Gram-negative bacteria (Figure 20).<sup>86,87</sup> From the time of their introduction through to today many of the most effective antibiotics have functioned by inhibiting peptidoglycan biosynthesis.

**Figure 20.** Schematic representation of peptidoglycan layer in bacterial cell wall



The ability to kill specific bacterial targets, however, has led many organisms to adapt by developing resistance to antibiotic therapeutics.<sup>88-90</sup> To combat antibiotic resistance new classes of therapeutics targeting a variety of cellular functions have been developed (Table 6).

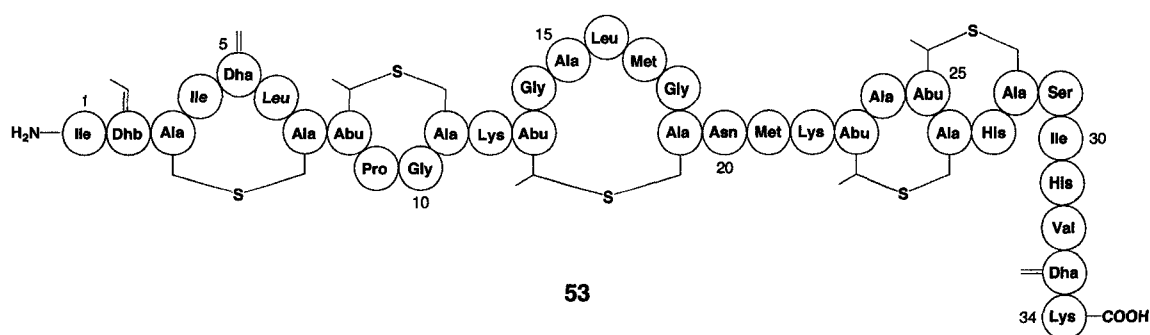
**Table 6.** Some common antibiotics and their cellular targets

<b>Drug Family</b>	<b>Function inhibited</b>
<b><math>\beta</math>-Lactams<sup>91</sup></b> Cephalosporins <sup>92</sup> Penicillins	Peptidoglycan biosynthesis
<b>Glycopeptides</b> Vancomycin <sup>93,94</sup> Teicoplanin	
<b>Aminoglycosides</b>	Protein synthesis
<b>Macrolides</b>	
<b>Oxazolidinones</b> Zyvox <sup>95-98</sup>	
<b>Streptogramins</b>	
<b>Tetracyclines</b>	
<b>Quinolones<sup>99-101</sup></b> Ciprofloxacin	DNA replication/transcription
<b>Rifamycins<sup>102,103</sup></b>	Transcription
<b>Sulphonamides<sup>104</sup></b>	Folate synthesis

## 2. Lantibiotic Two-Peptide Bacteriocins

In addition to conventional small molecule antibiotics, another class of antimicrobial agents called bacteriocins is slowly gaining recognition. Bacteriocins are bacterially produced peptides which display antimicrobial properties against other bacteria, often closely related to the producer strain.<sup>59,60</sup> The first bacteriocin was discovered in 1925,<sup>105</sup> and in the past twenty years there has been an increasing interest in such compounds as possible preservative agents for food and as potential supplements or replacements for currently used antibiotics. The ribosomal production of these small (2–6 kDa) antimicrobial peptides by Gram-positive bacteria, especially lactic acid bacteria, as a defense mechanism against other organisms is well documented and represents an intensive area of research.<sup>66,106</sup>

Among the known bacteriocins, two distinct families have emerged: the nonlantibiotics and the lantibiotics.<sup>107,108</sup> The latter contain the unusual amino acids lanthionine and  $\beta$ -methyllanthionine as part of additional intramolecular rings, and often possess other modified residues, frequently dehydro amino acids, which are formed after ribosomal translation. Nisin (**53**) (Figure 21) is the most highly studied lantibiotic<sup>109</sup> and illustrates these structural features.

**Figure 21. Nisin**

Currently used in food preservation worldwide, nisin is also being evaluated for use in a variety of other areas including antibiotic therapy.<sup>110-112</sup>

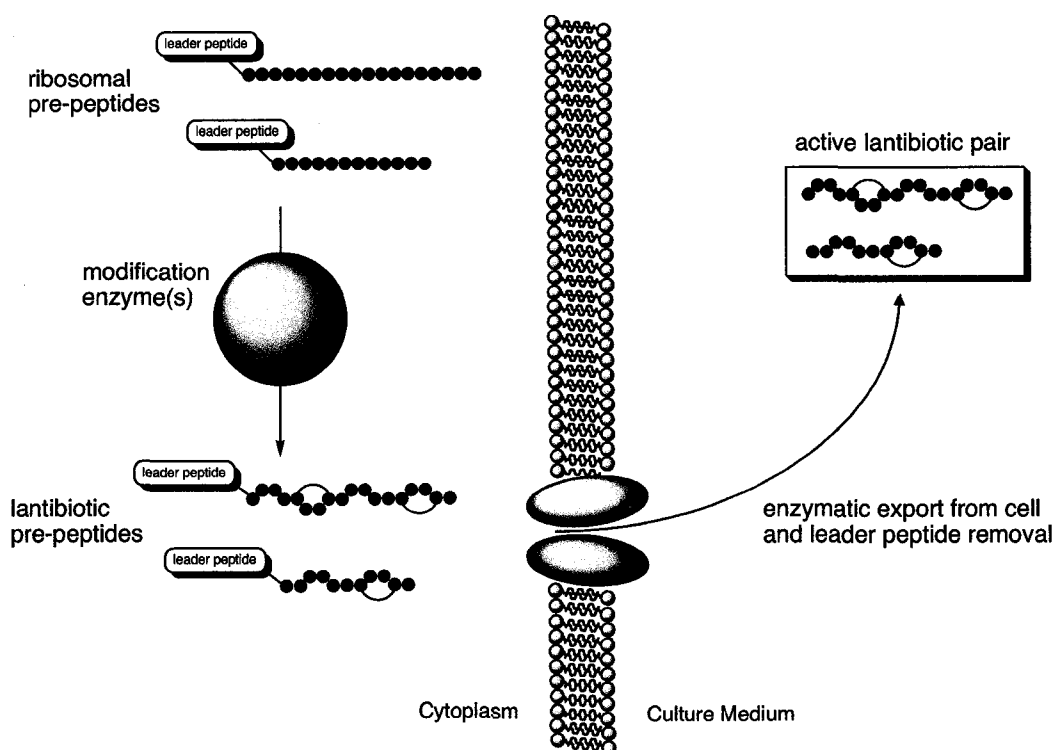
Both lantibiotic and nonlantibiotic bacteriocins are most often found as single active peptides, but a unique class of two-peptide systems, wherein both components act synergistically and are required for full activity, is now known. Two-component lantibiotic systems are rarer than their non-lantibiotic counterparts (the first two-component lantibiotic was reported in 1996<sup>113</sup>) and to date only 4 such systems are known.<sup>56</sup> Our efforts in this area have focused on the structural characterization of a new 2-peptide lantibiotic system, Lacticin 3147 originally identified by our collaborators (Paul Ross and Colin Hill, University College Cork, Ireland) in the late 1990's.<sup>114</sup>

## 2.1 Biosynthesis of Lantibiotics

The two-peptide lantibiotics are varied with respect to size, sequence and structure. These peptides, in contrast to the nonlantibiotics, are highly modified and are genetically encoded to contain many cysteine, serine, and threonine residues, which are

utilized in the post-translational formation of lanthionine bridges. They are ribosomally produced as prepeptides, which are enzymatically modified<sup>115</sup> followed by proteolytic removal of a leader peptide to generate the active species with concomitant export from the cell (Scheme 16).<sup>116,117</sup>

**Scheme 16.** Two-peptide lantibiotic production mechanisms

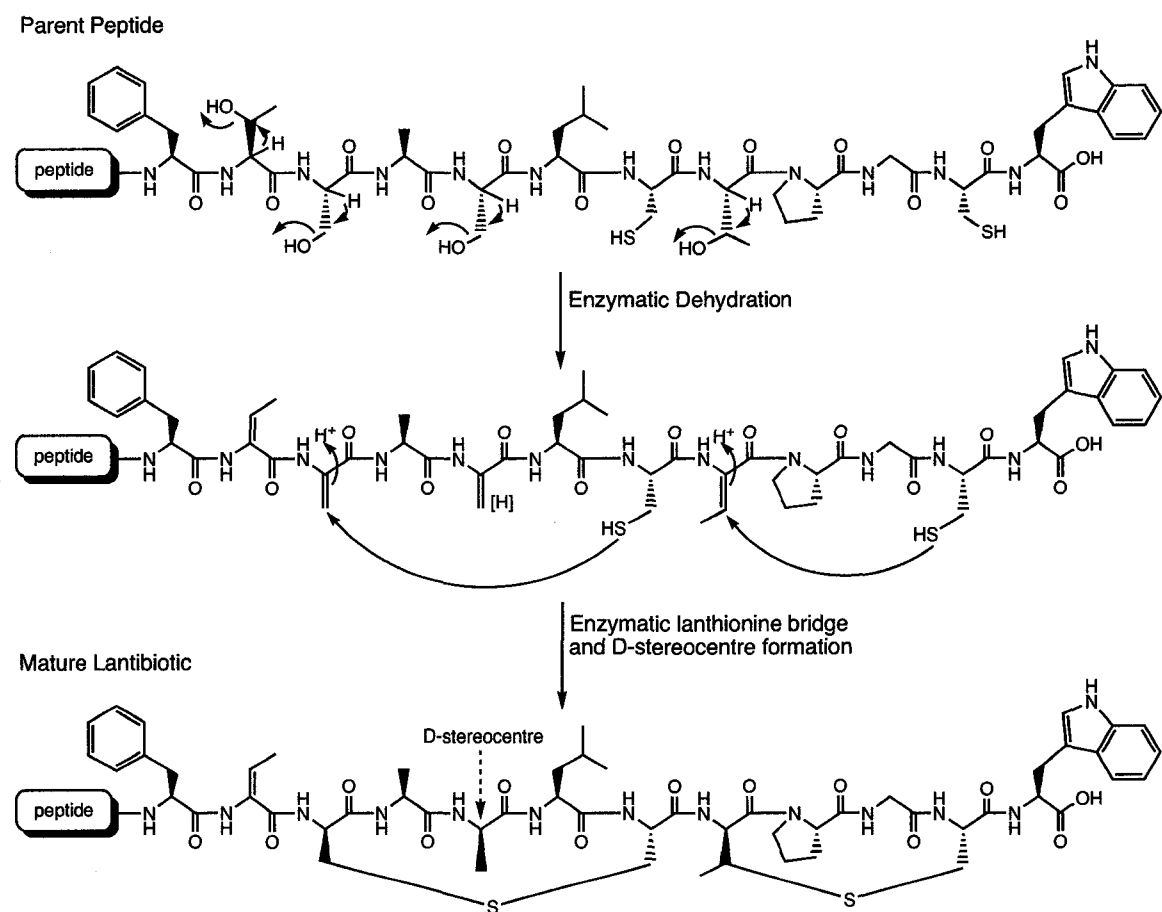


## 2.2 Lantibiotic Structural Features

In all lantibiotic peptides the initial enzymatic dehydration of a number of the serine and threonines present in the prepeptide yields an intermediate containing many dehydroalanine (Dha) and dehydroaminobutyric acid (Dhb) residues. The thiol moiety of a proximal cysteine side chain is then directed (in a stereospecific fashion) to condense

with one of the newly formed unsaturated sites via a 1,4-Michael addition.<sup>118,119,109</sup> The extent of dehydration and the number of cysteine side chains present, dictates the number of excess dehydro residues present after lanthionine bridge formation, with most lantibiotics in their mature form containing dehydro residues. However, in certain cases some of the remaining dehydro residues are enzymatically reduced,<sup>120</sup> to yield uncommon ribosomal peptides containing D-stereocentres (Scheme 17).

### Scheme 17. Lantibiotic peptide modifications

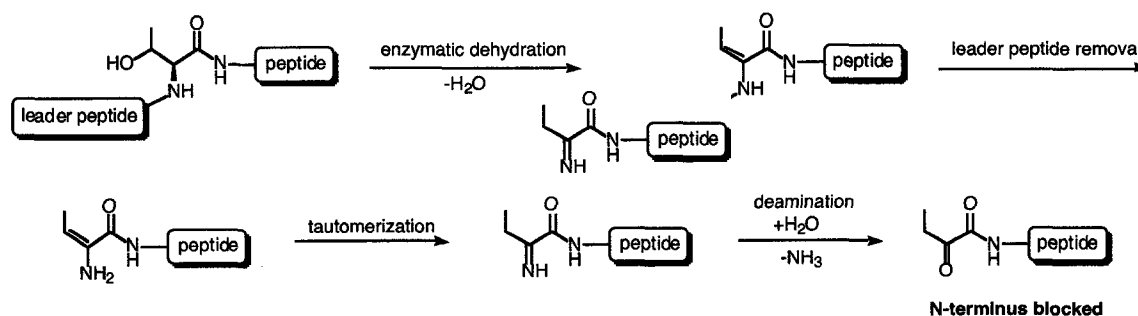


Other modifications found in lantibiotic peptides include formation of N-terminal  $\alpha$ -keto amides<sup>121</sup> and C-terminal ring formation by oxidative decarboxylation.<sup>122</sup> If the N-



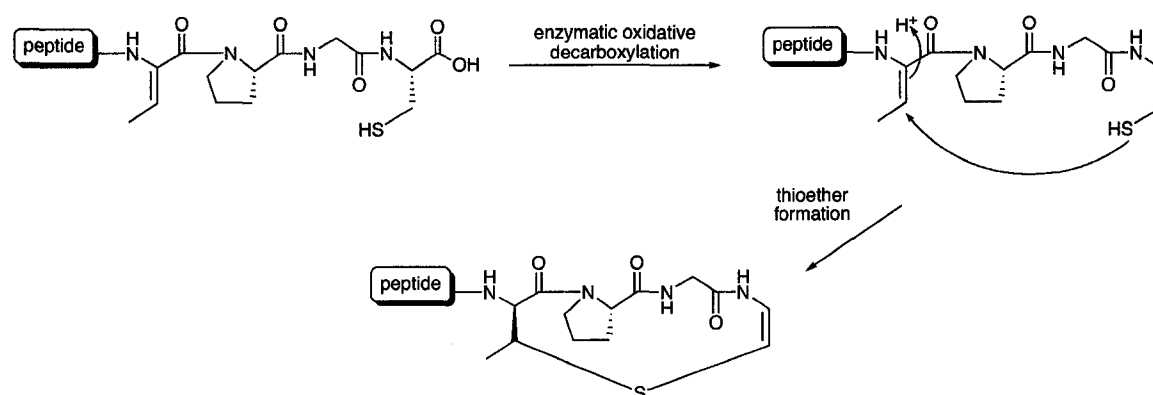
terminal residue (after removal of the leader peptide) is a dehydro residue it will spontaneously deaminate to yield an  $\alpha$ -keto-amide (Scheme 18).

**Scheme 18.**  $\alpha$ -Keto amide N-terminal blockage of lantibiotic peptides



In cases where a C-terminal cysteine residue exists, an enzymatic oxidative decarboxylation reaction may occur leading to a transient ene-thiol species which then condenses with a neighboring dehydro side chain to yield an unsaturated lanthionine ring (Scheme 19).<sup>123</sup>

**Scheme 19.** C-terminal cysteine oxidative decarboxylation and ring formation

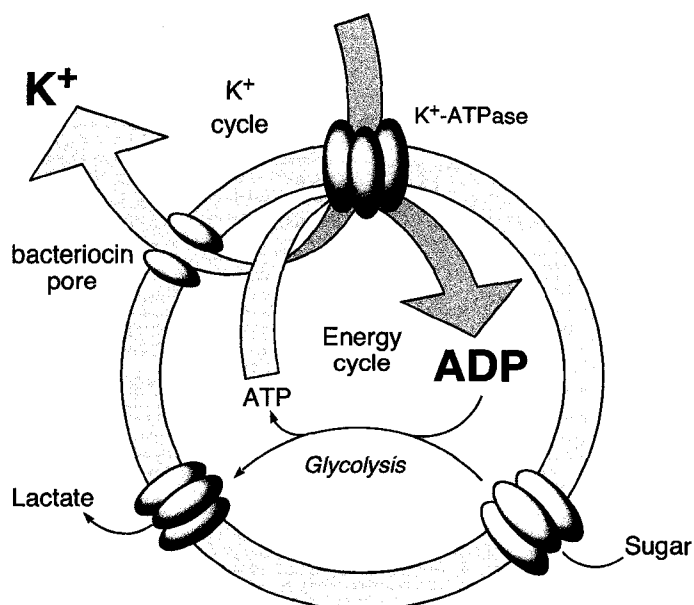


The unique structural features present in all lantibiotics make standard methods of peptide analysis, including the Edman degradation, difficult and often impossible.

### 2.3 Secondary Structure and Mode of Action of Lantibiotics

In all two-component systems studied to date, the optimal ratio of the synergistic peptides is approximately 1:1. For many two-peptide bacteriocins it has been shown that the bactericidal effect occurs as a result of permeabilization of the cell membrane.<sup>124</sup> This pore-forming ability causes cell leakage and the efflux of  $K^+$  ions leading to dissipation of membrane potential and inhibition of amino acid uptake. Cell death may be finally effected by a futile cycle of ATP-driven potassium uptake and bacteriocin mediated potassium release in combination with increased ATP hydrolysis by an ATPase<sup>125</sup> (Figure 22).

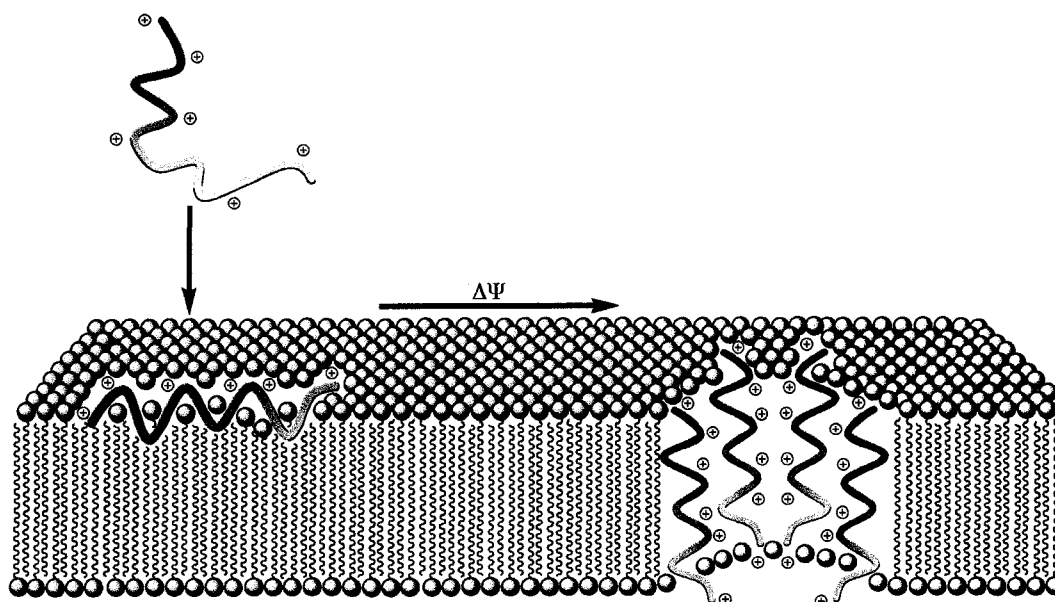
**Figure 22.** Model of cell killing by pore-forming bacteriocin



Due to the difficulties encountered in obtaining crystals and X-ray structures, conformational studies of lantibiotics have been confined to multidimensional NMR experiments and computer assisted modeling.<sup>126</sup> These studies have shown that in water, lantibiotic peptides (*e.g.* nisin A) often display high flexibility and are less ordered than might be expected considering the presence of multiple lanthionine bridges. In other solvents (trifluoroethanol or DMSO) or in the presence of micelles, however, the peptides appear to adopt the more ordered, amphiphilic structures expected for their membrane-depolarizing activity.<sup>127-129</sup> In certain unmodified (non-lantibiotic) single-peptide bacteriocins it has been shown that upon contact with membranes the otherwise random-coiled peptides adopt ordered helical structures.<sup>130</sup> The NMR solution structures of leucocin A and carnobacteriocin B2 in water and in structure-inducing solvents such as trifluoroethanol or dodecyl phosphocholine micelles illustrate this effect.<sup>131,132</sup>

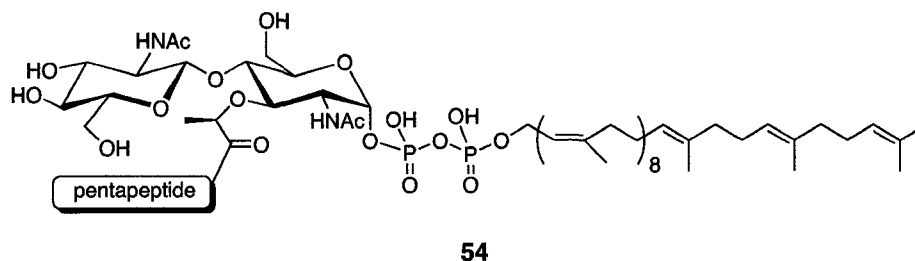
It has been widely proposed that the formation of such amphipathic helices is the critical conformational change required for pore formation by the barrel-stave or wormhole mechanism.<sup>133-136</sup> These mechanisms rely upon stabilizing interactions between membrane phospholipids and the cationic residues of the peptide allowing for insertion of hydrophobic regions into the outer leaflet of the membrane. Once associated with the membrane surface a number of the ordered bacteriocins could potentially aggregate. The bacteriocin complex can in principle completely span the membrane thereby forming a transient pore (Figure 23).

**Figure 23.** Barrel-stave/wormhole mechanism of pore formation by cationic bacteriocin



Recent work by Breukink and Sahl and their coworkers, however, has shown that the single-peptide lantibiotic nisin has a specific recognition for the peptidoglycan precursor lipid II **54** (Figure 24).<sup>137, 138</sup>

**Figure 24.** Lipid II

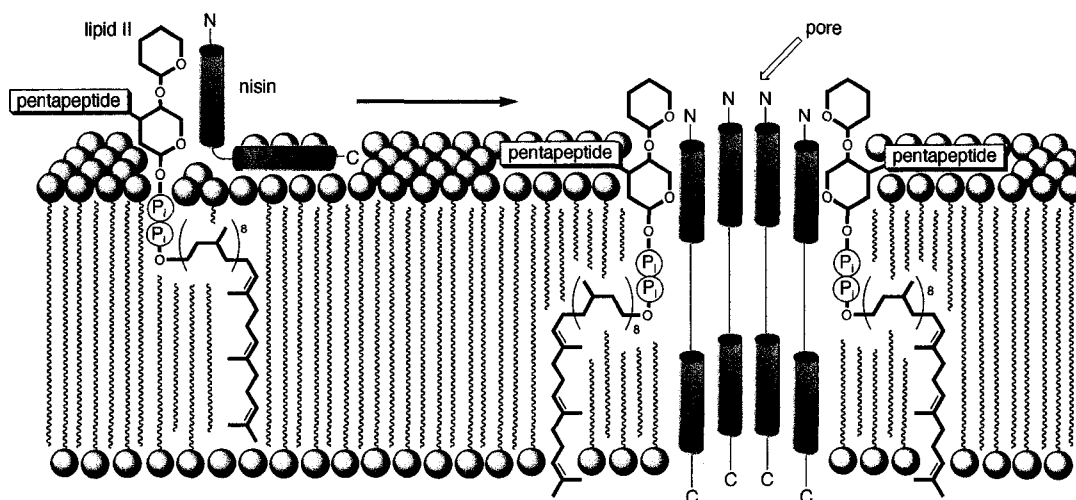


Although nisin does exhibit detergent-like pore forming abilities in artificial membranes, it was found that a much lower nisin concentration (*3 orders of magnitude*) could induce pore formation if an appropriate quantity of lipid II was incorporated into the artificial

membranes.<sup>138</sup> These observations offer an explanation for the differing sensitivities of various organisms based upon the lipid II content of their cell membrane. This type of receptor-based activity has also been proposed for non-lantibiotic single peptide bacteriocins such as leucocin A. Specifically, in the case of leucocin A, it is likely that a chiral recognition event is occurring as suggested by the observation that the enantiomeric peptide (constructed synthetically from D-amino acids), while identical to the natural peptide in all other respects, shows no antimicrobial activity.<sup>139</sup> Work by Héchard suggests that an extracellular portion of the mannose phosphotransferase system may be the target receptor for leucocin and other related bacteriocins.<sup>140</sup>

A recent proposal suggests that nisin displays a dual mode of action in lipid II mediated pore formation. By producing and testing nisin mutants, Sahl has shown that the N-terminal region of nisin is essential for lipid II recognition and prevention of peptidoglycan biosynthesis.<sup>68</sup> The C-terminal region of nisin and a flexible “hinge” region were then shown to be the essential pore-forming components (Figure 25).

**Figure 25.** Lipid II mediated pore formation by nisin



Examples of two-peptide lantibiotics are somewhat limited thus far, and of these systems only for lactacin 3147 have substantial efforts been reported to determine its cell killing effects and mode of action. Recent work by our collaborators (Ross and Hill) has shown that the optimal ratio of the two lactacin 3147 peptides is 1:1 with a MIC in the nanomolar regime (*unpublished results - personal communication*). It has also been shown that when combined, the lactacin 3147 peptides elicit their pore forming affects in target cells via lipid II recognition, as in the case of nisin. Upon permeabilization of the membrane a rapid efflux of  $K^+$  and phosphate ions is observed resulting in the dissipation of the proton motive force, hydrolysis of intracellular ATP, and ultimately cell death.<sup>141</sup>

#### **2.4 Lactacin 3147 Spectrum of Activity and Therapeutic Use**

The cytoplasmic membrane of Gram-positive bacteria is the primary target for the action of bacteriocins (Table 6). The outer membrane of Gram-negative bacteria, impenetrable to these antibiotic peptides, prevents their antimicrobial activity unless EDTA is added to enhance permeability. No two-component bacteriocins have been found to kill Gram-negative microorganisms. As a result, the inhibitory spectra of bacteriocins produced by Gram-positive bacteria might seem quite narrow. However, most two-peptide antimicrobial agents display activity against a wide variety of Gram-positive bacteria. Generally, nonlantibiotics have narrower spectra of inhibition than lantibiotics.

Lacticin 3147 inhibits the growth of a large range of Gram-positive bacteria. It is most potent towards staphylococci and streptococci.<sup>142</sup> The inhibition of streptococcal growth by lacticin 3147 has been shown to be useful in the treatment of bovine mastitis.<sup>142,143</sup> Lacticin 3147 is also active against a number of other bacterial (*Acetobacter*, *Bacillus*, *Clostridium*, *Enterococcus*, *Lactobacillus*, *Leuconostoc*, *Listeria*, *Pediococcus*, and *Staphylococcus*).<sup>144</sup> Tested for its sensitivity towards 54 strains of these various genera, lacticin 3147 was found to inhibit strains of lactococci commercially used in cheese making. Also active against *Listeria monocytogenes*, lacticin 3147 has proved to be effective as a protective culture in cottage cheese.<sup>145</sup> Most interestingly, lacticin 3147 is highly active against methicillin resistant *Staphylococcus aureus* (MRSA), vancomycin resistant *Enterococci* (VRE), penicillin resistant *Pneumococcus* (PRP), *Propionibacterium* and *Streptococcus mutans*.<sup>146</sup>

### **3. Project Objectives: New Methods for the Structure Elucidation of Lantibiotic Peptides**

In 1996 Ross and Hill identified a 2-component lantibiotic produced by *L. lactis* subsp. *lactis* DPC3147 which they termed lacticin 3147.<sup>114</sup> At the time, a partial purification and limited characterization of the antimicrobial peptides was achieved, after which our collaboration began with an aim to fully characterizing the active components.

The extensive modifications present in lantibiotics, as well as limited production of the active species by most producing organisms, present significant challenges to the

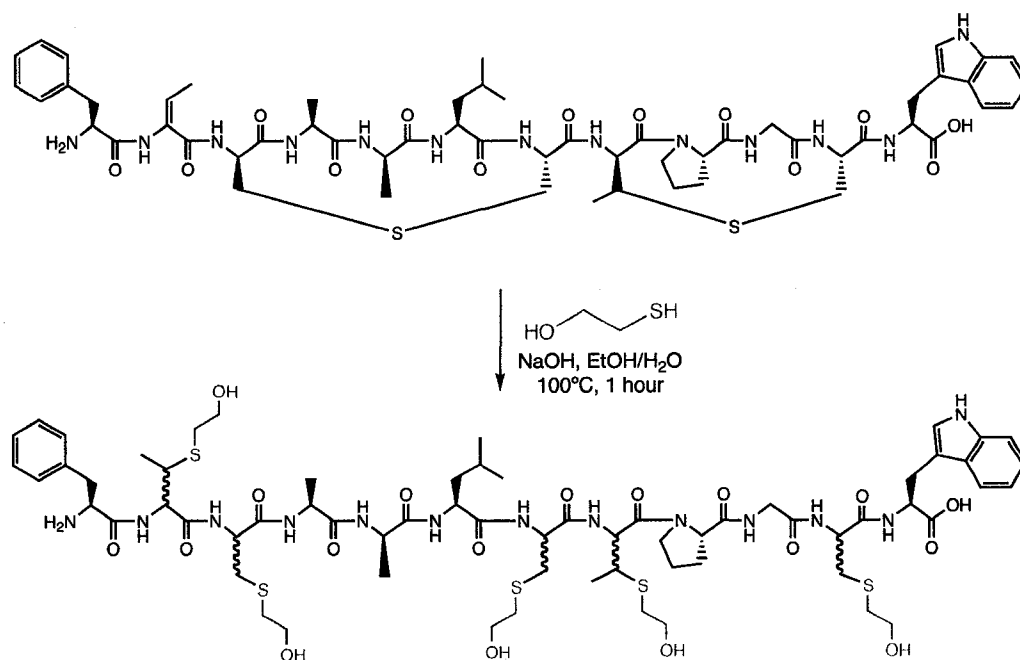
determination of primary structures. As mentioned above, standard analytical techniques, such as the Edman degradation, are often unsuccessful when investigating lantibiotics. Lanthionine bridges sequence poorly, yielding no detectable phenylthiohydantoin derivative, and dehydro residues within the peptide prevent sequencing once exposed at the N-terminus (presumably due to rapid deamination leading to a N-terminally blocked peptide). Also, the N-terminal  $\alpha$ -keto amide moiety found in some lantibiotics simply prevents any N-terminal sequencing.

No two-peptide, and only a small number of single-peptide, lantibiotics discovered to date have had their primary structures assigned. In all cases the final structural assignments have relied on multidimensional NMR.<sup>147-154</sup> In situations where the producing organism does not generate the milligram quantities of peptide required for NMR analysis the structure determination can be very difficult.

Early work on the structure elucidation of nisin and other lantibiotic peptides relied upon enzymatic or chemical cleavage strategies.<sup>155-158</sup> Such methods are often specific to the particular peptide and lack generality. For many lantibiotic peptides these cleavage approaches fail due to the unique structural properties of the peptide. A very limited number of more general methods have been developed by others,<sup>159</sup> which most often rely on thiol addition to convert both dehydro and lanthionine moieties to sequencer-friendly amino acids for Edman degradation (Scheme 20). While such methods are valuable, they are unable to give specific insights into the exact location of dehydro residues and the specific bridging patterns of lanthionine linkages.



**Scheme 20.** Thiol modification of lantibiotic peptide



Thiol modified peptide, fully sequenced by Edman degradation.  
 (modified residues indistinguishable as dehydro or lanthionine bridged in origin.)

The chemical modification strategies developed in our work target peptide sequencing via the Edman degradation but with differentiation of dehydro residues and those involved in lanthionine bridges. The methods described below have been successfully applied on minute quantities (*micrograms*) of nisin and both of the lactacin 3147 peptides. Our methodologies should make structure elucidation on the microscale viable for any lantibiotic.

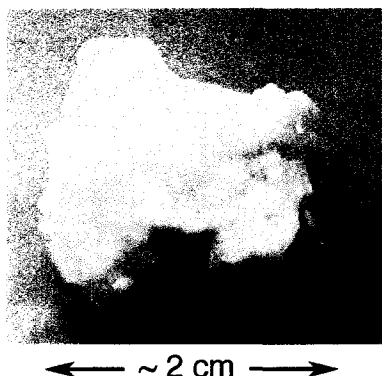
The second objective of the project was an improved isolation protocol providing access to greater quantities of the lactacin 3147 peptides to allow for structure elucidation by multidimensional NMR spectroscopy.

## RESULTS AND DISCUSSION

### 1. Isolation and Preliminary Characterization of Lacticin 3147

In the mid 1990's our collaborators (Ross and Hill) identified a new 2-peptide lantibiotic which they named Lacticin 3147.<sup>114</sup> The producing organism, *Lactococcus lactis* subsp. *lactis* DPC3147, had been obtained after screening a number of Irish kefir grains (Figure 26). Kefir grains have been used for generations in the production of Kefir, a fermented, probiotic milk beverage, and are indefinitely reusable.<sup>160</sup> Structurally comprised of protein, lipids, and a soluble polysaccharide (Kefiran), Kefirs are rich in a wide variety of lactobacilli, yeasts, and lactococci.<sup>161</sup>

**Figure 26.** Irish kefir grain

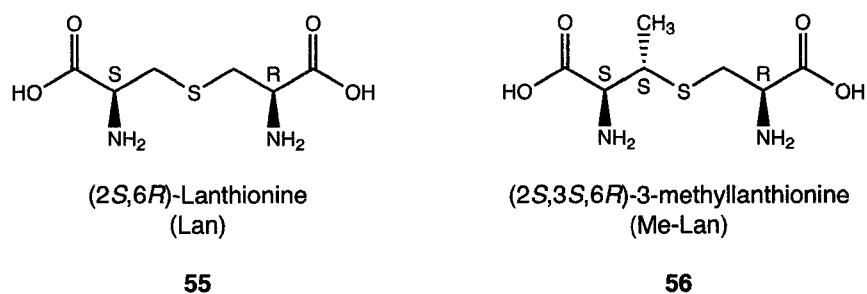


Based on the speculation that Kefir grains might contain bacteriocin-producing organisms (as an explanation for their longevity), a number of grains were collected from different regions of Ireland and assessed for antimicrobial activity. In four of the Kefirs studied identical lactococcal strains were found, each producing the bacteriocin later

identified as lacticin 3147.<sup>114</sup> After isolation and fermentation of the bacteriocin producing organism (*Lactococcus lactis* subsp. *lactis* DPC3147), two peptides, later termed lacticin 3147 A1 and A2, were isolated from the fermentation supernatant. These two peptides were identified as being responsible for a synergistic antibiotic activity against a wide array of Gram-positive organisms.<sup>162</sup>

Ross and Hill were also able to classify both lacticin peptides as lantibiotics based on the presence of lanthionine **55** and  $\beta$ -methylanthionine **56** in the acid hydrolysate mixture of both peptides.<sup>162</sup> These two unique amino acids are characteristic of lantibiotics and are enzymatically constructed in stereospecific fashion (Figure 27).<sup>119</sup>

**Figure 27.** Structures of lanthionine and  $\beta$ -methylanthionine

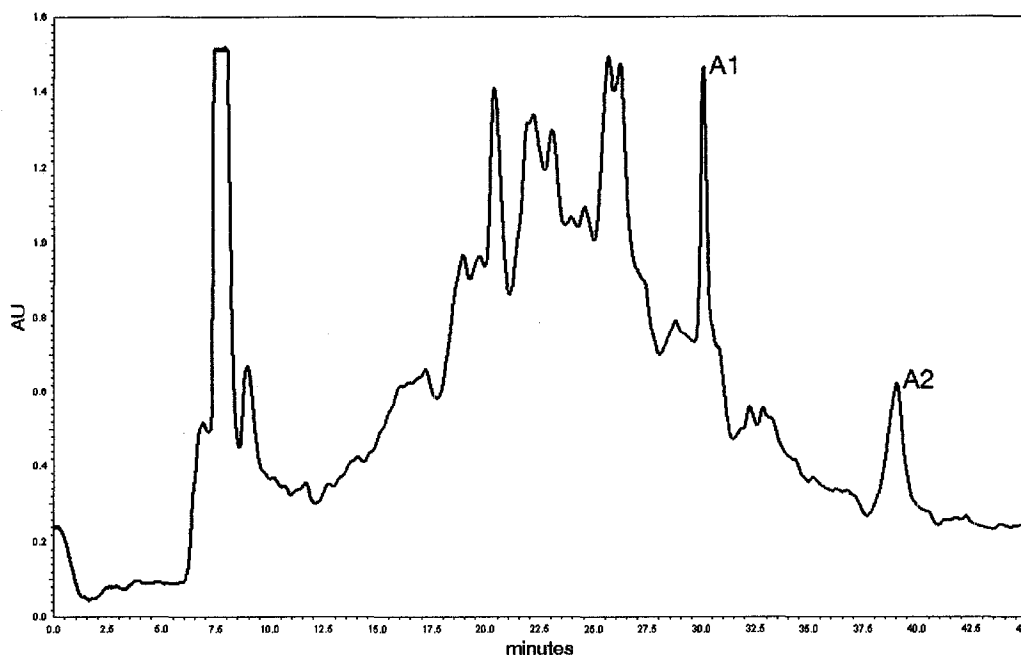


It was at this point that our collaboration began with the ambition of completing the structure elucidation of both of the lacticin 3147 peptides.

## 1.1 Mass Spectrometry and Preliminary Structural Features

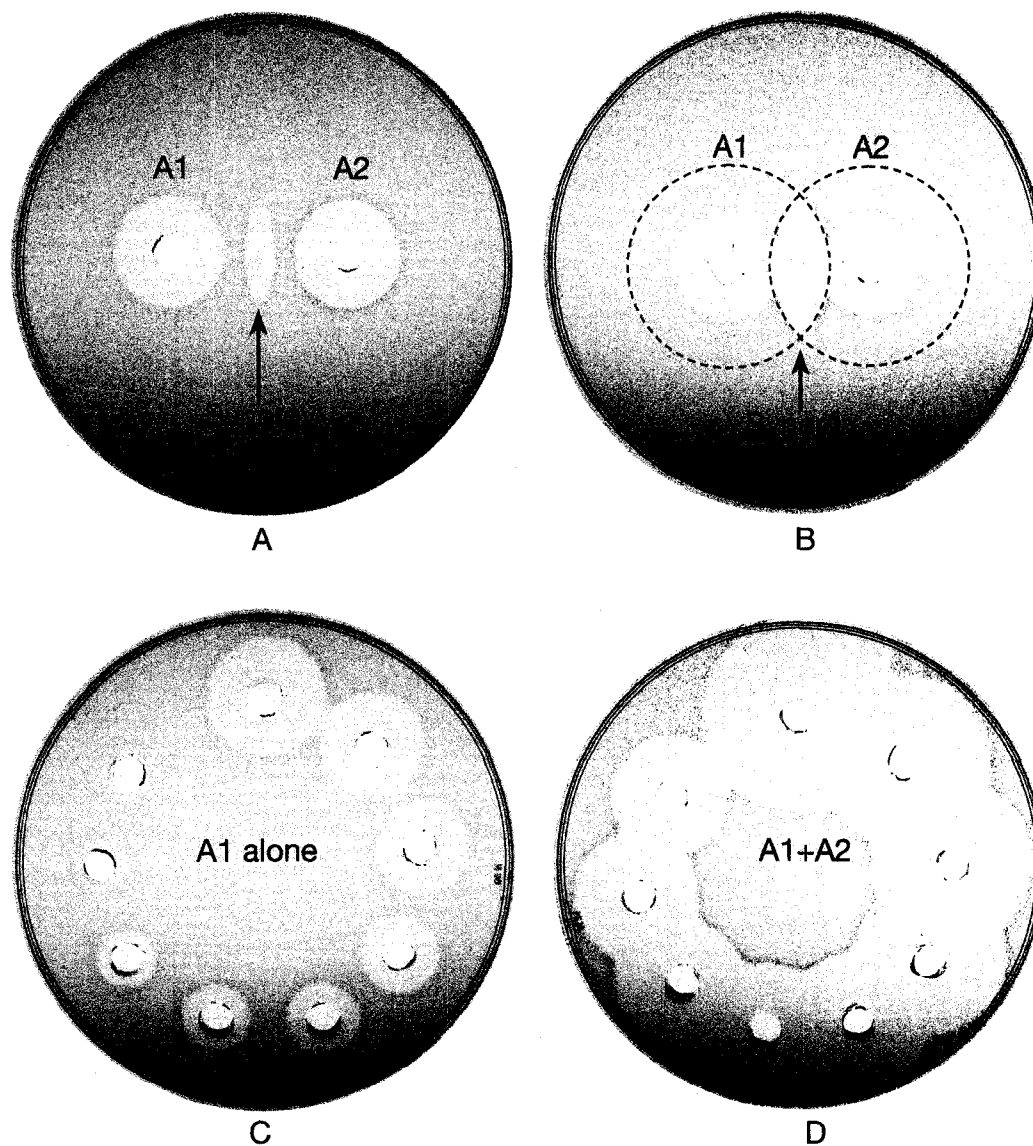
Initial isolation of the peptides in our laboratory focused on the fermentation supernatant. After overnight fermentation of the producing organism and cell removal by centrifugation, the lacticin peptides were recovered from the supernatant by a series of chromatographic procedures. The final HPLC step separated the lacticin peptides from one another and removed a large number of hydrophobic impurities (Figure 28).

**Figure 28.** HPLC separation of lacticin 3147 A1 and A2 peptides



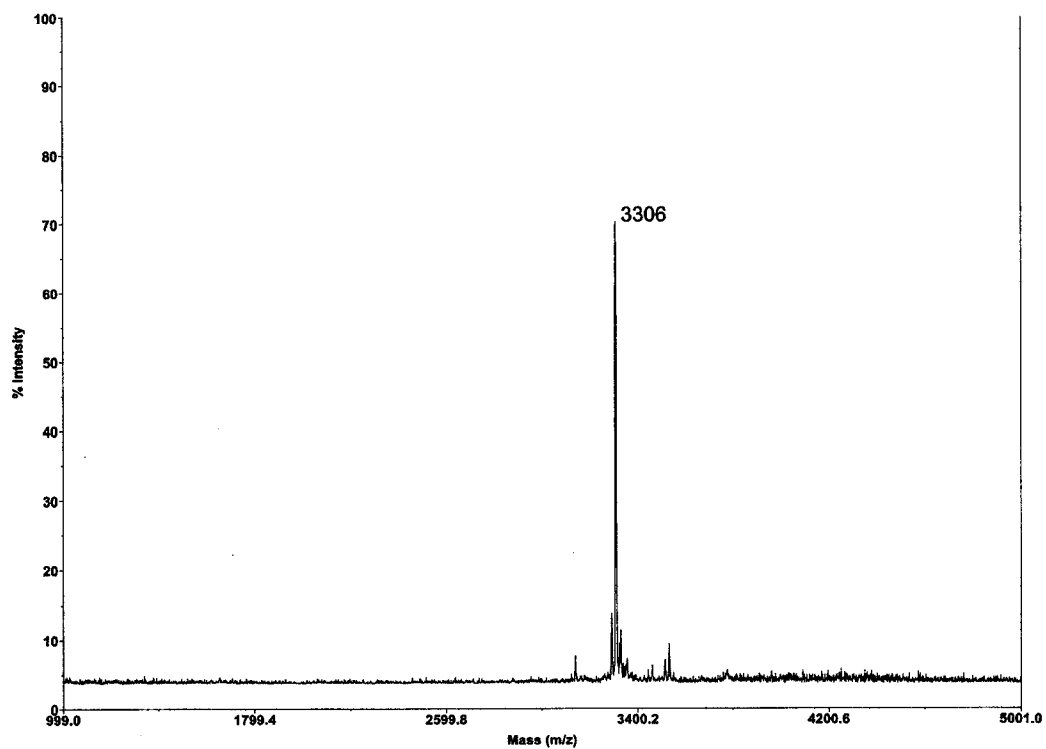
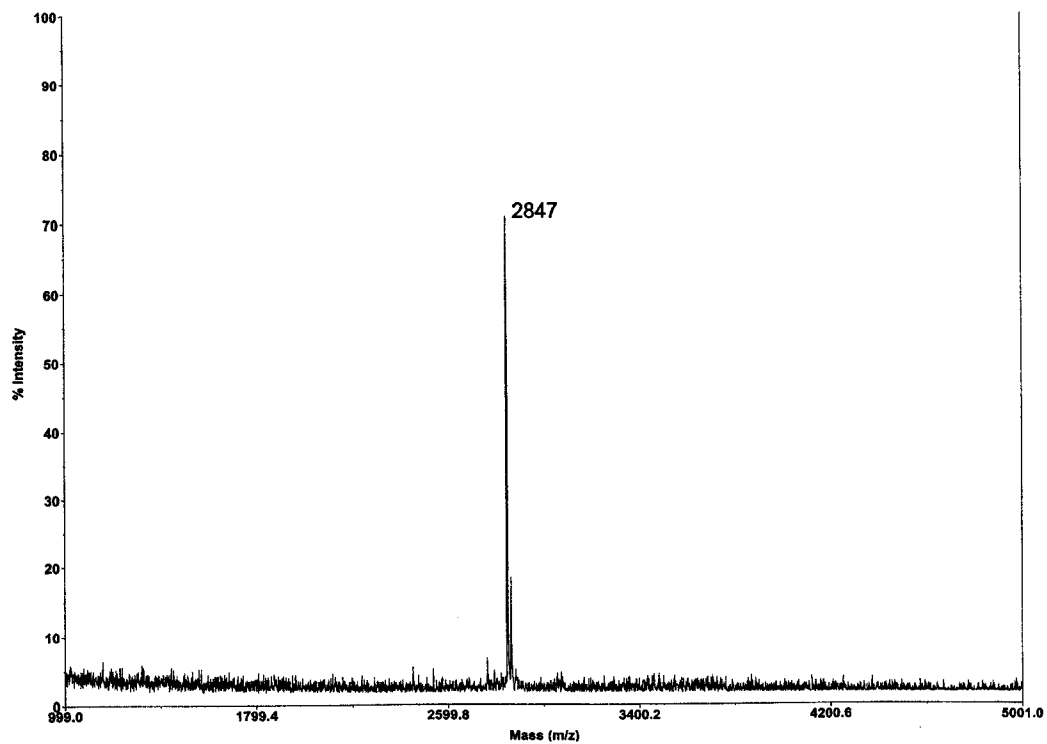
Once purified and separated, the antimicrobial activity of each lacticin peptide was assessed showing that both the A1 and A2 peptide maintain some degree of activity in isolation. When combined, however, the biological activity is drastically increased (Figure 29).

**Figure 29.** Complementary activity of lacticin A1 and A2 against *Lactococcus lactis* subsp. *cremoris* HP



The first two assays (A and B) show the synergy of the peptides as they are spotted side-by-side to form an inhibition zone wherein the two peptides have diffused together. The third assay (C) shows a serial, two-fold, dilution of the A1 peptide alone and the fourth assay (D) contains the same serial dilution of the A1 peptide with the addition of a matching quantity of the A2 peptide in each well.

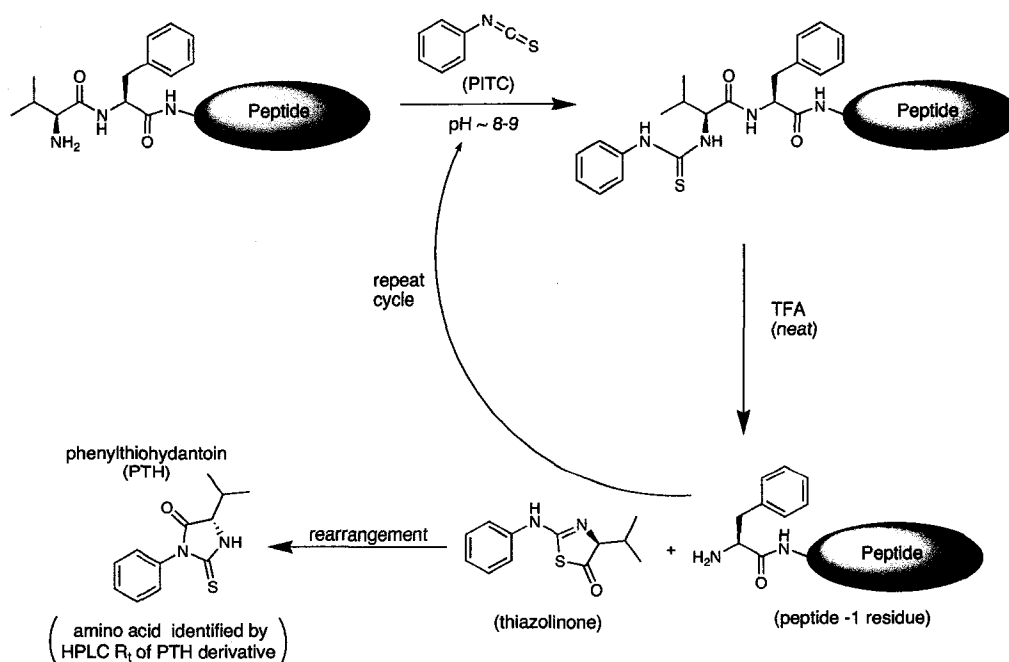
MALDI-TOF mass spectrometry was then employed to obtain the molecular weights of both peptides (Figures 30 and 31).

**Figure 30.** MALDI-TOF mass spectrum of lacticin 3147 A1**Figure 31.** MALDI-TOF mass spectrum of lacticin 3147 A2

## 2. Edman Chemistry and Lacticin 3147

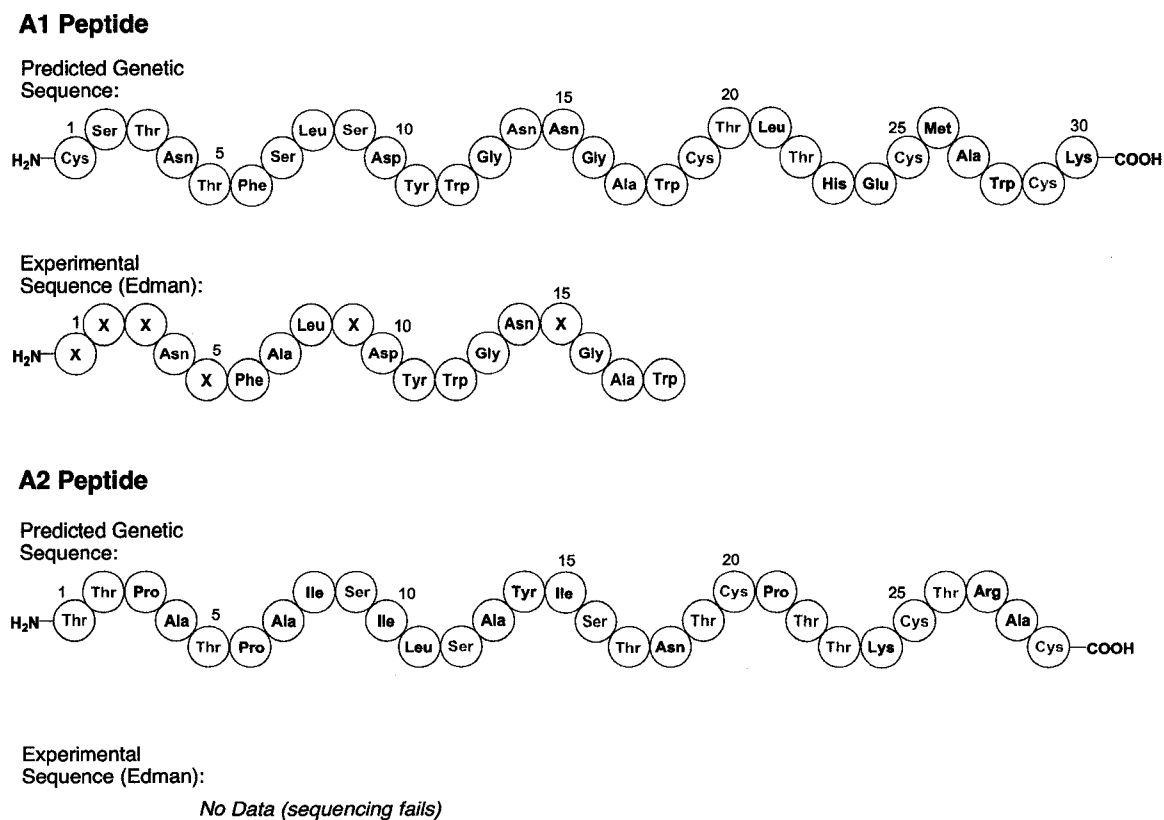
The Edman degradation has long been one of the standard methods of peptide analysis.<sup>163</sup> Its automation allows for the rapid N-terminal sequencing of peptides by the sequential derivitization and characterization of the N-terminal amino acid in a polypeptide chain (Scheme 21). After adsorbing the peptide sample onto a solid support, the first step in the process makes use of phenylisothiocyanate (PITC) which will react with the free amino group of the N-terminus. Cyclization of the PITC adduct with trifluoroacetic acid serves to cleave the derivatized amino acid from the peptide. The peptide is now shortened by one amino acid and the resulting thiazolinone species formed from the cleaved amino acid spontaneously rearranges to give a phenylthiohydantoin (PTH) species. The newly formed PTH is then characterized (most often by inline HPLC) to give the identity of the N-terminal amino acid.

**Scheme 21.** The Edman degradation



Early attempts at sequencing the mature lactacin peptides by Edman degradation gave little information. The sequence data obtained at this time did, however, provide enough insight for a limited confirmation of the structural genes (Figure 32). In conjunction with these results, our collaborators independently undertook genetic analysis of the producing organism which revealed a 60 kb conjugative, bacteriocin-producing plasmid.<sup>164</sup> Within the plasmid Ross and Hill were able to identify the structural genes for both peptides and complete amino acid sequences were then proposed.

**Figure 32.** Initial sequencing results and predicted genetic sequence of lactacin 3147



*(Residues highlighted in blue confirm genetic prediction, those in red are likely modified in the mature lantibiotic and generally give no data (X) in Edman sequencing. Ser to Ala conversion at position 7 in the A1 peptide suggests an enzyme generated D-Ala centre).*



## 2.1 Amino Acid Analysis

Based upon the difference between the genetically predicted and experimentally determined masses for each peptide it was possible to make some early estimates as to the modifications present in each of the peptides. Amino acid composition work revealed that in both the A1 and A2 peptides many of the hydroxy side-chain residues (serine and threonine) predicted were absent in the mature peptides. Also, our collaborators had previously detected D-alanine residues as well as lanthionine and  $\beta$ -methylanthionine in both mature peptides (Table 7).<sup>162</sup>

**Table 7.** Amino acid analysis of A1 and A2 peptides<sup>162</sup>

Amino acid	A1 peptide		A2 peptide	
	Predicted <sup>a</sup>	Detected	Predicted <sup>a</sup>	Detected
Ser	3	0.7	3	0.1
Thr	4	0.0	8	2.3
L-Ala <sup>c</sup>	2	2.3	4	4.3
D-Ala <sup>c</sup>	0	1.1	0	2.1
Cys	4	ND <sup>b</sup>	3	ND <sup>b</sup>
Lan/MeLan	0	3.2	0	2.9

<sup>a</sup> Predicted from gene sequences, <sup>b</sup> ND, not detectable by method employed, <sup>c</sup> D/L alanine ratio by chiral GCMS of hydrosylate.

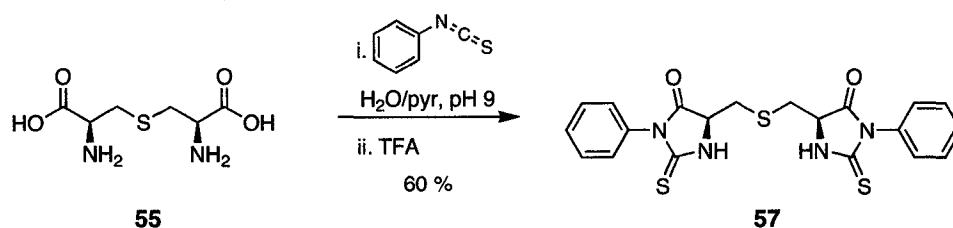
Based upon the number of dehydrations required, and the number of lanthionine or  $\beta$ -methylanthionine residues present in each peptide, predictions for the masses of the mature peptides were made. In the case of A1, the ribosomal peptide predicted by the structural gene has a mass of 3430.88 Da. Invoking seven dehydrations (-126.14 Da) and one reduction leading to a new D-alanine centre (+2.02 Da), a mass of 3306.76 Da is suggested, agreeing well with the experimental value of  $3306 \pm 1$  Da (Figure 30). The A2

ribosomal peptide predicted by the structural gene has a mass of 2986.44 Da. In this case, 8 dehydrations (-144.16 Da), two reductions leading to new D-alanine centres (+4.04 Da), and a N-terminal deamination to an  $\alpha$ -keto amide (+1.01 Da *see Scheme 18*), suggests a mass of 2847.33 Da, also agreeing well with the experimental value of  $2847 \pm 1$  Da (Figure 31). These preliminary calculations, and the number of lanthionine or  $\beta$ -methylanthionine residues detected, suggest the presence of two dehydro side chains in each mature lantibiotic peptide.

## 2.2 Compatibility of Lantibiotics with the Edman Degradation

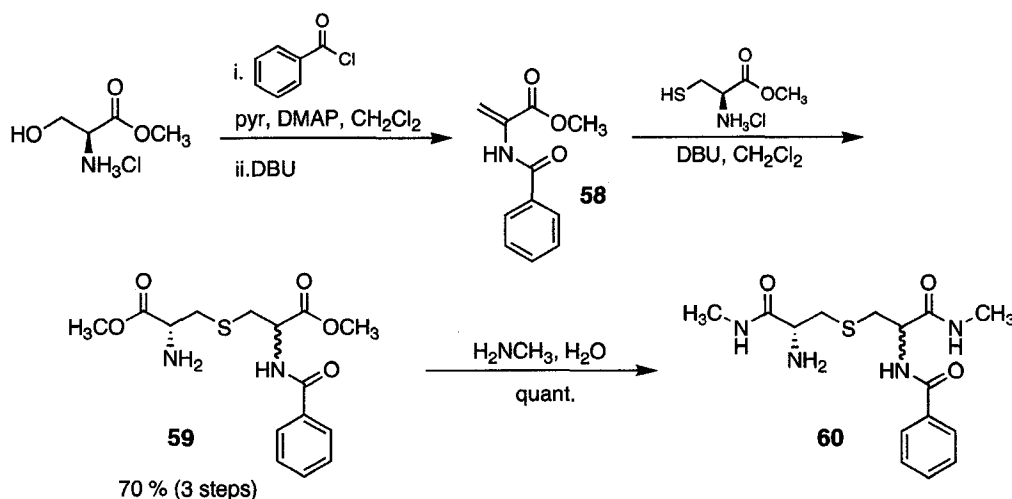
As Figure 32 shows, for each site in the A1 peptide where a lantibiotic modification (lanthionine bridge or dehydro residue) might have occurred, a blank cycle in the Edman sequence is encountered. In the case of the A2 peptide no data was obtained by Edman sequencing. Clearly the dehydro side chains present in lantibiotics would be expected to block the Edman degradation by the tautomerization/deamination mechanism outlined in Scheme 18. The fact that lanthionine bridges also seem to conflict with Edman chemistry, however, had yet to be addressed. Most often in the sequencing of lantibiotics when a residue participating in a lanthionine bridge is encountered, a blank in the corresponding HPLC cycle appears. In the subsequent Edman cycle a severe drop in signal intensity or complete lack of signal results, prematurely terminating the sequencing process. To investigate the compatibility of lanthionine with the chemistry of the Edman degradation, a sample of meso lanthionine (**55**) was treated under the standard conditions used for forming PTH derivatives of amino acids (Scheme 22).

**Scheme 22.** Lanthionine bis-PTH preparation

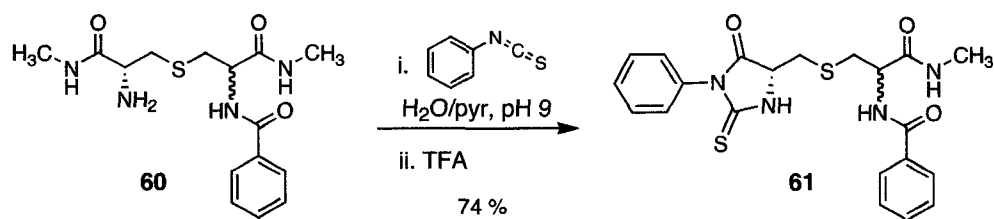


The moderate (unoptimized) yield for the formation of the bis-PTH of lanthionine **57** under standard conditions suggests that the formation of the desired PTH derivative is not the obstacle to sequencing lantibiotic peptides. In an attempt to better mimic the environment of a lanthionine residue within a peptide, an orthogonally protected lanthionine species **60** was also prepared (Scheme 23).

**Scheme 23.** Preparation of orthogonally protected lanthionine



When treated under standard Edman conditions, the orthogonally protected lanthionine species **60** also provided the expected mono-PTH product **61** in good yield (Scheme 24).

**Scheme 24.** Lanthionine mono-PTH preparation

These results suggest that the chemistry of the Edman degradation is compatible with lanthionine residues. However, an investigation of the solubility properties of the original lanthionine bis-PTH **57** (performed by Glen Armstrong, summer student 2003), suggested an explanation for the difficulties encountered (Table 8).

**Table 8.** Lanthionine bis-PTH **57** solubility study

Solvent	Insoluble	Partially soluble	Soluble
Acetone			✓
Acetonitrile			✓
Chloroform	✓		
Cyclohexane		✓	
Dichloromethane		✓	
Dimethylformamide			✓
Diethyl Ether	✓		
Ethanol	✓		
Ethyl Acetate	✓		
Hexane	✓		
Methanol			✓
Pentane		✓	
2-Propanol		✓	
Tetrahydrofuran			✓
Toluene		✓	
Triethylamine		✓	
Trifluoroacetic acid			✓
Water	✓		

Scheme 21 illustrates the process by which PTH amino acids are formed and processed in the automated Edman degradation. At each stage of the operation a different solvent is employed, with ethyl acetate serving as a “transport solvent” utilized for moving the PTH amino acid from the micro reactor of the sequencer to the injection loop prior to HPLC analysis. All of the 20 standard PTH amino acids are soluble in ethyl acetate so it would stand to reason that the insolubility of lanthionine bis-PTH **57** in ethyl acetate explains the failures encountered in automated Edman degradation. As Table 8 indicates, the use of an alternative solvent (methanol or acetonitrile) may circumvent the problem (yet to be attempted).

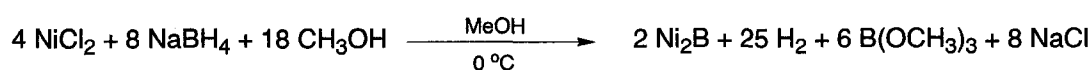
### **3. Ni<sub>2</sub>B Modification of Lantibiotics**

Modern peptide structure elucidation most often relies on either X-ray crystallography or multidimensional NMR spectroscopy, for which multi milligram quantities of peptide are required. However, in the case of lacticin 3147, the lack of a suitable mass of material made both techniques impossible. In the optimized isolation of the lacticin peptides from the fermentation supernatant of *L. lactis* DPC 3147 the amount of each peptide obtained was approximately 100 µg/L.

With these challenges, the major focus of the project became the chemical modification of lantibiotics to yield peptides compatible with the Edman degradation. As described in the previous section, the presence of both lanthionine bridges and dehydro side chains in lantibiotics often interfere with Edman chemistry. A desired chemical

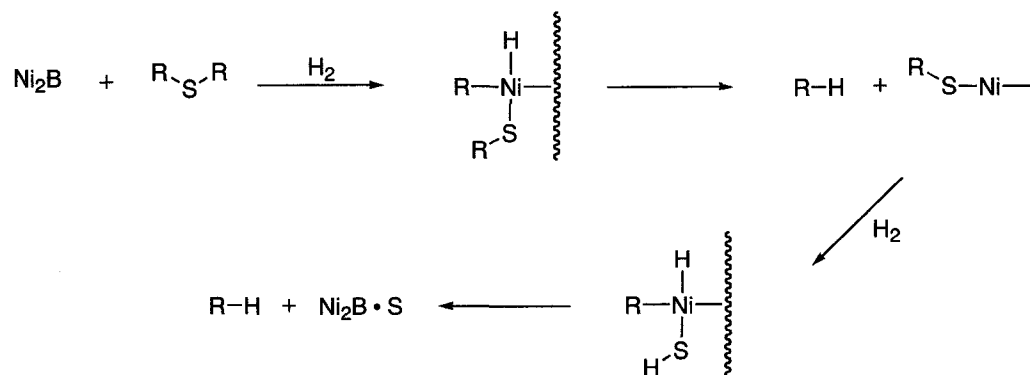
modification process for these peptides would ideally transform both lanthionine bridges and dehydro side chains to sequencer-friendly moieties while leaving the peptide and all other functional groups unaffected. Nickel boride ( $\text{Ni}_2\text{B}$ ) is one such reducing and desulfurizing agent when used in the presence of hydrogen. The original structure elucidation of Nisin relied on Raney nickel W-6 for lanthionine desulfurization without reduction of dehydro residues.<sup>155,156</sup> Nickel boride ( $\text{Ni}_2\text{B}$ ), however, has been used both in thioether desulfurization<sup>165</sup> and olefin reduction.<sup>166</sup> Nickel boride forms rapidly in situ when nickel chloride is treated with sodium borohydride in protic solvent<sup>167</sup> (Scheme 25).

**Scheme 25.** Formation of nickel boride in protic solvent



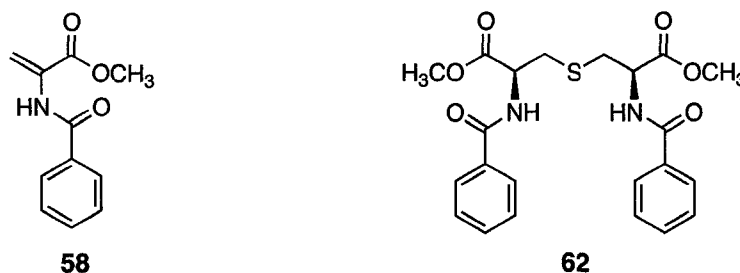
While the detailed structure of nickel boride is unknown, its elemental composition is consistent with the formula  $\text{Ni}_2\text{B}$  and contains hydrogen that is gradually released upon heating.<sup>167</sup>

Mechanistic studies by Back and coworkers rule out a process involving activation of the substrate by complexation of its sulfur atom with nickel boride, followed by hydride attack from sodium borohydride upon the  $\alpha$ -carbon.<sup>167</sup> Similarly, labeling experiments with hydrogen donor solvents, as well as the observed stereospecificity, are inconsistent with a radical mechanism. Back's results support the oxidative addition-reductive elimination mechanism illustrated in Scheme 26.<sup>167</sup>

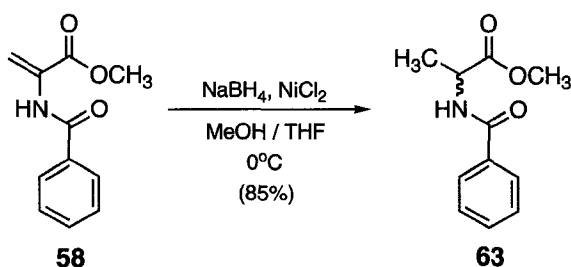
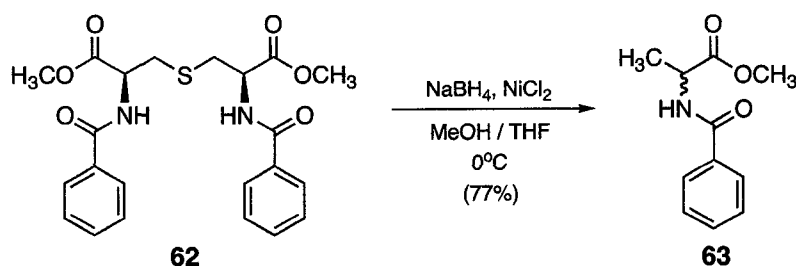
**Scheme 26.** Proposed mechanism for Ni<sub>2</sub>B desulfurization

### 3.1 Model Studies

Analogues of dehydroalanine **58** and lanthionine **62** were prepared to serve as model compounds (Figure 33) for the reduction and desulfurization of the unique functional groups found in lantibiotic peptides.

**Figure 33.** Dehydroalanine and lanthionine analogues prepared

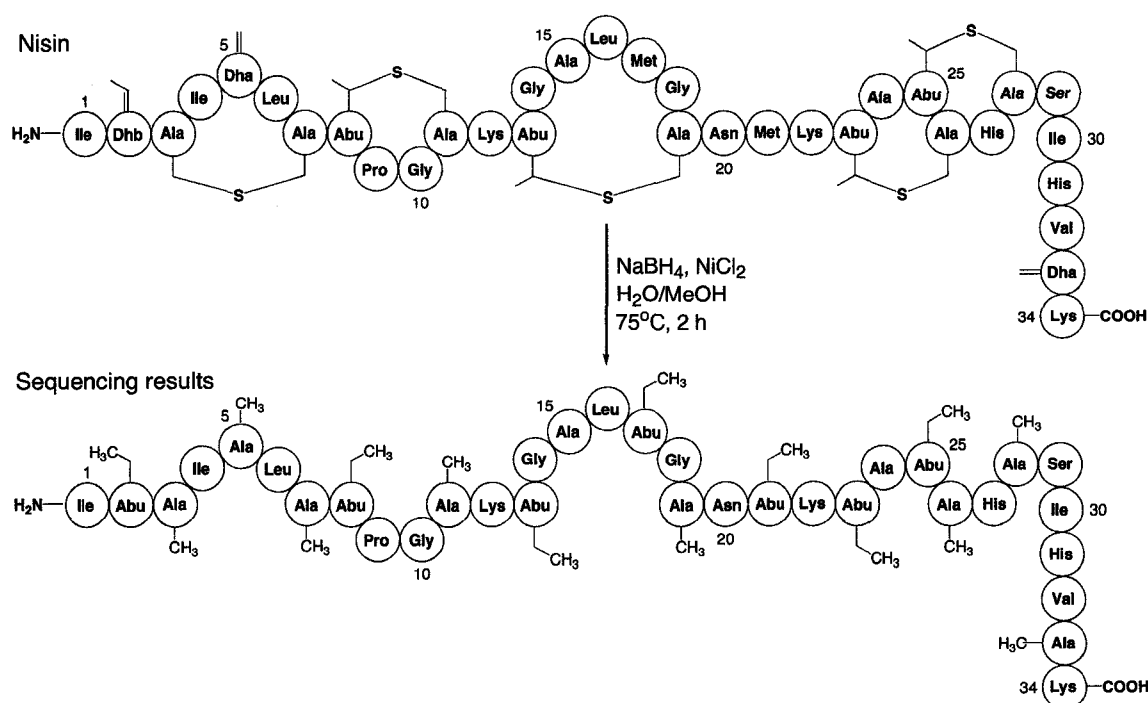
Both compounds, when treated with nickel boride under identical conditions, generate the expected alanine analogue **63** (Schemes 27 and 28).

**Scheme 27.** Nickel boride reduction of dehydroalanine analogue **58****Scheme 28.** Nickel boride desulfurization of lanthionine analogue **62**

With promising results for both the reduction and desulfurization of the model compounds, the commercially available lantibiotic peptide nisin (**53**) (Figure 21) was next investigated. After treating pure nisin with nickel boride, the product peptide was isolated and subjected to sequence analysis. The results indicated that the dehydro residues had been reduced and the lanthionine bridges desulfurized, yielding a peptide completely compatible with Edman sequencing (Scheme 29).



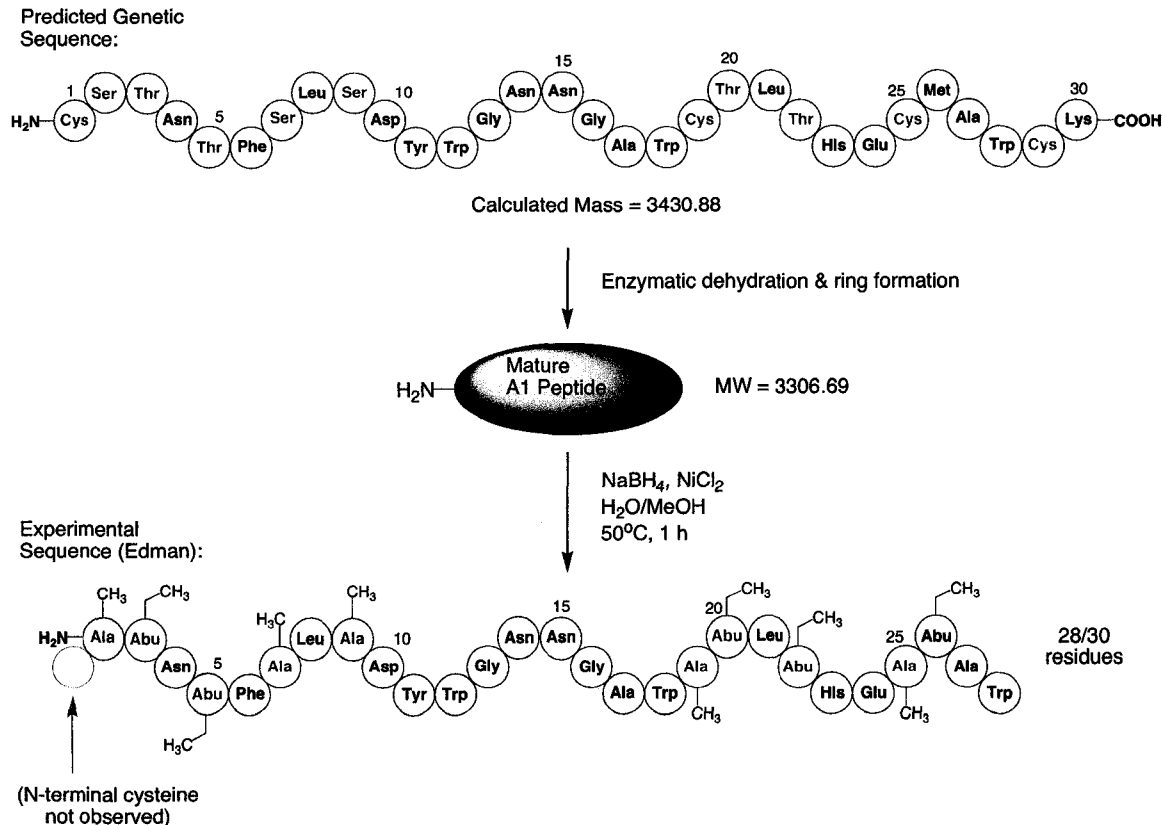
### Scheme 29. Nickel boride modification of nisin



### 3.2 $\text{Ni}_2\text{B}$ Desulfurization and Reduction of Lacticin 3147 A1 and A2

With sound evidence for the utility of nickel boride in the desulfurization and reduction of lantibiotic models, the lacticin 3147 A1 and A2 peptides were next investigated. A sample of pure lacticin A1 was treated under the same conditions used for nisin and the isolated peptide product subjected to Edman sequencing. Scheme 30 outlines the predicted sequence of the A1 peptide based on the structural gene, the enzymatically modified active lantibiotic, and the product of its treatment with nickel boride as determined by Edman degradation.

**Scheme 30.** Nickel boride modification of the lacticin 3147 A1 peptide

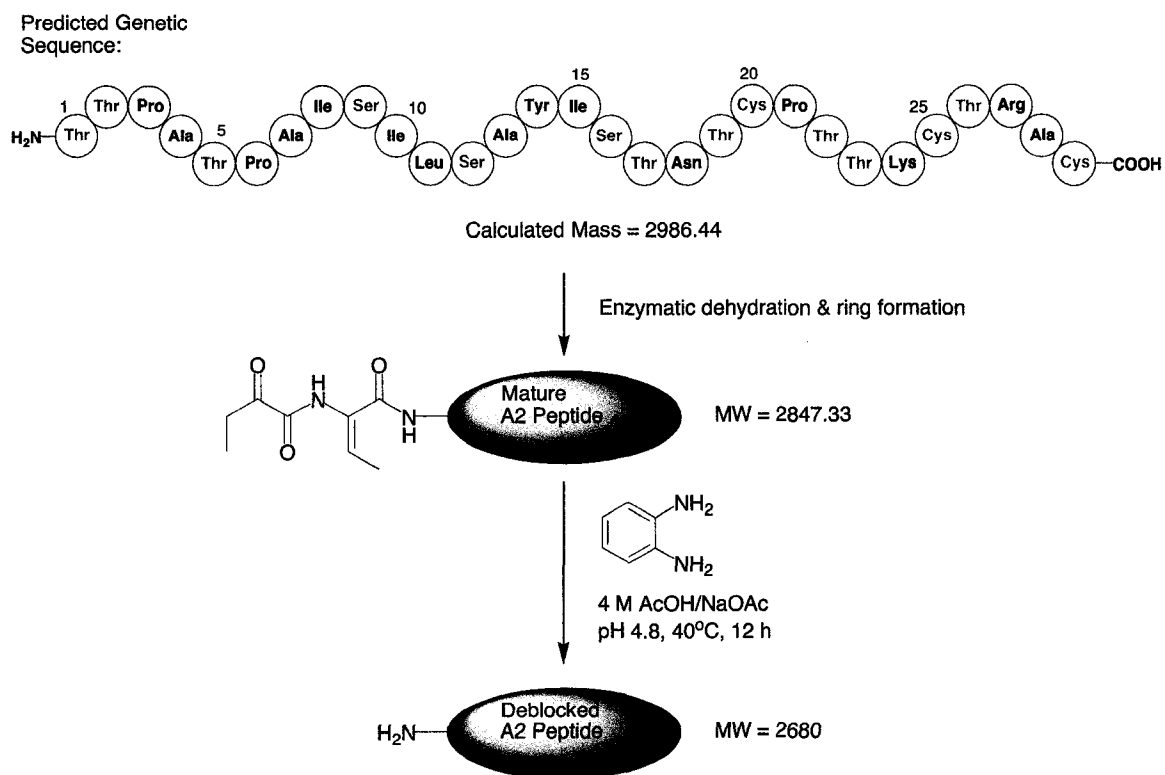


*Residues highlighted in red are likely modified in the mature lantibiotic.*

These results further support the sequence proposed by Ross and Hill<sup>162</sup> based on the structural gene and provide a more complete peptide sequence than the original sequencing attempts using the native peptide (compare with Figure 32). Unexpectedly, the proposed N-terminal cysteine residue (expected to be involved in a lanthionine bridge) appears to have been clipped from the peptide during the nickel boride modification process. Sequencing otherwise proceeded cleanly up to the 28<sup>th</sup> of 30 amino acids.

The lactacin A2 peptide was not immediately amenable to the nickel boride modification strategy. Initial sequencing work with the native peptide returned no data (Figure 32) suggesting a N-terminal block of some kind. The first two N-terminal residues are predicted to be threonine, based on the structural gene. However, if both residues are enzymatically dehydrated, an  $\alpha$ -keto amide moiety would result, blocking N-terminal sequencing (*see Scheme 18*). Using a dinucleophile, 1,2-diaminobenzene, in strong acetic acid/sodium acetate buffer, it was possible to chemically remove the two N-terminal residues (Scheme 31).

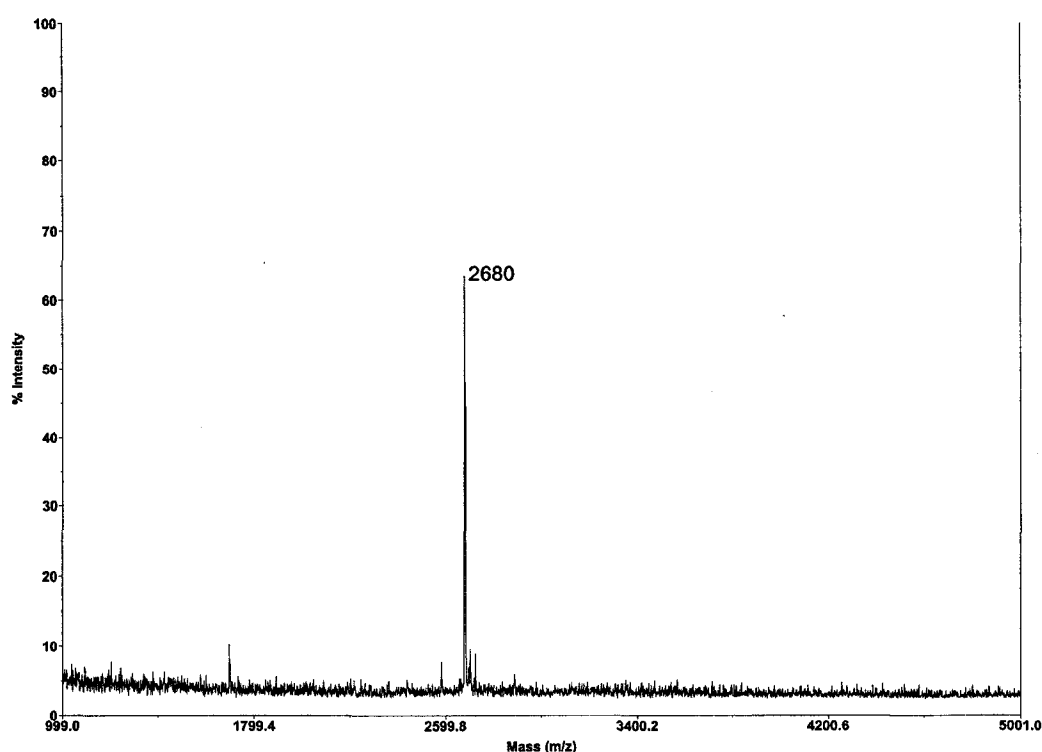
### Scheme 31. N-terminal deblocking of lactacin A2



*Residues highlighted in red are likely modified in the mature lantibiotic.*

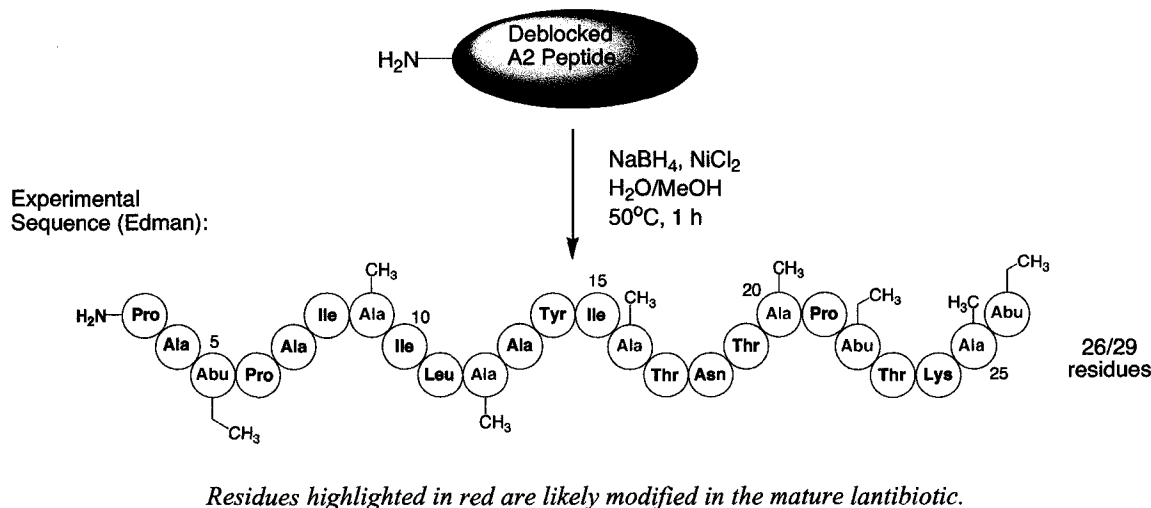
Evidence for the successful deblocking of the peptide was provided by MALDI-TOF mass spectrometry. The expected mass of the deblocked peptide can be estimated by subtracting the mass of the N-terminal blocking moiety (167.18 Da for  $C_8H_9NO_3$ ) from mass of the mature peptide (2847.33 Da) to arrive at a predicted mass of 2680.15 Da agreeing well with the experimental value of  $2680 \pm 1$  Da (Figure 34).

**Figure 34.** MALDI-TOF mass spectrum of deblocked lacticin 3147 A2



The deblocked peptide was then treated with nickel boride to produce a peptide that was readily sequenced by Edman degradation (Scheme 32).

**Scheme 32.** Nickel boride modification of the deblocked lacticin 3147 A2 peptide



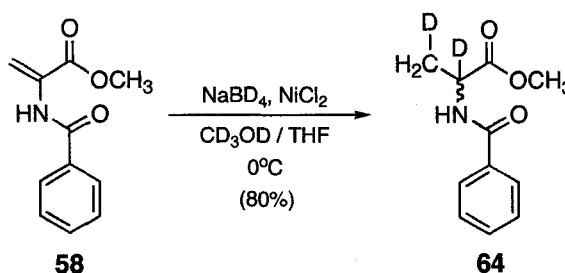
These results represented the first sequence data obtained for the A2 peptide and confirmed the genetic prediction. Also of interest is the indication that threonines 19 and 23 are preserved in the mature lantibiotic and not dehydrated or involved in lanthionine bridges.

### 3.3 Deuterating Desulfurization/Reduction of Lantibiotics with $\text{Ni}_2\text{B}$

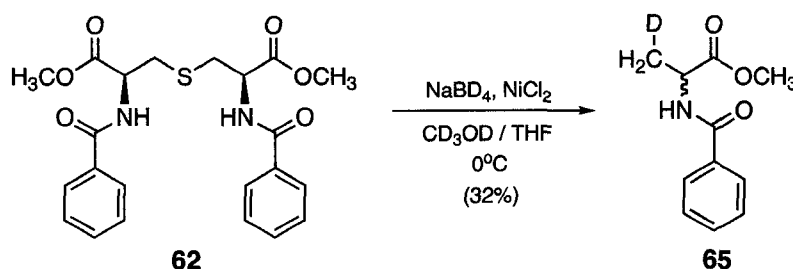
The results of the previous section illustrate how nickel boride desulfurization and reduction allow for more thorough Edman sequencing when dealing with lantibiotic peptides. The information obtained through this approach, however, is still limited in that one cannot distinguish between residues that were dehydrated or part of lanthionine bridges in the native lantibiotic. To make this differentiation possible it was speculated that a “deuterated” variant of the nickel boride modification might be used. Using  $\text{NaBD}_4$  in deuterated solvent, the original model compounds **58** and **62** were reduced and

desulfurized (Schemes 33 and 34). Lanthionine linkages are desulfurized with the concomitant incorporation of a single deuterium atom at each of the residues participating in the sulfur bridge while dehydro residues are reduced with incorporation of two deuterium atoms.

**Scheme 33.** Deuterating nickel boride reduction of dehydroalanine analogue **58**



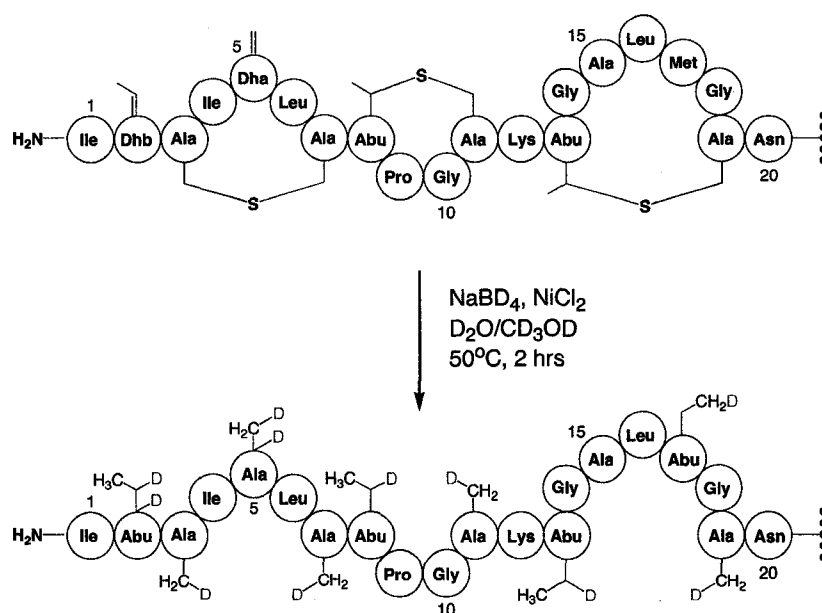
**Scheme 34.** Deuterating nickel boride desulfurization of lanthionine analogue **62**



For peptides analyzed by Edman degradation, mass spectrometry can then be used to identify the specific deuterium incorporation for the PTH derivative of each modified residue in the lantibiotic. This approach should provide information about the location of dehydro residues and lanthionine linkages. After successful trials with model compounds, nisin was again used as a model lantibiotic (Scheme 35). After treatment with nickel boride under deuterating conditions, the product peptide was subjected to Edman

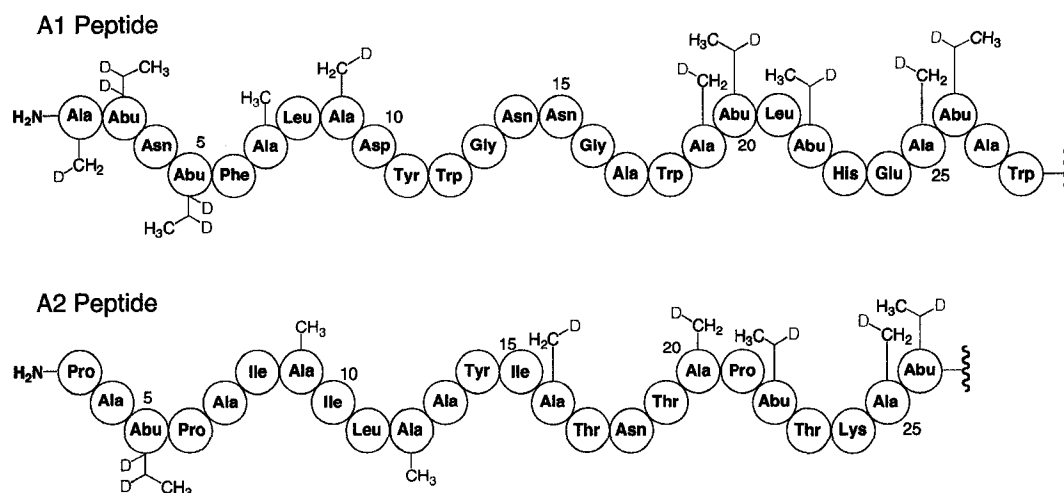
sequencing and those residues (within the first 20) known to be dehydrated, or part of lanthionine bridges in the native peptide, were collected for mass analysis. The results clearly allow for distinction of those residues involved in lanthionine bridges and those that are dehydrated in the native peptide (Scheme 35).

**Scheme 35.** Deuterating nickel boride modification of nisin



With the successful deuterium incorporation of nisin the same modification and analysis protocol was next applied to the lactacin peptides (Figure 35).

**Figure 35.** Dehydro residue / lanthionine bridge location in lacticin A1 and A2 peptides



*Deuterium incorporation indicated in red shows likely positions of lanthionine linkages and dehydro side chains in the mature lantibiotic peptide. Alanines in blue indicate likely site(s) of D-alanine residues produced by enzymatic reduction of dehydroalanine. Note: again the A1 peptide is clipped by one residue at the N-terminus; for the A2 peptide two residues are removed by 1,2-diaminobenzene N-terminal deblocking.*

While this methodology does not reveal all aspects of a lantibiotic peptide's structure (precise lanthionine bridging patterns in particular) it remains a valuable tool. The microscale capability of this approach is especially valuable when dealing with quantities of peptide too small for conventional approaches like multi-dimensional NMR and crystallography. Nickel boride chemistry as well as Edman sequencing are reliably used with sub milligram quantities of peptide and mass spectrometric analysis of the PTH derivatives is routinely performed on the nanogram scale.

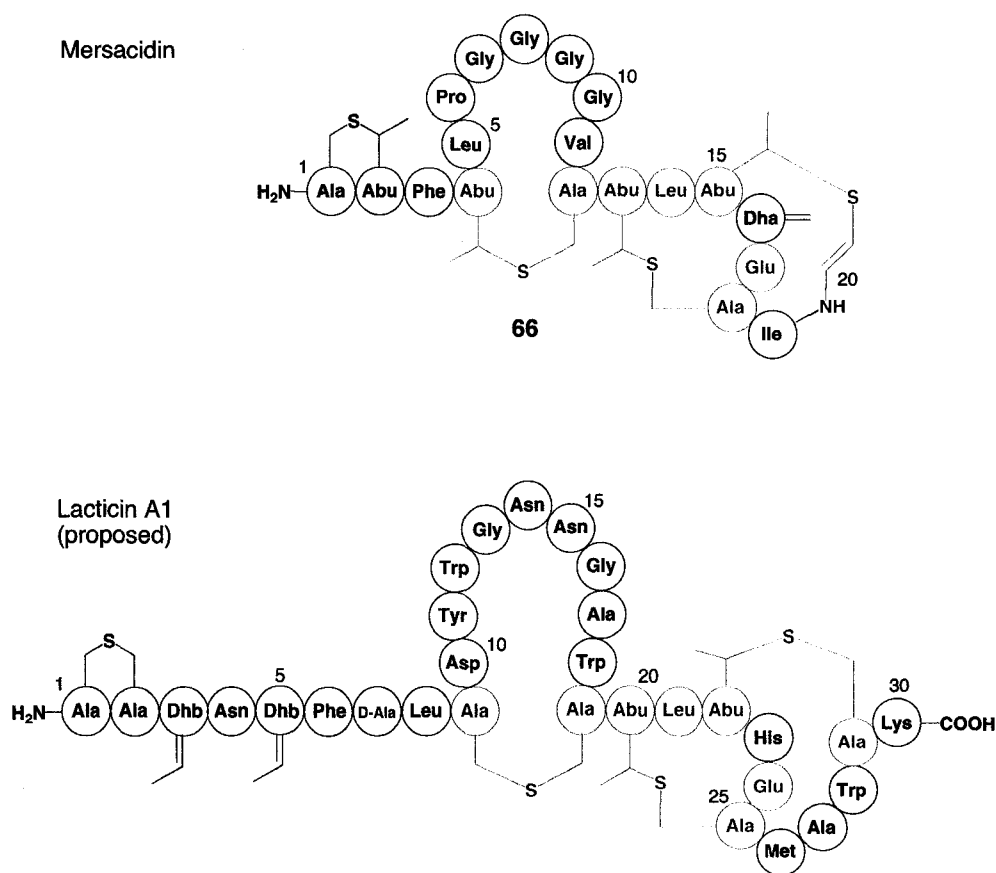
### 3.4 Proposed Structures

The nickel boride deuteration experiments provided valuable information about which residues were likely to be part of lanthionine bridges, dehydrated, and new



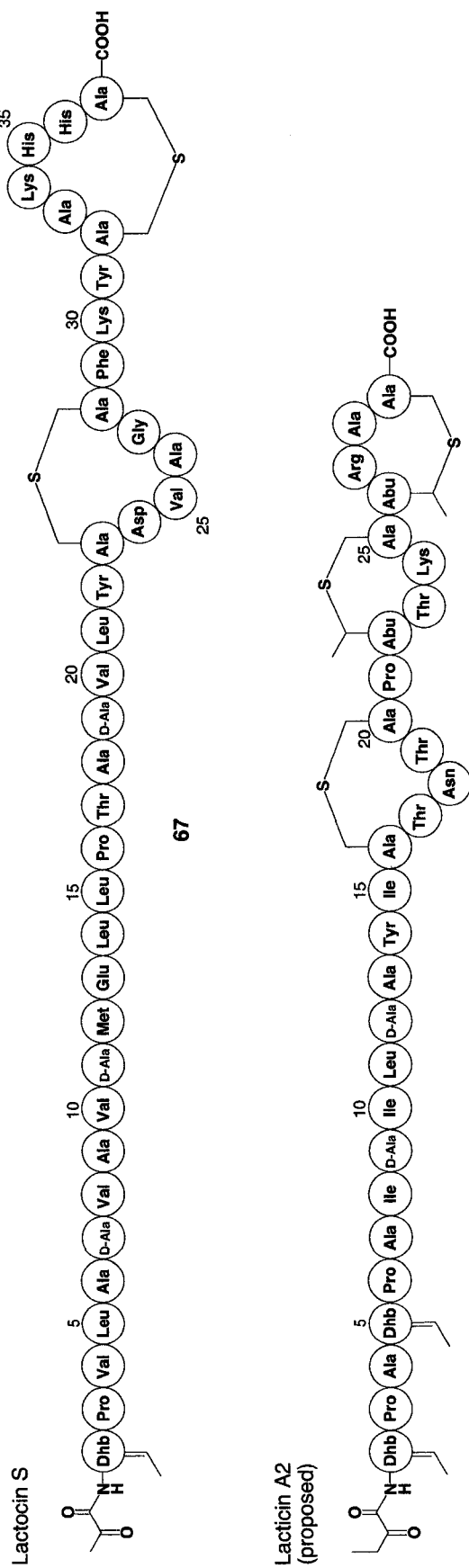
(enzymatic) D-alanine centres. With these results it is possible to make structural predictions for the lacticin peptides based on comparison with structures of known lantibiotics. Lanthionine bridging patterns can be suggested for the A1 peptide by comparison with mersacidin<sup>150,168</sup> (66) (Figure 36). Also, the A2 peptide may have similarity to lactocin S (67), the only other lantibiotic proven to contain D-alanine<sup>120</sup> (Figure 37).

**Figure 36.** Mersacidin structure and proposal for A1 peptide



*Residues in red indicate possible shared structural features.*

**Figure 37.** Lactocin S structure and proposal for A2 peptide

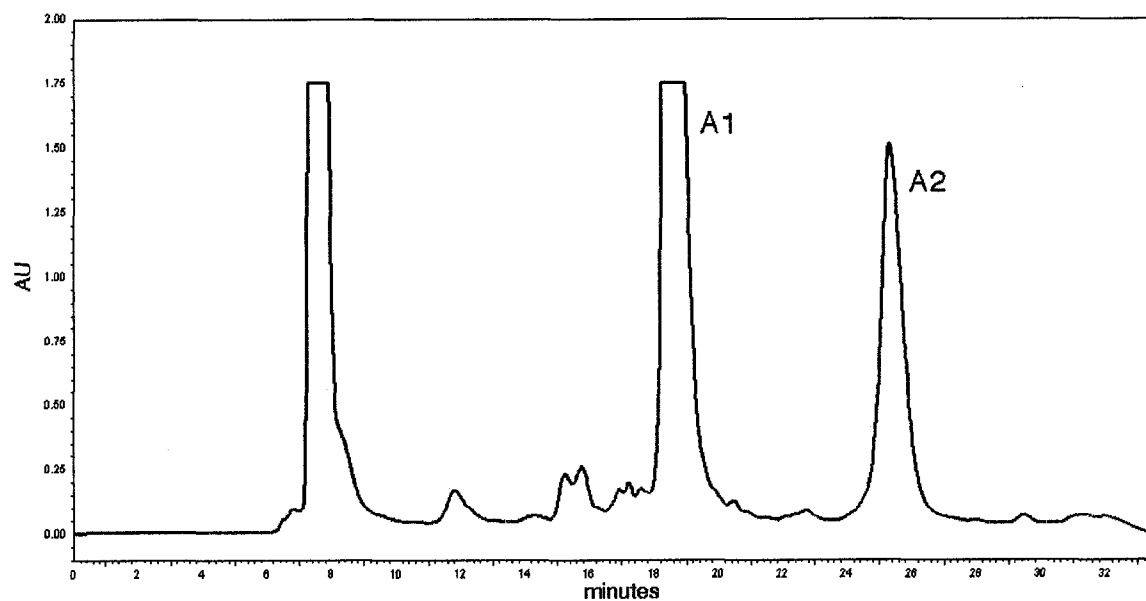


#### 4. Improved Isolation of Lacticin 3147

The original isolation strategy for the lacticin A1 and A2 peptides focused on their recovery from the fermentation supernatant. While this was a reasonable tactic based upon conventional thinking (*see Scheme 16*), the cells themselves had not been investigated for their ability to retain or bind the lacticin peptides upon centrifugation. Both of the peptides are quite hydrophobic and it was reasoned that the cell surface might present a more stabilizing environment than the aqueous supernatant. Also, at this stage of the project, our collaborators provided us with an engineered organism, which had been designed to overproduce the lacticin 3147 peptides.

A modified procedure was developed making use of the new overproducing strain and focusing exclusively on isolation of the lacticin peptides from the cells after centrifugation. Recovery of the peptides in this manner provided a mixture of the A1 and A2 peptides that contained very little contamination prior to HPLC. The number of fractionating, chromatographic steps was drastically reduced, thereby enhancing yields. After HPLC, pure material was obtained in approximately half the time of the initial procedure. Also, the new protocol significantly reduced the deleterious oxidation of both the A1 and A2 peptides, which had consistently decreased isolation yields. In this way a vast increase in the amount of the lacticin peptides obtained was achieved, approaching a 10-fold increase (~1 mg/L). Figure 38 displays a typical HPLC trace illustrating the improved isolation (compare with Figure 28).

**Figure 38.** HPLC separation of lacticin 3147 A1 and A2 peptides – improved isolation

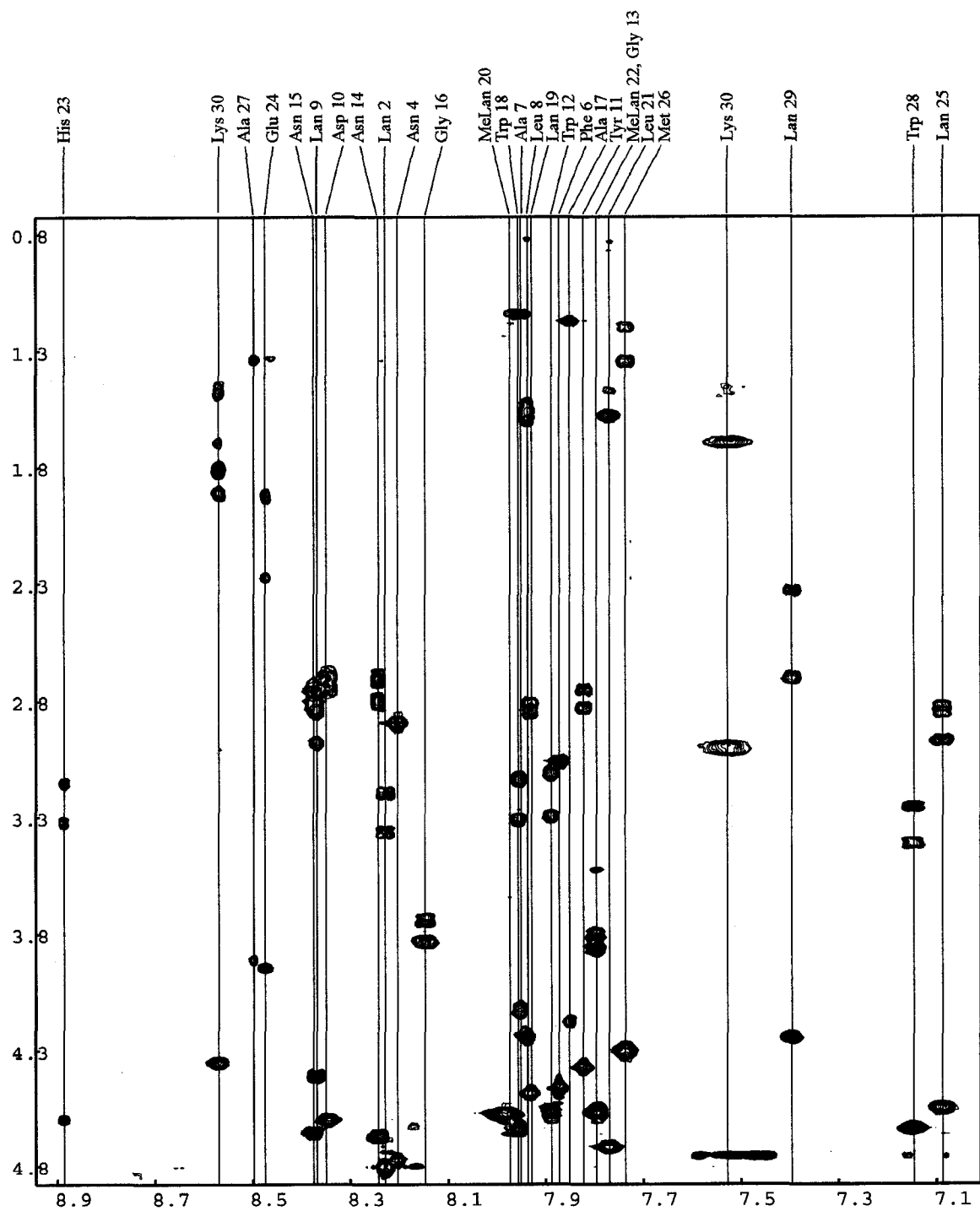


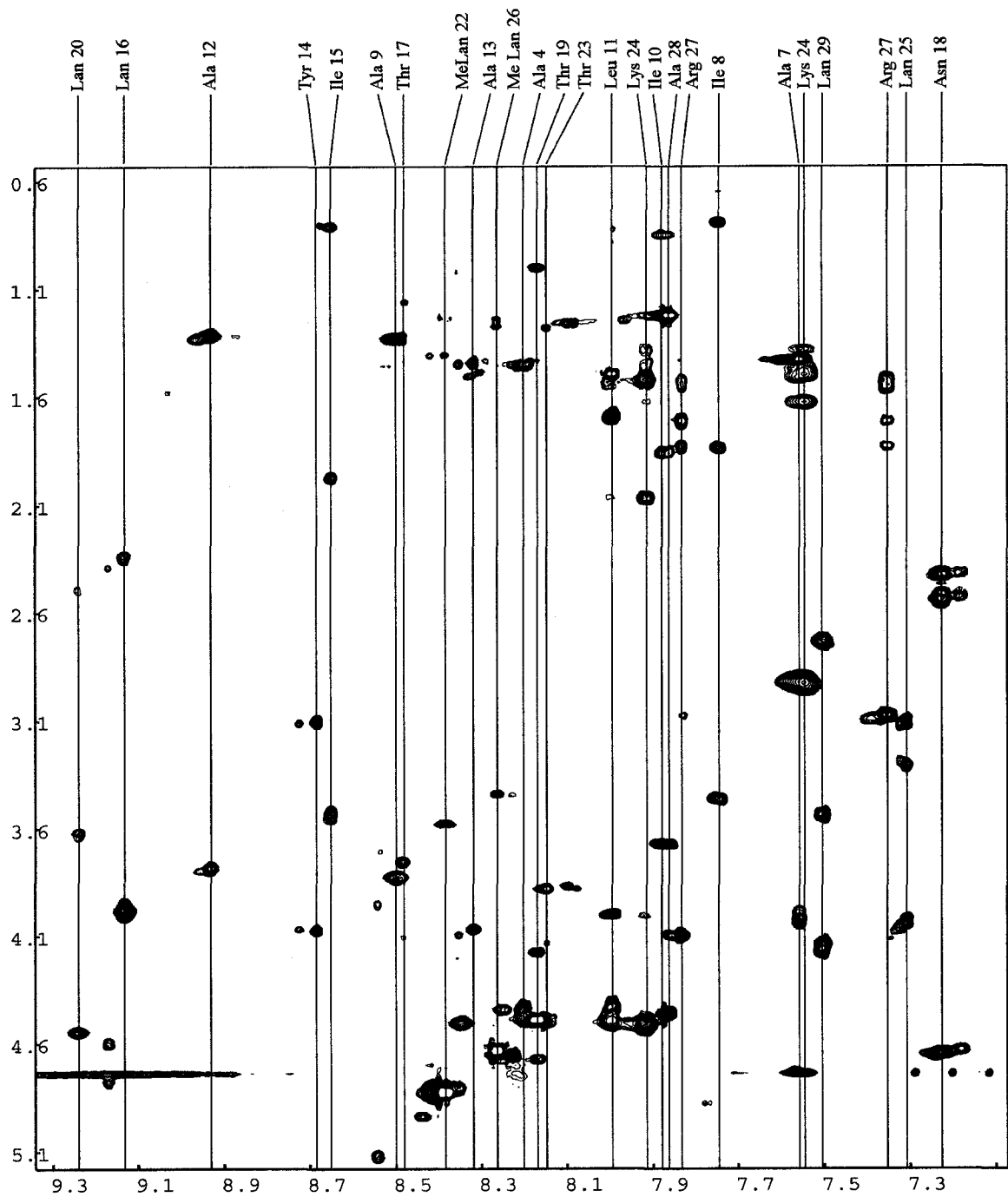
#### 4.1 NMR Spectroscopy

Ready access to milligram quantities of both peptides meant the structure elucidation could now make use of multidimensional NMR spectroscopy. The most important structural challenge still remaining was that of the lanthionine bridging patterns in both peptides. With much help from Dr. Tara Sprules (*Vederas group postdoctoral fellow, 2003*), a number of two-dimensional NMR experiments were performed with each of the lacticin 3147 peptides.

The spin systems in the TOCSY spectra of lacticin A1 and A2 were assigned to the respective residues by taking into consideration the characteristic frequencies and numbers of resonances (Figures 39a and 39b). In the spectra of both peptides all expected residues are apparent.

**Figure 39a.** TOCSY spectrum identifying spin systems for all residues in A1 peptide

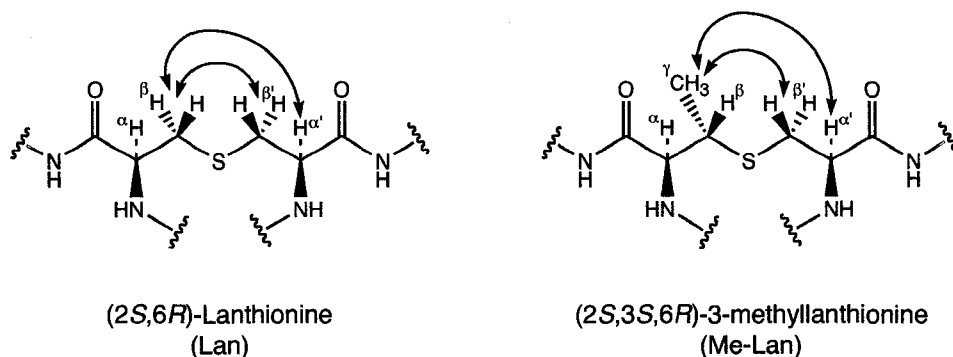


**Figure 39b.** TOCSY spectrum identifying spin systems for all residues in A2 peptide

Sequential assignment of the peptides agreed completely with results from the Edman degradation and was achieved using the connectivities suggested by  $d_{\alpha N}(i,i+1)$  and  $d_{NM}(i,i+1)$  connectivities in the NOESY spectra.

Finally, intra-bridge NOEs were used to establish the connectivities of the lanthionine and  $\beta$ -methylanthionine linkages in each peptide. The most useful correlations detected in this analysis were the  $\alpha/\beta'$  and  $\beta/\beta'$  interactions in all the bridges as well as the  $\gamma/\alpha'$  and  $\gamma/\beta'$  interactions present for  $\beta$ -methylanthionine moieties (Figure 40).

**Figure 40.** Intra-bridge NOE's used in Lan/MeLan bridging pattern assignment



Figures 41a and 41b are expansions of the most useful regions of the NOESY spectra acquired for each peptide and illustrate the relevant correlations used to assign the lanthionine bridging patterns.

**Figure 41a.** Intra-bridge NOEs for lanthionine and  $\beta$ -methylanthionine linkages in A1 peptide

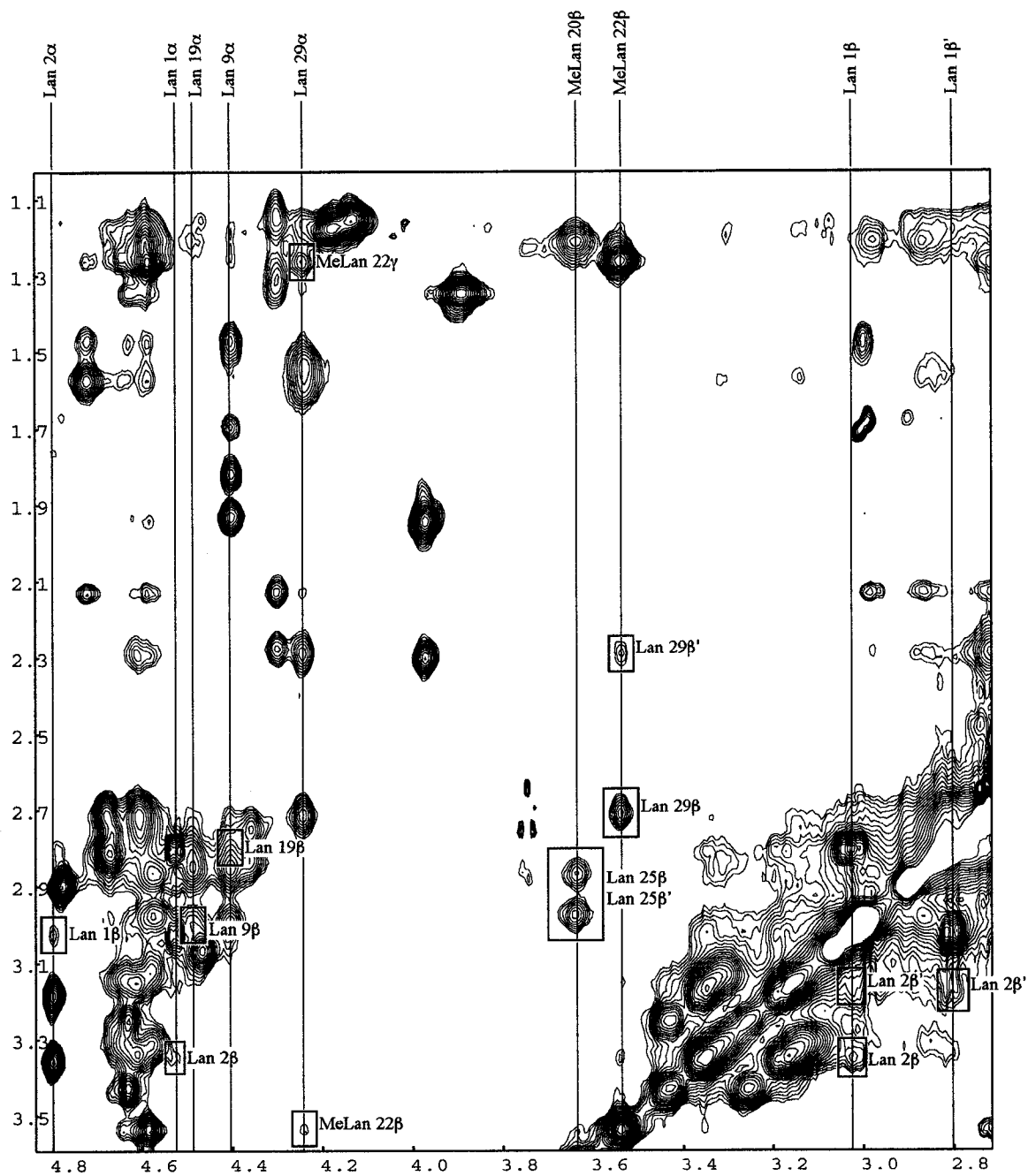
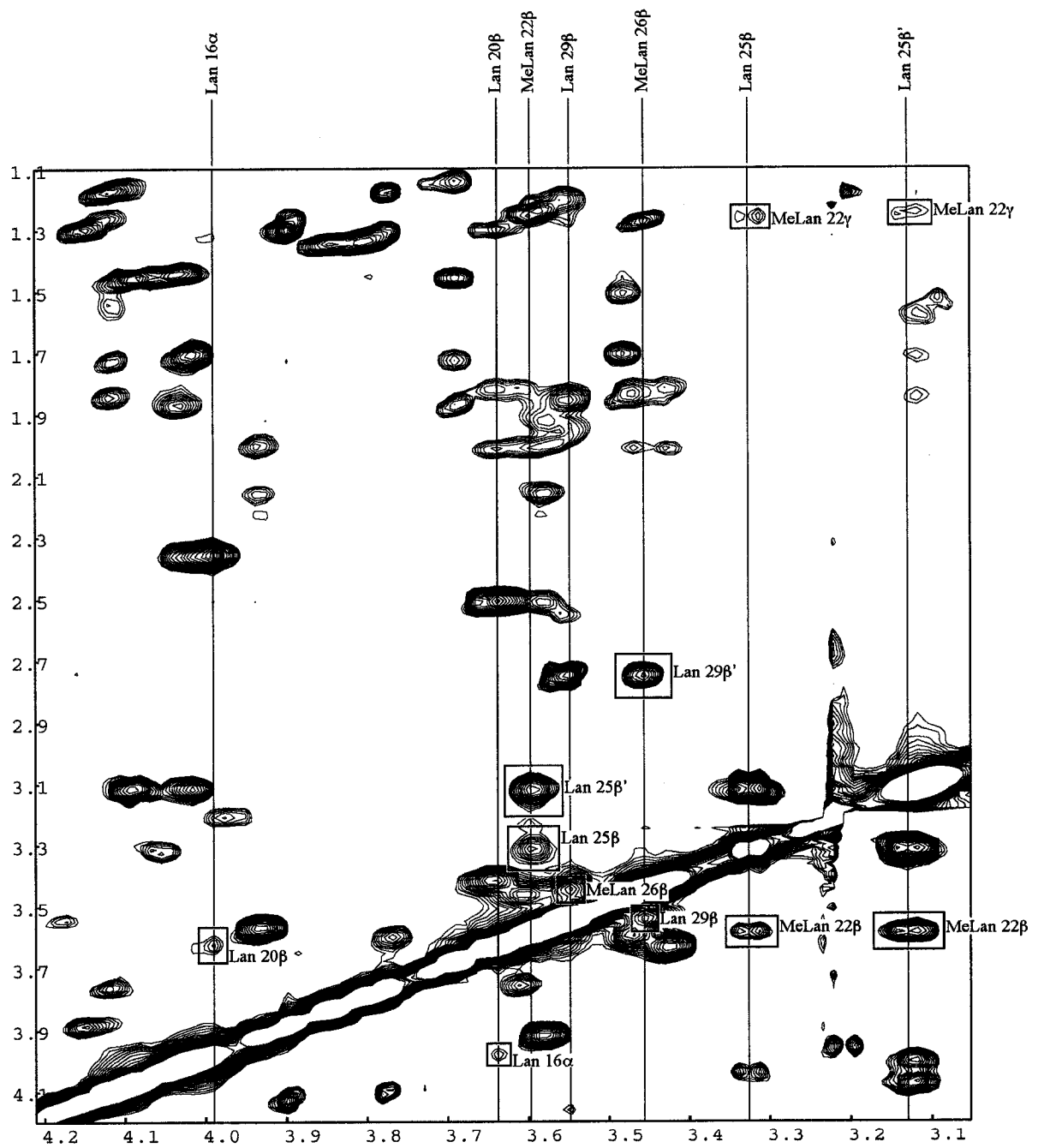




**Figure 41b.** Intra-bridge NOEs for lanthionine and  $\beta$ -methylanthionine linkages in A2 peptide



## 4.2 Solved Structures of Lacticin A1 and A2

The structures and bridging patterns suggested by the NMR spectroscopy results are in complete agreement with all data previously obtained for the peptides via the nickel boride desulfurization/reduction and Edman degradation (Figures 42a and 42b).

**Figure 42a.** Lacticin A1

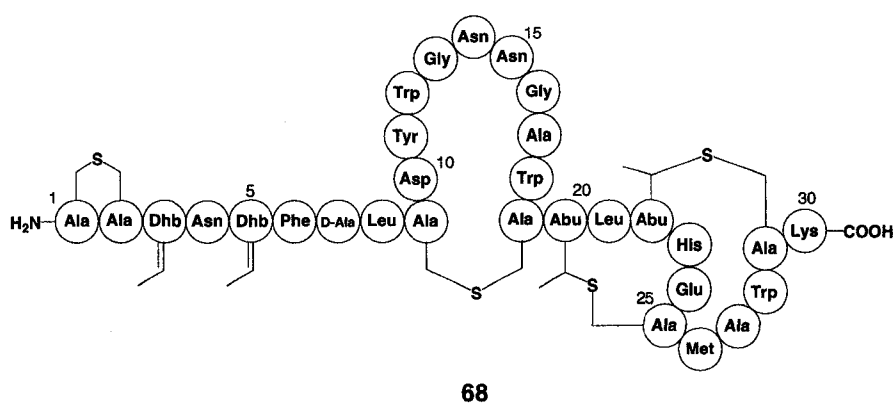
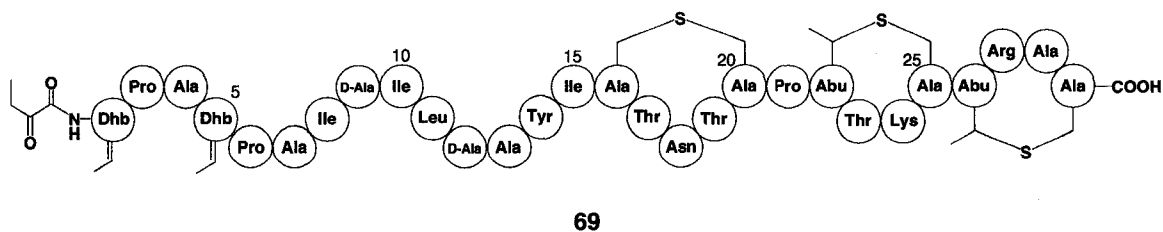


**Figure 42b.** Lacticin A2



## 5. Conclusions and Future Directions

The principal objective of the project has been realized - the primary structures of both lactacin peptides are now known. Along with this achievement advances have been made that should benefit other researchers working in the area of lantibiotic peptide structure elucidation. The combined use of nickel boride desulfurization/reduction chemistry, Edman degradation, and mass spectrometry represents a novel and general method that should work with any lantibiotic peptide.

With the successful determination of the primary structures of both lactacin peptides new questions emerge. In most lantibiotic structure elucidations performed to date, the stereochemistry of the lanthionine and  $\beta$ -methylanthionine residues is taken to be identical to that found for nisin (see Figure 27). These assumptions will be tested in ongoing work with the lactacin peptides and the stereochemistry of each lanthionine linkage.

As well, given the now ready access to milligram quantities of both lactacin peptides, an opportunity for further NMR studies presents itself. Following on the recent work of others with nisin<sup>169-171</sup> and mersacidin,<sup>172</sup> the interaction of the lactacin peptides with the cell wall precursor lipid II will be undertaken. Such studies should help shed light on the mode of action of the peptides. Ross and Hill have proposed that the A1 peptide is responsible for interaction with lipid II and that the A2 peptide then recognizes the A1-lipid II association complex after which pore formation proceeds. No other two-

component lantibiotic has been fully characterized presenting the opportunity to make an original contribution to the understanding of their pore forming abilities. Finally, the lactacin 3147 peptides are already being used in food preservation and veterinary medicine. A detailed understanding of the three-dimensional structures of both peptides, as well as the influences of residue modification on biological activity, may lead to new lacticins for use in human therapy.

## CHAPTER 4. EXPERIMENTAL PROCEDURES

### 1. General Procedures

#### 1.1 Reagents, solvents and solutions

All reactions involving air or moisture sensitive reactants were done under a positive pressure of dry argon using oven-dried glassware. All reagents employed were of American Chemical Society (ACS) grade or finer and were used without further purification unless otherwise stated. For anhydrous reactions, solvents were dried according to Perrin *et al.*<sup>173</sup> and Vogel.<sup>174</sup> Tetrahydrofuran and diethyl ether were distilled over sodium and benzophenone under an atmosphere of dry argon. Acetonitrile, dichloromethane, methanol, pyridine and triethylamine were distilled over calcium hydride. Removal of solvent was performed under reduced pressure below 40 °C using a Büchi rotary evaporator, followed by evacuation (< 0.1 mm Hg) to constant sample weight. Deionized water was obtained from a Milli-Q reagent water system (Millipore Co., Milford, MA). Unless otherwise specified, solutions of NH<sub>4</sub>Cl, NaHCO<sub>3</sub>, HCl, NaOH, and KOH refer to aqueous solutions. Brine refers to a saturated aqueous solution of NaCl.

## 1.2 Purification Techniques

All reactions and fractions from column chromatography were monitored by thin layer chromatography (TLC) using glass plates with a UV fluorescent indicator (normal SiO<sub>2</sub>, Merck 60 F<sub>254</sub>; reversed-phase, Merck RP-8 and RP-18 F<sub>254S</sub>). One or more of the following methods were used for visualization: UV absorption by fluorescence quenching; iodine staining; phosphomolybdic acid:ceric sulfate:sulfuric acid:H<sub>2</sub>O (10 g:1.25 g:12 mL:238 mL) spray; and 50% sulfuric acid spray. Flash chromatography was performed according to the method of Still *et al.*<sup>175</sup> using Merck type 60, 230-400 mesh silica gel.

## 1.3 Instrumentation for Compound Characterization

Melting points are uncorrected and were determined on a Thomas-Hoover or a Büchi oil immersion apparatus using open capillary tubes. Optical rotations were measured on a Perkin Elmer 241 polarimeter with a microcell (10 cm, 1 mL) at ambient temperature and are reported in units of 10<sup>-1</sup> deg cm<sup>2</sup> g<sup>-1</sup>. All optical rotations reported were referenced against air and were measured at the sodium D line and values quoted are valid within ±1°. Infrared spectra (IR) were recorded on a Nicolet Magna 750 or a 20SX FT-IR spectrometers. Cast refers to the evaporation of a solution on a NaCl plate. Mass spectra (MS) were recorded on a Kratos AEIMS-50 high resolution (HRMS), electron impact ionization (EI), MS-9 fast atom bombardment with argon (FAB), and Micromass ZabSpec Hybrid Sector-TOF positive mode electrospray ionization (ES),

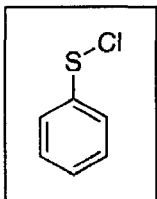
instruments. Microanalyses were obtained using a Perkin Elmer 240 or Carlo Erba 1108 elemental analyzers.

Nuclear magnetic resonance (NMR) spectra were obtained on Bruker AM-300 and WM-360 or Inova Varian 300, 500 and 600 MHz spectrometers.  $^1\text{H}$  NMR chemical shifts are reported in parts per million (ppm) downfield relative to tetramethylsilane (TMS) using the residual proton resonance of solvents as reference:  $\text{CDCl}_3$   $\delta$  7.24,  $\text{CD}_2\text{Cl}_2$   $\delta$  5.32,  $\text{D}_2\text{O}$   $\delta$  4.72, and  $\text{CD}_3\text{OD}$   $\delta$  3.30.  $^{13}\text{C}$  NMR chemical shifts are reported relative to  $\text{CDCl}_3$   $\delta$  77.0,  $\text{CD}_2\text{Cl}_2$   $\delta$  53.8, and  $\text{CD}_3\text{OD}$   $\delta$  49.0.  $^1\text{H}$  NMR data are reported in the following order: multiplicity (s, singlet; d, doublet; t, triplet; q, quartet; qn, quintet and m, multiplet), number of protons, coupling constant ( $J$ ) in Hertz (Hz) and assignment. When appropriate, the multiplicity is preceded by br, indicating that the signal was broad. All literature compounds had IR,  $^1\text{H}$  NMR, and mass spectra consistent with the assigned structures.

## 2. Sulfenimines and Pseudoxazolones

### 2.1 Experimental Data for Compounds

#### Benzenesulfonyl Chloride (10).



To an ice cooled solution of benzenethiol (11.0 g, 10.2 mL, 0.10 mol) in  $\text{CCl}_4$  (175 mL) was added triethylamine (15 drops) followed by sulfuryl chloride (14.8 gm, 8.8 mL, 0.11 mol). The reaction mixture was stirred at  $0^\circ\text{C}$  for 30 minutes followed by solvent removal under reduced pressure to yield a dark red oil. The desired product was purified from the mixture by vacuum distillation, boiling at  $110^\circ\text{C}$  under a measured vacuum of 9 torr as expected based on literature preparation.<sup>176</sup> The product was isolated as a red oil (12.4 g, 86%) and immediately stored under Ar at  $-40^\circ\text{C}$  (without further characterization) to minimize the facile degradation of the product to the corresponding disulfide. Attempts at spectroscopic characterization showed only the disulfide degradation product as indicated in the literature.<sup>176</sup>

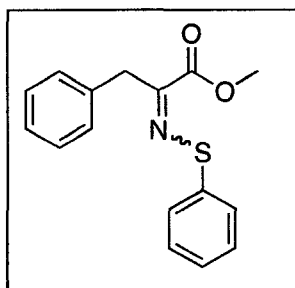
#### General Procedure for Preparation of Amino Acid Ester Sulfenimines (11-18).

The amino acid ester hydrochloride (10.0 mmol) was slurried in a mixture of dry  $\text{CH}_2\text{Cl}_2$  (50 mL) and propylene oxide (5.0 mL) at  $0^\circ\text{C}$  under Ar. Triethylamine (1.4 mL, 10.0 mmol) and 4 Å molecular sieves (5.0 g) were next added followed by benzenesulfonyl chloride (4.3 g, 3.5 mL, 30.0 mmol). The mixture was stirred for 3 hours with

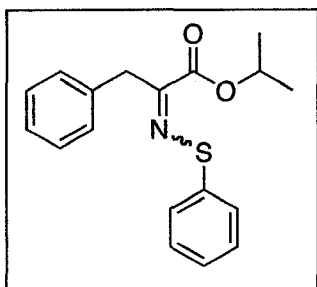


temperature maintained between 0 and 5 °C after which it was heated to reflux temperature for an additional two hours. The sieves were separated from the mixture by filtration and the solvent removed under reduced pressure. The crude product was pre-purified by treatment with ethyl acetate and filtration to remove the insoluble phenyl disulfide followed by final purification via flash chromatography (SiO<sub>2</sub>, 1:1 hexane/CH<sub>2</sub>Cl<sub>2</sub>, R<sub>f</sub> typically 0.2 – 0.4).

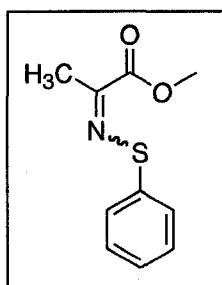
**Methyl α-[(phenyl)thio]imino]benzenepropionate (11).**



Yellow solid (91%), *E/Z* isomers ~ 3:1; mp 53-55 °C; IR (CHCl<sub>3</sub> cast) 3060, 3027, 2950, 1716, 1582, 1494, 1479 cm<sup>-1</sup>; <sup>1</sup>H NMR (CDCl<sub>3</sub>, 300 MHz) δ 7.57 (m, ~1.5H, major isomer Ar-H), 7.48 (m, ~0.5H, minor isomer Ar-H), 7.41-7.20 (m, 8H, both isomers Ar-H), 4.11 (s, ~1.5H, major isomer benzylic -CH<sub>2</sub>-), 4.11 (s, ~0.5H, minor isomer benzylic -CH<sub>2</sub>-), 3.85 (s, ~0.5H, minor isomer -OCH<sub>3</sub>), 3.83 (s, ~1.5H, major isomer -OCH<sub>3</sub>); <sup>13</sup>C NMR (CDCl<sub>3</sub>, 75 MHz) δ 161.5, 159.8 (C=O both isomers), 155.9, 150.7 (C=N both isomers), 141.1, 137.6, 136.7, 134.4, 129.3, 129.1, 128.9, 128.7, 128.6, 128.3, 126.9, 126.5, 125.1, 124.7 (ArC both isomers), 70.0, 69.6 (O-CH(CH<sub>3</sub>)<sub>2</sub> both isomers), 43.3, 39.3 (-CH<sub>2</sub>- both isomers), 21.7 (O-CH(CH<sub>3</sub>)<sub>2</sub> both isomers); HRMS (EI) Calcd for C<sub>18</sub>H<sub>19</sub>NO<sub>2</sub>S 313.11365, found 313.11374 M<sup>+</sup>; Anal. Calcd for C<sub>18</sub>H<sub>19</sub>NO<sub>2</sub>S: C, 68.98; H, 6.11; N, 4.47. Found: C, 69.24; H, 6.15; N, 4.49.

**Propyl  $\alpha$ -[[phenylthio]imino]benzenepropionate (12).**

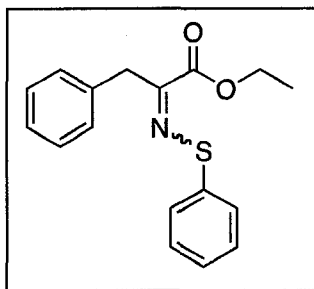
Yellow oil (96%), *E/Z* isomers ~ 3:2; IR (CHCl<sub>3</sub> cast) 3061, 3028, 2980, 2934, 1708, 1583, 1495 cm<sup>-1</sup>; <sup>1</sup>H NMR (CDCl<sub>3</sub>, 300 MHz)  $\delta$  7.57 (m, ~1.2H, major isomer Ar-H), 7.48 (m, ~0.8H, minor isomer), 7.41-7.20 (m, 8H, both isomers), 5.10 (septet, 1H, both isomers  $-\text{OCH}(\text{CH}_3)_2$ ,  $J = 6.2$  Hz), 4.10 (s, ~1.2H, major isomer benzylic  $-\text{CH}_2-$ ), 4.00 (s, ~0.8H, minor isomer benzylic  $-\text{CH}_2-$ ), 1.29 (d, ~3.6H, major isomer  $-\text{OCH}(\text{CH}_3)_2$ ,  $J = 6.2$  Hz), 1.26 (d, ~2.4H, minor isomer  $-\text{OCH}(\text{CH}_3)_2$ ,  $J = 6.2$  Hz); <sup>13</sup>C NMR (CDCl<sub>3</sub>, 75 MHz)  $\delta$  162.6, 160.5 ( $\text{C}=\text{O}$  both isomers), 155.5, 149.9 ( $\text{C}=\text{N}$  both isomers), 140.9, 137.3, 136.6, 134.2, 129.3, 129.2, 129.1, 128.8, 128.7, 128.5, 127.3, 127.0, 126.6, 125.8, 124.6 (ArC both isomers), 52.9, 52.6 (O-CH<sub>3</sub> both isomers), 43.1, 39.2 ( $-\text{CH}_2-$  both isomers); HRMS (EI) Calcd for C<sub>16</sub>H<sub>15</sub>NO<sub>2</sub>S 285.08234, found 285.08229 M<sup>+</sup>; Anal. Calcd for C<sub>16</sub>H<sub>15</sub>NO<sub>2</sub>S: C, 67.34; H, 5.30; N, 4.91. Found: C, 67.47; H, 5.28; N, 4.85.

**Methyl 2-[[phenylthio]imino] propionate (13).**

Yellow solid (72%), *E/Z* isomers ~ 10:1; mp 38-40 °C; IR (CHCl<sub>3</sub> cast) 3060, 2950, 1718, 1584, 1479, 1439, 1366 cm<sup>-1</sup>; <sup>1</sup>H NMR (CDCl<sub>3</sub>, 300 MHz)  $\delta$  7.57 (m, 2H, both isomers Ar-H), 7.38 (m, 2H, both isomers), 7.25 (m, 1H, both isomers), 3.84 (s, 0.2H, minor isomer  $-\text{OCH}_3$ ), 3.82 (s, 2.8H, major isomer  $-\text{OCH}_3$ ), 2.36 (s, 0.2H, minor isomer  $-\text{CH}_3$ ); 2.31 (s, 2.8H, major isomer  $-\text{CH}_3$ ); <sup>13</sup>C NMR (CDCl<sub>3</sub>, 75 MHz)  $\delta$  162.6 ( $\text{C}=\text{O}$  major isomer), 154.3 ( $\text{C}=\text{N}$  major isomer), 137.3, 129.1, 127.3, 126.0 (ArC major isomer), 52.8

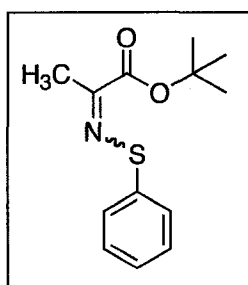
(O-CH<sub>3</sub> major isomer), 19.2 (-CH<sub>3</sub> major isomer); HRMS (EI) Calcd for C<sub>10</sub>H<sub>11</sub>NO<sub>2</sub>S 209.05106, found 209.05117 M<sup>+</sup>; Anal. Calcd for C<sub>10</sub>H<sub>11</sub>NO<sub>2</sub>S: C, 57.39; H, 5.30; N, 6.69. Found: C, 57.53; H, 5.28; N, 6.45.

**Ethyl  $\alpha$ -[[(phenyl)thio]imino]benzenepropionate (14).**



Yellow solid (89%), *E/Z* isomers ~ 2:1; mp 33-34 °C; IR (CHCl<sub>3</sub> cast) 3061, 3028, 2981, 2936, 2903, 1711, 1583 cm<sup>-1</sup>; <sup>1</sup>H NMR (CDCl<sub>3</sub>, 300 MHz)  $\delta$  7.57 (m, ~1.3H, major isomer Ar-H), 7.49 (m, ~0.7H, minor isomer), 7.40 – 7.20 (m, 8H, both isomers), 4.28 (q, 2H, both isomers –OCH<sub>2</sub>CH<sub>3</sub>, *J* = 7.14 Hz), 4.10 (s, ~1.3H, major isomer benzylic –CH<sub>2</sub>-), 4.01 (s, ~0.7H, minor isomer benzylic –CH<sub>2</sub>-), 1.32 (q, 3H, both isomers –OCH<sub>2</sub>CH<sub>3</sub>, *J* = 7.14 Hz); <sup>13</sup>C NMR (CDCl<sub>3</sub>, 75 MHz)  $\delta$  162.1, 160.5 (C=O both isomers), 155.8, 150.3 (C=N both isomers), 141.1, 137.6, 136.8, 134.3, 129.4, 129.3, 129.1, 128.9, 128.8, 127.1, 127.0, 126.7, 126.6, 125.5, 124.8 (ArC both isomers), 62.0 (O-CH<sub>2</sub>CH<sub>3</sub> both isomers), 43.3, 39.3 (-CH<sub>2</sub>- both isomers), 14.2, 14.1 (O-CH<sub>2</sub>CH<sub>3</sub> both isomers); HRMS (EI) Calcd for C<sub>17</sub>H<sub>17</sub>NO<sub>2</sub>S 299.09799, found 299.09814 M<sup>+</sup>; Anal. Calcd for C<sub>17</sub>H<sub>17</sub>NO<sub>2</sub>S: C, 68.20; H, 5.72; N, 4.68. Found: C, 67.96; H, 5.65; N, 4.60.

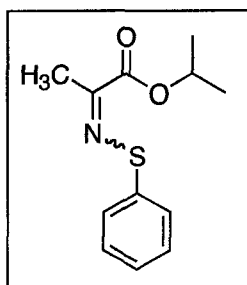
**Butyl 2-[[(phenyl)thio]imino] propionate (15).**



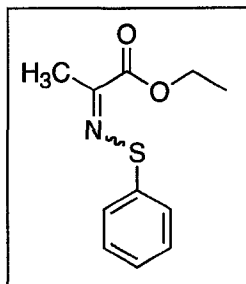
Yellow solid (87%), *E/Z* isomers ~ 4:1; mp 46-47 °C; IR (CHCl<sub>3</sub> cast) 3060, 2978, 2932, 1708, 1584, 1479, 1458 cm<sup>-1</sup>; <sup>1</sup>H NMR (CDCl<sub>3</sub>, 300 MHz)  $\delta$  7.58 (m, 2H, both isomers Ar-H), 7.36 (m, 2H, both isomers), 7.22 (m, 1H, both isomers), 2.32 (s, ~0.6H, minor

isomer  $-\underline{\text{CH}}_3$ ), 2.25 (s,  $\sim 2.4\text{H}$ , major isomer  $-\underline{\text{CH}}_3$ ), 1.56 (s,  $\sim 1.8\text{H}$ , minor isomer  $-\text{OC}(\underline{\text{CH}}_3)_3$ ), 1.54 (s,  $\sim 7.2\text{H}$ , major isomer  $-\text{OC}(\underline{\text{CH}}_3)_3$ );  $^{13}\text{C}$  NMR ( $\text{CDCl}_3$ , 75 MHz)  $\delta$  161.1, 160.0 ( $\underline{\text{C}}=\text{O}$  both isomers), 155.6, 150.3 ( $\underline{\text{C}}=\text{N}$  both isomers), 141.2, 137.9, 128.9, 128.8, 126.7, 126.5, 125.1, 125.0 ( $\text{Ar}\underline{\text{C}}$  both isomers), 83.2, 82.0 ( $\text{O}-\underline{\text{C}}(\text{CH}_3)_3$  both isomers), 28.0, 27.9 ( $\text{O}-\underline{\text{C}}(\text{CH}_3)_3$  both isomers), 24.1, 19.1 ( $\underline{\text{C}}\text{H}_3$  both isomers); HRMS (EI) Calcd for  $\text{C}_{13}\text{H}_{17}\text{NO}_2\text{S}$  251.09801, found 251.09782  $\text{M}^+$ ; Anal. Calcd for  $\text{C}_{13}\text{H}_{17}\text{NO}_2\text{S}$ : C, 62.12; H, 6.82; N, 5.57. Found: C, 62.15; H, 7.04; N, 5.54.

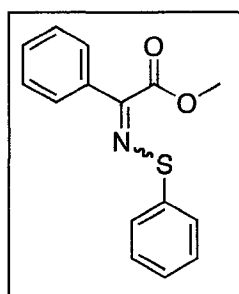
**<sup>1</sup>Propyl 2-[[*(phenyl)thio*]imino] propionate (16).**



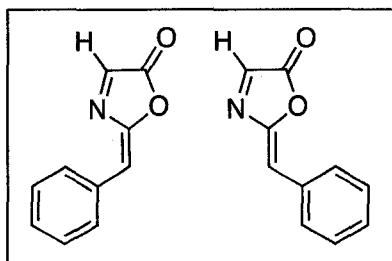
Yellow oil (93%), *E/Z* isomers  $\sim 6:1$ ; IR ( $\text{CHCl}_3$  cast) 3061, 2981, 2937, 1709, 1584, 1479, 1467  $\text{cm}^{-1}$ ;  $^1\text{H}$  NMR ( $\text{CDCl}_3$ , 300 MHz)  $\delta$  7.57 (m, 2H, both isomers Ar-H), 7.36 (m, 2H, both isomers), 7.22 (m, 1H, both isomers), 5.13 (m, 1H, both isomers  $\text{O}-\underline{\text{C}}\text{H}(\text{CH}_3)_2$ ), 2.34 (s,  $\sim 0.4\text{H}$ , minor isomer  $-\underline{\text{C}}\text{H}_3$ ), 2.28 (s,  $\sim 2.6\text{H}$ , major isomer  $-\underline{\text{C}}\text{H}_3$ ), 1.35 (d,  $\sim 0.8\text{H}$ , minor isomer  $\text{O}-\underline{\text{C}}\text{H}(\text{CH}_3)_2$ ,  $J = 6.2$  Hz), 1.33 (d,  $\sim 5.2\text{H}$ , major isomer  $\text{O}-\underline{\text{C}}\text{H}(\text{CH}_3)_2$ ,  $J = 6.2$  Hz);  $^{13}\text{C}$  NMR ( $\text{CDCl}_3$ , 75 MHz)  $\delta$  167.8, 166.3 ( $\underline{\text{C}}=\text{O}$  both isomers), 161.7, 154.9 ( $\underline{\text{C}}=\text{N}$  both isomers), 138.4, 137.7, 129.0, 128.8, 126.9, 126.7, 125.4, 125.2 ( $\text{Ar}\underline{\text{C}}$  both isomers), 70.0, 69.6 ( $\text{O}-\underline{\text{C}}\text{H}(\text{CH}_3)_2$  both isomers), 21.9, 21.8 ( $\text{O}-\underline{\text{C}}\text{H}(\text{CH}_3)_2$  both isomers); HRMS (EI) Calcd for  $\text{C}_{12}\text{H}_{15}\text{NO}_2\text{S}$  237.08235, found 237.08209  $\text{M}^+$ ; Anal. Calcd for  $\text{C}_{12}\text{H}_{15}\text{NO}_2\text{S}$ : C, 60.73; H, 6.37; N, 5.90. Found: C, 60.48; H, 6.39; N, 5.70.

**Ethyl 2-[[phenylthio]imino]propionate (17).**

Yellow oil (82%), *E/Z* isomers ~ 8:1; IR (CHCl<sub>3</sub> cast) 3060, 2981, 1712, 1583, 1479, 1441, 1393 cm<sup>-1</sup>; <sup>1</sup>H NMR (CDCl<sub>3</sub>, 300 MHz) δ 7.57 (m, 2H, both isomers Ar-H), 7.36 (m, 2H, both isomers), 7.24 (m, 1H, both isomers), 5.13 (m, 2H, both isomers O-CH<sub>2</sub>CH<sub>3</sub>), 2.35 (s, ~0.3H, minor isomer -CH<sub>3</sub>), 2.30 (s, ~2.7H, major isomer -CH<sub>3</sub>), 1.35 (t, 3H, both isomers O-CH<sub>2</sub>CH<sub>3</sub>), *J* = 7.15 Hz); <sup>13</sup>C NMR (CDCl<sub>3</sub>, 75 MHz) δ 162.2, (C=O major isomer), 154.7 (C=N major isomer), 137.5, 128.8, 127.1, 125.7 (ArC major isomer), 61.9 (O-CH<sub>2</sub>CH<sub>3</sub> major isomer), 19.2 (-CH<sub>3</sub> major isomer), 14.2 (O-CH<sub>2</sub>CH<sub>3</sub> major isomer); HRMS (EI) Calcd for C<sub>11</sub>H<sub>13</sub>NO<sub>2</sub>S 223.06670, found 223.06631 M<sup>+</sup>; Anal. Calcd for C<sub>11</sub>H<sub>13</sub>NO<sub>2</sub>S: C, 59.17; H, 5.87; N, 6.27. Found: C, 58.91; H, 5.77; N, 5.89.

**Methyl α-[[phenylthio]imino]benzeneacetate (18).**

Yellow solid (86%), *E/Z* isomers ~ 3:1; mp 57-58 °C; IR (CHCl<sub>3</sub> cast) 3063, 2951, 1707, 1580, 1529, 1494, 1477 cm<sup>-1</sup>; <sup>1</sup>H NMR (CDCl<sub>3</sub>, 300 MHz) δ 7.74 – 7.21 (m, 10H, both isomers Ar-H), 3.98 (s, ~2.2H, major isomer -OCH<sub>3</sub>), 3.88 (s, ~0.8H, minor isomer -OCH<sub>3</sub>); <sup>13</sup>C NMR (CDCl<sub>3</sub>, 75 MHz) δ 162.3 (C=O major isomer), 150.5 (C=N major isomer), 129.8, 129.4, 128.8, 128.3, 128.0, 126.9, 125.6, 125.2 (ArC major isomer), 52.7 (O-CH<sub>3</sub> major isomer); HRMS (EI) Calcd for C<sub>15</sub>H<sub>13</sub>NO<sub>2</sub>S 271.06671, found 271.06623 M<sup>+</sup>; Anal. Calcd for C<sub>15</sub>H<sub>13</sub>NO<sub>2</sub>S: C, 66.40; H, 4.83; N, 5.16. Found: C, 66.20; H, 4.80; N, 5.12.

**21a (E)- and 21b (Z)-2-Benzylidene-2H-oxazol-5-one**

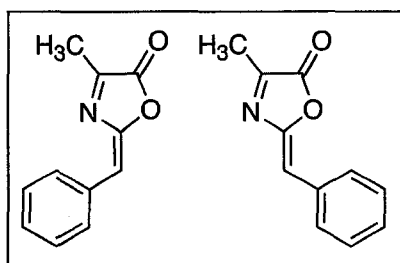
The title compounds were prepared by a modification of the procedure of King.<sup>37</sup> To a solution of glycine (0.93 g, 23.0 mmol) in H<sub>2</sub>O (7.5 mL), THF (3 mL) and NaOH (1.09 g, 27.30 mmol) at 0–5 °C was added DL-2-chloro-2-phenylacetyl chloride (2.0 mL, 13.0 mmol). The reaction mixture was stirred for 30 min then warmed to room temperature over 30 min. The mixture was basified with 1 M NaOH and then washed with EtOAc (2 × 15 mL). The aqueous layer was acidified to pH 1 with 4 M HCl, extracted with EtOAc (3 × 15 mL) and dried over MgSO<sub>4</sub>. Evaporation of the solvent followed by recrystallization of the residue from MeOH–diethyl ether–hexane furnished the α-chloro acid as a white solid (0.84 g, 37%). A portion of the acid (0.5 g, 2.2 mmol) was dissolved in acetic anhydride (20 mL) and pyridine (5 mL). The mixture was stirred for 1 h after which it was evaporated *in vacuo*. The crude product was taken up in EtOAc (15 mL) and washed successively with 1 M HCl (2 × 10 mL) and then saturated aq. NaHCO<sub>3</sub> (2 × 10 mL). The EtOAc extract was dried over MgSO<sub>4</sub> and concentrated *in vacuo*. The crude product was purified by column chromatography (SiO<sub>2</sub>, Et<sub>2</sub>O–hexane 4:1, R<sub>f</sub> 0.58, 0.44) to afford the title products which were recrystallized from hexane to give yellow crystalline solids.

Data for **21a**: (0.03 g, 9%, over 2 steps); mp 94–96 °C; IR (CHCl<sub>3</sub> cast) 3065, 1837, 1789, 1670, 1602, 1498, 1087 cm<sup>-1</sup>; <sup>1</sup>H NMR (acetone-*d*<sub>6</sub>, 300 MHz) δ 8.12 (d, 1H, CHN, *J* = 2.0 Hz), 7.99–7.94 (m, 2H, ArH), 7.49–7.36 (m, 3H, ArH), 6.72 (d, 1H, CHC, *J* = 2.0 Hz); <sup>13</sup>C NMR (acetone-*d*<sub>6</sub>, 125 MHz) δ 163.5 (CO<sub>2</sub>), 156.6 (CCH), 151.4 (CHN),

133.5 (Ar-C quaternary), 132.0, 130.4, 126.7 (Ar-CH), 113.6 (CHC); HRMS (EI) calcd for C<sub>10</sub>H<sub>7</sub>O<sub>2</sub>N 173.0477, found 173.0476 M<sup>+</sup>.

Data for **21b**: (0.14 g, 37%, over 2 steps); mp 92–94 °C; IR (CHCl<sub>3</sub> cast) 3036, 1838, 1780, 1672, 1508, 1451, 1361, 1284, 1088; <sup>1</sup>H NMR (acetone-*d*<sub>6</sub>, 300 MHz) δ 8.05 (d, 1H CHN, *J* 1.0 Hz), 7.86–7.80 (m, 2H, ArH), 7.52–7.38 (m, 3H, ArH), 6.62 (s, 1H, CHC); <sup>13</sup>C NMR (acetone-*d*<sub>6</sub>, 125 MHz) δ 164.3 (CO<sub>2</sub>), 156.0 (CCH), 148.7 (CHN), 133.3 (Ar-C quaternary), 131.8, 130.8, 129.9 (Ar-CH), 114.5 (CHC); HRMS (EI) calcd for C<sub>10</sub>H<sub>7</sub>O<sub>2</sub>N 173.0477, found 173.0479 M<sup>+</sup>.

#### **22a (E)- and 22b (Z)-2-Benzylidene-4-methyl-2H-oxazol-5-one**



The title compounds were prepared as described for **19a** and **19b**. Reaction of *D/L* alanine (1.0 g, 11.2 mmol), NaOH (0.93 g, 23.0 mmol) and DL-2-chloro-2-phenylacetyl chloride (2.0 mL, 13.1 mmol) gave the

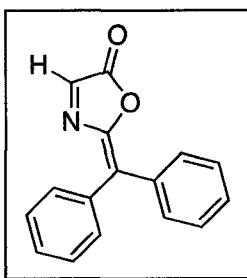
corresponding chloro acid which was cyclized with acetic anhydride (30 mL) and pyridine (6 mL). Purification by column chromatography (SiO<sub>2</sub>, 100% CH<sub>2</sub>Cl<sub>2</sub>, R<sub>f</sub> 0.55, 0.35) gave the title products which were recrystallized from hexane to give yellow crystalline solids.

Data for **22a**: (778 mg, 38%, over 2 steps); mp 145–146 °C; IR (CHCl<sub>3</sub> cast) 3066, 1774, 1651, 1451, 1377, 1368, 1222 cm<sup>-1</sup>; <sup>1</sup>H NMR (CDCl<sub>3</sub>, 300 MHz) δ 7.88–7.82 (m, 2H ArH), 7.42–7.29 (m, 3H ArH), 6.40 (s, 1H CHC), 2.44 (d, 3H CH<sub>3</sub>, *J* = 0.9 Hz); <sup>13</sup>C NMR (CDCl<sub>3</sub>, 75 MHz) δ 163.3 (CO<sub>2</sub>), 159.9 (CN), 153.7 (CHC), 132.5 (Ar-C), 130.9,

129.3, 128.6 (Ar-CH), 111.2 (CHC), 14.0 (CH<sub>3</sub>); HRMS (EI) calcd for C<sub>11</sub>H<sub>9</sub>O<sub>2</sub>N 187.0633, found 187.0629 M<sup>+</sup>.

Data for **22b**: (782 mg, 38%, over 2 steps); mp 126–127 °C; IR (CHCl<sub>3</sub> cast) 3052, 2946, 1785, 1659, 1492, 1379, 1350, 1290, 1235 cm<sup>-1</sup>; <sup>1</sup>H NMR (CDCl<sub>3</sub>, 300 MHz) δ 7.78–7.74 (m, 2H ArH), 7.44–7.31 (m, 3H ArH), 6.32 (s, 1H CHC), 2.40 (d, 3H CH<sub>3</sub>, *J* = 0.82 Hz); <sup>13</sup>C NMR (CDCl<sub>3</sub>, 75 MHz) δ 163.6 (CO<sub>2</sub>), 156.9 (CN), 134.5 (CHC), 132.3 (Ar-C), 130.9, 129.8, 129.0 (Ar-CH), 112.4 (CHC), 13.7 (CH<sub>3</sub>); HRMS (EI) calcd for C<sub>11</sub>H<sub>9</sub>O<sub>2</sub>N 187.0633, found 187.0635 M<sup>+</sup>.

### 2-(Diphenylmethylene)-2H-oxazol-5-one (**24**)

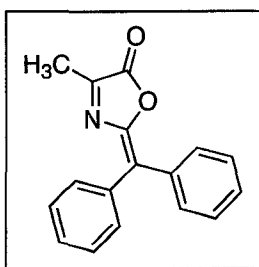


2-Chloro-2,2-diphenylacetyl chloride **23** (6.6 g, 25.0 mmol) was dissolved in dry EtOAc (100 mL) under an argon atmosphere. Propylene oxide (1.75 mL, 25.0 mmol) was added, followed by glycine (1.7 g, 22.5 mmol). The mixture was heated to reflux and stirred overnight. The reaction mixture was cooled to room temperature, filtered and concentrated *in vacuo*. Recrystallization from EtOAc–petroleum ether gave the α-chloro-diphenylacetyl glycine as a white solid (6.48 g, 94%). A portion of this compound (1.0 g, 3.30 mmol) was dissolved in dry MeCN (40 mL) under an argon atmosphere. 1,3-Dicyclohexylcarbodiimide (0.75 g, 3.6 mmol) was added, followed by propylene oxide (0.70 g, 9.9 mmol). The mixture was stirred overnight, filtered and concentrated *in vacuo*. Purification by flash chromatography (SiO<sub>2</sub>, petroleum ether–diethyl ether 3:1, *R<sub>f</sub>* 0.45) gave the title compound **24** (0.70 g, 85%) as a yellow solid: mp 111–113 °C; IR (CHCl<sub>3</sub> cast) 3057, 1792, 1770, 1099 cm<sup>-1</sup>; <sup>1</sup>H NMR (CDCl<sub>3</sub>, 300 MHz) δ 7.74 (s, 1H, CHN),



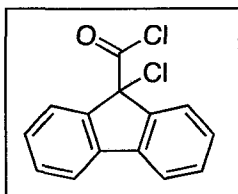
7.55–7.36 (m, 10H, ArH);  $^{13}\text{C}$  NMR ( $\text{CDCl}_3$ , 75 MHz)  $\delta$  163.7 ( $\text{CO}_2$ ), 153.3 ( $\text{CCPh}_2$ ), 146.9 ( $\text{CHN}$ ), 136.3, 136.1 (Ar-C quaternary), 132.2, 131.7, 130.0 (Ar-CH), 129.7 ( $\text{Ph}_2\text{CC}$ ), 129.6, 128.4, 128.1 (Ar-CH); HRMS (EI) Calcd for  $\text{C}_{16}\text{H}_{11}\text{O}_2\text{N}$  249.07898, found 249.07862  $\text{M}^+$ ; Anal. Calcd for  $\text{C}_{16}\text{H}_{11}\text{O}_2\text{N}$ : C, 77.10; H, 4.45; N, 5.62. Found: C, 76.70; H, 4.34; N, 5.46.

### 2-(Diphenylmethylene)-4-methyl-2H-oxazol-5-one (25)



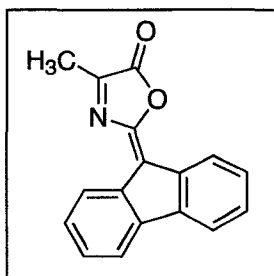
D/L Alanine (2.0 g, 22.5 mmol) was suspended in ethyl acetate (50 mL) containing propylene oxide (1.75 mL, 25.0 mmol). To the mixture was added a solution of 2-chloro-2,2-diphenylacetyl chloride **23** (6.6 g, 25.0 mmol) in EtOAc (50 mL). After heating at reflux under argon for 24 h a homogenous solution was obtained. The solvent was removed *in vacuo* and the reaction mixture was cooled to 0 °C and treated with TFAA (7.5 mL, 53 mmol). Within 10 minutes of the TFAA addition a large amount of bright orange precipitate formed. The mixture was quenched with 100 mL of ice-water and the crude solid recovered was recrystallized from acetonitrile-isopropyl alcohol to yield bright yellow crystals (4.0 g, 68% over 2 steps); mp 158–159 °C, lit.,<sup>177</sup> mp 155–156 °C; IR ( $\text{CHCl}_3$  cast) 3055, 1767, 1727, 1625, 1537, 1490  $\text{cm}^{-1}$ ;  $^1\text{H}$  NMR ( $\text{CDCl}_3$ , 300 MHz)  $\delta$  7.45–7.36 (m, 10H, ArH), 2.40 (s, 3H,  $\text{CH}_3$ );  $^{13}\text{C}$  NMR ( $\text{CDCl}_3$ , 75 MHz)  $\delta$  164.2 ( $\text{CO}_2$ ), 157.6 ( $\text{CN}$ ), 151.4 ( $\text{CCPh}_2$ ), 136.6, 136.5 (Ar-C quaternary), 132.0, 131.4, 129.3, 129.1, 128.3, 128.1, (Ar-CH), 125.9 ( $\text{Ph}_2\text{CC}$ ), 13.9 ( $\text{CH}_3$ ); HRMS (EI) Calcd for  $\text{C}_{17}\text{H}_{13}\text{O}_2\text{N}$  263.0946, found 263.0946  $\text{M}^+$ .

### 9-Chloro-9H-fluorene-9-carbonyl chloride (27)



The title compound was prepared using the method of Stolle.<sup>40</sup> 9H-fluorene-9-carboxylic acid **26** (5.0 g, 23.8 mmol) and thionyl chloride (17 mL, 238 mmol) were combined and heated to reflux under argon. After 48 h a small aliquot of the mixture was removed and analysed by <sup>1</sup>H NMR to look for the disappearance of the 9-H proton, indicating reaction completion. The excess thionyl chloride was removed *in vacuo* and the residue recrystallized from benzene to yield yellow crystals (1.81 g, 29%); mp 110–112 °C, lit.<sup>40</sup> mp 113 °C; <sup>1</sup>H NMR (CDCl<sub>3</sub>, 300 MHz) δ 7.72 (d, 2H, ArH, *J* = 7.5 Hz), 7.62 (d, 2H, ArH, *J* = 7.6 Hz), 7.50 (dd, 2H, ArH, *J* = 7.5 Hz), 7.40 (dd, 2H, ArH, *J* = 7.6 Hz); HRMS (EI) Calcd for C<sub>14</sub>H<sub>8</sub>O<sub>3</sub>Cl<sub>2</sub> 261.9952, found 261.9952 M<sup>+</sup>.

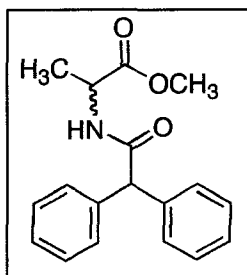
### 2-Fluoren-9-ylidene-4-methyl-2H-oxazol-5-one (28)



D/L Alanine (300 mg, 3.4 mmol) was suspended in ethyl acetate (15 mL) containing propylene oxide (0.30 mL, 4.0 mmol). To the mixture was added a solution of 9-chloro-9H-fluorene-9-carbonyl chloride **27** (987 mg, 3.75 mmol) in EtOAc (15 mL). After heating at reflux under argon for 24 hours the mixture was bright orange with a precipitate present. After solvent removal *in vacuo* the residue was redissolved in CH<sub>2</sub>Cl<sub>2</sub> and cooled to 0 °C. The solution was stirred under Ar, during which TFAA (1.0 mL, 7.0 mmol) was added. After warming to room temperature over 2 h the mixture was quenched with 30 mL aqueous 5% NaHCO<sub>3</sub>. After being washed with H<sub>2</sub>O (3 × 50 mL) and brine (50 mL), the organic layer was dried over sodium sulfate. Solvent removal *in vacuo* yielded a

bright orange solid which was recrystallized from toluene to yield the title compound (0.68 g, 76%, over 2 steps); mp 255 °C (decomp.); IR (CHCl<sub>3</sub> cast) 3059, 1882, 1777, 1652, 1604, 1447, 1376, 1357, 1290 cm<sup>-1</sup>; <sup>1</sup>H NMR (CDCl<sub>3</sub>, 300 MHz) δ, 8.46–8.40 (d, 1H, ArH, *J* = 7.8 Hz), 8.18–8.12 (d, 1H, ArH, *J* = 7.8 Hz), 7.68–7.60 (m, 2H, ArH), 7.40–7.24 (m, 4H, ArH), 2.55 (s, 3H, CH<sub>3</sub>); <sup>13</sup>C NMR (CDCl<sub>3</sub>, 75 MHz) δ 163.3 (CO<sub>2</sub>), 158.4 (CN), 151.1 (Ar<sub>2</sub>CC), 141.7, 141.3, 135.8, 135.2 (Ar-C quaternary), 130.3, 129.7, 127.9, 127.7, 127.6, 127.5, 120.2, 120.1 (Ar-CH), 119.4 (Ar<sub>2</sub>CC), 14.2 (CH<sub>3</sub>); HRMS (EI) calcd for C<sub>17</sub>H<sub>11</sub>O<sub>2</sub>N 261.0791, found 261.0790 M<sup>+</sup>.

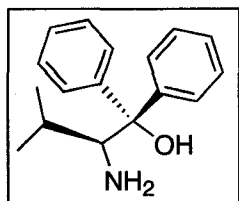
**(*R,S*)-2-(2,2-Diphenyl-acetyl-amino)-propionic acid methyl ester (29)**



Alanine diphenyl pseudoxazolone **25** (66 mg, 0.25 mmol) was dissolved in dry chloroform (2.0 mL) and added at -50 °C to a solution of NaBH<sub>4</sub> (15 mg, 0.38 mmol) in chloroform (5.0 mL) and methanol (0.25 mL). The mixture was left to stir under argon for the night and quenched the following morning by addition of methanol (10.0 mL) containing concentrated HCl (15 drops). After solvent removal and purification by flash column chromatography (SiO<sub>2</sub>, 100% EtOAc, *R<sub>f</sub>* 0.85) the title compound was obtained as a white solid (63 mg, 85%); mp 123-124 °C; IR (CHCl<sub>3</sub> cast) 3242, 3062, 3027, 3007, 2951, 1733, 1700, 1663, 1640, 1597 cm<sup>-1</sup>; <sup>1</sup>H NMR (CDCl<sub>3</sub>, 500 MHz) δ, 7.38–7.24 (m, 10H, ArH), 6.21 (d br, 1H, NH, *J* = 6.6 Hz), 4.93 (s, 1H, Ph<sub>2</sub>CH-CO-), 4.61 (pent, 1H, -NCH-CO<sub>2</sub>Me, *J* = 7.1 Hz), 3.72 (s, 3H, -OCH<sub>3</sub>), 1.35 (d, 3H, -NHC-CH<sub>3</sub>); <sup>13</sup>C NMR (CDCl<sub>3</sub>, 75 MHz) δ 173.3 (CO<sub>2</sub>), 171.5 (-CON), 139.2 (Ar-C quaternary), 128.9, 128.7, 127.3 (Ar-CH), 58.8 (-OCH<sub>3</sub>), 52.4 (Ar<sub>2</sub>CC), 48.3 (-NCHCH<sub>3</sub>), 18.2 (CH<sub>3</sub>CHN-); HRMS

(EI) calcd for  $C_{18}H_{19}O_3N$  297.1365, found 297.1360  $M^+$ ; Anal. Calcd for  $C_{18}H_{19}O_4N$ : C, 72.71; H, 6.44; N, 4.71. Found: C, 72.40; H, 6.50; N, 4.66.

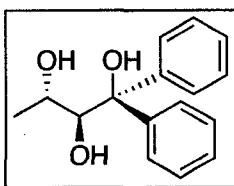
**(2*S*)-Amino-3-methyl-1,1-diphenyl-butan-1-ol (32)**



The known compound **32**<sup>43</sup> was prepared using the following procedure. In a flame dried 500 mL round bottom flask fitted with a reflux condenser and addition funnel was placed freshly ground magnesium turnings (2.5g, 100 mmol). The addition funnel was charged with dry THF (75 mL) and freshly distilled bromobenzene (14.1 g, 9.5 mL, 90 mmol). A portion of the bromobenzene solution (10 mL) was immediately added, and upon heating, the reaction initiated and was maintained by dropwise addition of the remaining bromobenzene/THF solution (~ 20 minutes total addition time). The mixture was then refluxed for 1 hour after which the Grignard solution was cooled to 0°C in an ice bath. L-Valine methyl ester hydrochloride (3.0 gm, 18.0 mmol) was then slowly added to the Grignard. The mixture was allowed to warm gradually to room temperature and left to stir under argon overnight. The following morning the mixture was diluted by addition of diethyl ether (75 mL) and quenched by addition of saturated  $NH_4Cl$  (75 mL). After stirring for 30 minutes, the organic layer was separated and dried with brine (2 x 75 mL) and  $Na_2SO_4$ . Following solvent removal under vacuum, the crude white residue was recrystallized from ethanol/water to yield white needles. The crystals were recovered, dissolved in  $Et_2O$  (100 mL), and dried with  $MgSO_4$ . Upon evaporation of solvent the desired product **32** was obtained (1.5 g, 35%) as a white solid: mp 94-95 °C (lit.<sup>43</sup> mp 94-95 °C);  $[\alpha]_D^{26}$  -123.4° (*c* 7.28,  $CHCl_3$ ) (lit.<sup>43</sup>  $[\alpha]_D^{20}$  -127.7° (*c* 0.639,  $CHCl_3$ )); IR ( $CHCl_3$  cast) 3345, 3283, 3085,

3056, 3022, 2963, 2927, 2875, 1951, 1652, 1594, 1490  $\text{cm}^{-1}$ ;  $^1\text{H}$  NMR ( $\text{CDCl}_3$ , 300 MHz) (lit.<sup>43</sup>)  $\delta$  7.60 (m, 2H, ArH), 7.48 (m, 2H, ArH), 7.32-7.10 (m, 6H, ArH), 4.40 (s br, 1H, -OH), 3.83 (d, 1H,  $J = 2.1$  Hz,  $-\text{NH}_2\text{CHC}-$ ), 1.74 (d sept, 1H,  $J = 7.0$  Hz,  $J = 2.1$  Hz,  $(\text{CH}_3)_2\text{CHNH}_2$ ), 1.60-1.10 (s br, 2H,  $-\text{NH}_2$ ), 0.91 (d, 3H,  $J = 7.1$  Hz,  $-\text{CH}_3$ ), 0.87 (d, 3H,  $J = 6.8$  Hz,  $-\text{CH}_3$ );  $^{13}\text{C}$  NMR ( $\text{CDCl}_3$ , 75 MHz)  $\delta$  148.1, 144.9 (ArC quaternary), 128.4, 128.0, 126.6, 126.3, 125.9, 125.5 (ArCH), 79.7 ( $-\text{OCPh}_2$ ), 60.2 ( $-\text{NH}_2\text{CH}-$ ), 27.9 ( $(\text{CH}_3)_2\text{CH}$ ), 23.0 ( $\text{CH}_3$ ), 16.1 ( $\text{CH}_3$ ); HRMS (CI) Calcd for  $\text{C}_{17}\text{H}_{22}\text{NO}$  256.1701, found 256.1678  $[\text{M}+\text{H}]^+$ ; Anal. Calcd for  $\text{C}_{17}\text{H}_{21}\text{NO}$ : C, 79.96; H, 8.29; N, 5.49. Found: C, 79.40; H, 8.30; N, 5.43.

#### (2*S*,3*S*)-1,1-Diphenylbutane-1,2,3-triol (40)

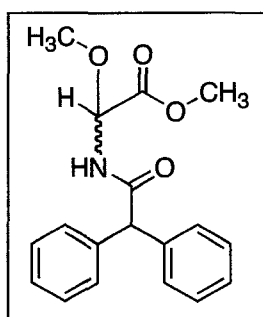


The title compound was generated based upon an existing method starting from L-threonine.<sup>178</sup> L-Threonine (4.4 g, 37 mmol) suspended in water (10 mL) at  $-5^\circ\text{C}$  was treated simultaneously with a solution of  $\text{NaNO}_2$  (2.8 g, 40 mmol in 4.0 mL water) and  $\text{H}_2\text{SO}_4$  (1.2 mL, 20 mmol, in 3.0 mL water). The two solutions were added at a rate such that the temperature was maintained between 0 and  $5^\circ\text{C}$ . After stirring overnight at room temperature, the water was evaporated and the residue dissolved in ethanol. Filtration to remove salts followed by evaporation yielded the dihydroxy acid as a light yellow oil. The crude dihydroxy acid was directly transformed to the methyl ester by treatment with HCl saturated methanol (5.0 mL) at reflux temperature overnight. Evaporation of the solvent gave the crude dihydroxy ester, which was directly transformed into the 1,3-dioxolane derivative by treatment with acetone (5.0 mL), 2,2-dimethoxypropane (15 mL), and *p*-

toluenesulfonic acid (100 mg). After stirring at room temperature for 24 hours, the solvent was evaporated and the product was partitioned between water and ethyl acetate. After drying the organic layer with brine and Na<sub>2</sub>SO<sub>4</sub>, solvent was removed under vacuum and the (4*S*)-*trans*-2,2,5-trimethyl-1,3-dioxolane-4-carboxaldehyde was purified by Kugelrohr distillation. The protected dihydroxy ester (1.9 gm, 10.9 mmol) was then slowly added (as a solution in 10.0 mL THF) to freshly prepared phenyl magnesium bromide (35.0 mmol in 30.0 mL THF) at 0 °C. The mixture was warmed gradually to room temperature and left to stir under argon overnight. The following morning the mixture was diluted by addition of diethyl ether (45 mL) and quenched with saturated NH<sub>4</sub>Cl (45 mL). After stirring for 10 minutes the organic layer was separated and dried with brine (2 x 50 mL) and Na<sub>2</sub>SO<sub>4</sub> followed by solvent removal under vacuum to yield a yellow solid (shown to be the desired product in major proportion by <sup>1</sup>H NMR). The crude Grignard product was directly deprotected by first dissolving in THF (50 mL) followed by addition of 1 M aqueous HCl (50 mL). After heating at 60°C for 4 hours the deprotection was deemed complete by TLC (EtOAc/hexane 1:10, R<sub>f</sub> (starting material) = 0.3, R<sub>f</sub> (product) = 0.0) after which the mixture was cooled to room temperature and neutralized by addition of saturated NaHCO<sub>3</sub> (80 mL). The product was extracted with diethyl ether (3 x 50 mL), and the combined ether extracts were washed with brine (2 x 50 mL) followed by drying over Na<sub>2</sub>SO<sub>4</sub>. Following solvent removal a light yellow solid remained. Recrystallization from EtOAc/hexane yielded white needles (1.21 g, 43% over 2 steps): mp 81-84°C; [α]<sub>D</sub><sup>26</sup> -146.4° (c 4.75, CHCl<sub>3</sub>); IR (CHCl<sub>3</sub> cast) 3558, 3417, 3088, 3063, 3031, 2983, 2935, 1956, 1597, 1500, 1488, 1447 cm<sup>-1</sup>; <sup>1</sup>H NMR (CDCl<sub>3</sub>, 300 MHz) δ 7.55 (m, 2H, ArH), 7.44-7.15 (m, 8H, ArH), 4.31 (m, 2H, CH<sub>3</sub>CHO- and -

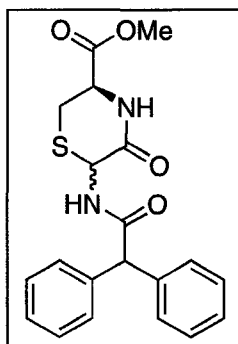
CCHOH overlapped), 3.81 (s br, 1H, -OH), 2.81 (s br, 1H, -OH), 2.55 (s br, 1H, -OH), 1.18 (d, 3H,  $J = 6.5$  Hz, -CH<sub>3</sub>); <sup>13</sup>C NMR (CDCl<sub>3</sub>, 75 MHz)  $\delta$  144.8, 144.6 (ArC quaternary), 128.5, 127.3, 127.0, 126.3, 125.2 (ArCH), 81.8 (-OCPh<sub>2</sub>), 75.3 (-CCHO-), 67.3 (CH<sub>3</sub>CHO-), 20.7 (CH<sub>3</sub>); HRMS (ES) Calcd for C<sub>16</sub>H<sub>18</sub>O<sub>3</sub> 258.1256, found 281.0 [M+Na]<sup>+</sup>; Anal. Calcd for C<sub>17</sub>H<sub>21</sub>NO: C, 74.39; H, 7.02. Found: C, 74.20; H, 6.90.

**(*R,S*)-2-(2,2-Diphenyl-acetyl-amino)-methoxy-acetic acid methyl ester (41)**



Glycine diphenyl pseudoxazolone **24** (100 mg, 0.40 mmol) was dissolved in dry methanol (5.0 mL) and stirred at room temperature under argon for 3 hours. During this time the bright yellow color of the imine dissipated. After solvent removal and purification by flash column chromatography (SiO<sub>2</sub>, diethyl ether/hexane, 1:1, R<sub>f</sub> 0.25) the title compound was obtained as a white solid (100 mg, 80%); mp 113-116 °C; IR (CHCl<sub>3</sub> cast) 3315, 3061, 3028, 2952, 2834, 1958, 1752, 1666, 1599, 1520 cm<sup>-1</sup>; <sup>1</sup>H NMR (CDCl<sub>3</sub>, 300 MHz)  $\delta$ , 7.39–7.20 (m, 10H, ArH), 6.50 (d br, 1H, NH,  $J = 7.4$  Hz), 5.55 (d, 1H, -OCHN-,  $J = 7.4$  Hz), 4.95-4.90 (s, 1H, Ph<sub>2</sub>CH-CO-), 3.78 (s, 3H, -OCH<sub>3</sub>), 3.42 (s, 3H, -OCH<sub>3</sub>); <sup>13</sup>C NMR (CDCl<sub>3</sub>, 75 MHz)  $\delta$  175.3 (CO<sub>2</sub>), 169.8 (-CON), 140.7 (Ar-C quaternary), 129.9, 129.5, 128.2 (Ar-CH), 80.0 (Ar<sub>2</sub>CC), 58.8 (-OCH<sub>3</sub>), 56.3 (-OCH<sub>3</sub>), 53.1 (OCHN); HRMS (EI) calcd for C<sub>18</sub>H<sub>19</sub>O<sub>4</sub>N 313.1314, found 313.1312 M<sup>+</sup>; Anal. Calcd for C<sub>18</sub>H<sub>19</sub>O<sub>4</sub>N: C, 68.99; H, 6.11; N, 4.47. Found: C, 68.70; H, 5.84; N, 4.29.

**(3*R*,6*RS*)-6-(2,2-Diphenyl-acetylamino)-5-oxo-thiomorpholine-3-carboxylic acid methyl ester (45)**



L-Cysteine methyl ester hydrochloride **44** (69 mg, 0.40 mmol) and triethylamine (56  $\mu$ L, 1 eq.) were added to diethyl ether (10 mL). To the mixture was added a solution of the glycine diphenyl pseudoxazolone **24** (100 mg, 0.40 mmol) and glacial acetic acid (50  $\mu$ l) in diethyl ether (8 mL). After stirring at room temperature under argon for 24 hours the bright yellow color of the imine had dissipated and a white precipitate was present. After solvent removal *in vacuo*, the residue was redissolved in hot methanol and adsorbed onto silica gel followed by purification by flash column chromatography (SiO<sub>2</sub>, CH<sub>2</sub>Cl<sub>2</sub>/MeOH, 95:5, R<sub>f</sub> 0.5). Solvent removal *in vacuo* yielded the title compound as a 4:1 mixture of diastereomers (122 mg, 79%); mp 121 - 123 °C; IR (CHCl<sub>3</sub> cast) 3306, 3028, 2942, 1745, 1678, 1652, 1524, 1496, 1455 cm<sup>-1</sup>; <sup>1</sup>H NMR (CDCl<sub>3</sub>, 300 MHz)  $\delta$ , 7.35–7.20 (m, 10H, both diastereomers ArH), 6.80-6.70 (m, 1H, both diastereomers -NH), 6.60–6.50 (m, 1H, both diastereomers -NH), 5.45-5.40 (m, 1H, both diastereomers -SCHN-), 4.95-4.90 (m, 1H, both diastereomers Ph<sub>2</sub>CH-CO-), 4.43-4.31 (m, 1H, both diastereomers -CH<sub>2</sub>CHN-), 3.80-3.75 (m, 3H, both diastereomers -OCH<sub>3</sub>), 3.35-2.90 (m, 2H, both diastereomers -SCH<sub>2</sub>CHN-); <sup>13</sup>C NMR (CDCl<sub>3</sub>, 75 MHz)  $\delta$  171.7 (CO<sub>2</sub>), 168.9 (-CON), 166.7 (-CON), 138.7 (Ar-C quaternary), 128.9, 128.8, 127.4 (Ar-CH), 58.7 (Ar<sub>2</sub>CC), 54.1 (SCHN), 53.6 (CH<sub>2</sub>CHCO<sub>2</sub>), 48.8 (-OCH<sub>3</sub>), 30.9 (SCH<sub>2</sub>CHN); HRMS (EI) calcd for C<sub>20</sub>H<sub>20</sub>O<sub>4</sub>N<sub>2</sub>S 384.1144, found 384.1147 M<sup>+</sup>; Anal. Calcd for C<sub>20</sub>H<sub>20</sub>O<sub>4</sub>N<sub>2</sub>S: C, 62.48; H, 5.24; N, 7.29. Found: C, 62.64; H, 5.07; N, 7.15.



**Crystallographic Data for 21b and 22a.**

All data was acquired by Dr. Robert McDonald (X-ray Crystallography Laboratory, University of Alberta) using a Bruker P4/RA/SMART 1000 CCD diffractometer. All intensity measurements were performed using graphite monochromated Mo-K $\alpha$  radiation ( $\lambda = 0.71073 \text{ \AA}$ ).

*Crystal data for pseudoxazolone 21b:* C<sub>10</sub>H<sub>7</sub>NO<sub>2</sub>:  $M = 173.17$ , triclinic,  $a = 5.5390(6) \text{ \AA}$ ,  $b = 7.2645(8) \text{ \AA}$ ,  $c = 10.4291(11) \text{ \AA}$ ,  $\alpha = 83.673(2)^\circ$ ,  $\beta = 83.789(2)^\circ$ ,  $\gamma = 80.624(8)^\circ$ ,  $U = 409.77(8) \text{ \AA}^3$ ,  $T = 193 \text{ K}$ , space group  $P\bar{1}$  (No. 2),  $Z = 2$ ,  $\mu(\text{Mo-K}\alpha) = 0.100 \text{ mm}^{-1}$ , 2179 reflections measured, 1641 unique ( $R_{\text{int}} = 0.0164$ ) which were used in all least squares calculations,  $R_1(F) = 0.0374$  (for 1365 reflections with  $F_o^2 \geq 2\sigma(F_o^2)$ ),  $wR_2(F^2) = 0.1037$  (for all unique reflections). Data deposited in Cambridge crystallography database.

*Crystal data for pseudoxazolone 22a:* C<sub>11</sub>H<sub>9</sub>NO<sub>2</sub>:  $M = 187.19$ , triclinic,  $a = 6.0008(8) \text{ \AA}$ ,  $b = 7.2370(11) \text{ \AA}$ ,  $c = 10.9282(16) \text{ \AA}$ ,  $\alpha = 95.403(2)^\circ$ ,  $\beta = 101.029(3)^\circ$ ,  $\gamma = 102.046(3)^\circ$ ,  $U = 451.10(11) \text{ \AA}^3$ ,  $T = 193 \text{ K}$ , space group  $P\bar{1}$  (No. 2),  $Z = 2$ ,  $\mu(\text{Mo-K}\alpha) = 0.096 \text{ mm}^{-1}$ , 2409 reflections measured, 1827 unique ( $R_{\text{int}} = 0.0422$ ) which were used in all least squares calculations,  $R_1(F) = 0.0449$  (for 1207 reflections with  $F_o^2 \geq 2\sigma(F_o^2)$ ),  $wR_2(F^2) = 0.1113$  for all unique reflections). Data deposited in Cambridge crystallography database.

### **3. Mattacin and Polymyxin B Peptides**

#### **3.1 Bacterial Strains and Culture Conditions**

The producer strain, *Paenibacillus kobensis* M, was isolated from a soil/manure sample mix by our collaborators and grown aerobically at 30 °C on tryptic soy agar (TSA) or in broth (TSB) with shaking (250 rpm). *Escherichia coli* BF2, a laboratory strain, was used as the standard sensitive strain. *E. coli* strains were grown aerobically at 37 °C on Luria-Bertani (LB) agar or in broth with shaking (250 rpm).

#### **3.2 Antimicrobial Activity Monitoring During Purification**

Antimicrobial activity was monitored by inhibition of indicator strain growth on agar plates. Plates were prepared by inoculating 200 mL of molten (48 °C) TSA (40 g/L) with 1.0 mL of a culture of the indicator organism *E. coli* BF2 (0.5% inoculum). The molten agar was swirled gently and then dispensed in 20 mL aliquots onto sterile Petri plates, allowed to cool, and then stored at 4 °C. When performing activity assays, small wells (4.6 mm diameter) were made in the seeded agar plates, and 50 µL aliquots of the solutions to be tested were dispensed into each well. The plates were then incubated at 30 °C with growth of the indicator being visible within as a little as three hours.

#### **3.3 Isolation of Mattacin (52)**

In a 10 mL culture tube of TSB, a pre-culture of *Paenibacillus kobensis* M was grown for 24 hours with shaking (200 rpm) at 30 °C. A 1 liter batch of TSB was then prepared by first passing through a column (2.5 x 30 cm) packed with 40 g of Amberlite

XAD-16 resin (Sigma) to remove hydrophobic components from the media that would otherwise interfere with the isolation of the hydrophobic peptide. After sterilization (15 min at 121 °C) and cooling, this modified TSB was inoculated with the entire 10 mL *P. kobensis* M preculture (1% inoculum). After a total growth time of 16 to 24 h at 30 °C with shaking (200 rpm), the cells were removed by centrifugation (20 min, 8000 rpm). The supernatant was then passed through a column (2.5 x 50 cm) containing 60 g of Amberlite XAD-16 resin at a flow rate of 15 mL/min with the aid of a peristaltic pump. The column was then washed with 30% ethanol (500 mL). The active peptide was then removed from the Amberlite column by washing with 500 mL of 70% isopropanol (pH 2 by addition of 1 M HCl). All fractions were assessed for activity using the well-plate assay described above. The active 70% isopropanol (pH 2) fraction was evaporated to dryness by rotary evaporation and the yellow residue was redissolved/suspended in 5.0 mL of purified (milli-Q system, Millipore, Bedford, Mass.) water. This concentrated solution was next applied to a column (2.5 x 50 cm) containing G25 superfine Sephadex (Amersham Pharmacia, Uppsala, Sweden) at a flow rate of 1.0 mL/min. The column was eluted with purified (milli-Q) water overnight and 10 mL fractions were collected. Each fraction was again assayed for activity as described above. The active fractions 17-20 were then pooled, evaporated, and redissolved in 10 mL of 20% isopropanol in preparation for reverse phase HPLC. Complete isolation of mattacin required 2 separate HPLC methods both employing a C<sub>18</sub> steel-walled column (Vydac, 10 x 250 mm, 5 mm). During the initial HPLC work, all isolable peaks were assessed for antimicrobial activity using the aforementioned well-plate assay until the retention time of mattacin was well established. In the first method, a 1.0 mL injection was applied and a gradient of water

and isopropanol (0.1% TFA), starting at 20% and climbing to 30% isopropanol over 25 min, was used (flow rate = 2.5 mL/min, detection at 225 nm). Using this method, most of the polar impurities were removed with mattacin eluting in a broad peak ( $R_t=18-20$  min) somewhat later. The active fractions were pooled, evaporated to dryness, and redissolved in 6.0 mL of 45% methanol. The second method employed the same  $C_{18}$  column using a gradient of water and methanol (0.1% TFA), starting at 45% and climbing to 60% methanol over 15 min (flow rate = 4.0 mL/min, detection at 225 nm). Under these conditions, mattacin was isolated as a single peak ( $R_t = 10-11$  min). Using 1.0 mL sample injections, the entire sample was purified, and after pooling, evaporation of the methanol, and lyophilization, as much as 5 mg of pure mattacin was obtained as a white powder from a 1 litre culture.

### 3.4 Amino Acid Analysis

Mattacin (100  $\mu$ g) was hydrolyzed at 160 °C for 1 h with 100  $\mu$ L of 5.7 M HCl/0.1% phenol in a sealed, evacuated tube. The solvent was removed by vacuum centrifugation (Speed-Vac), and the dried hydrolysate was redissolved in 0.2 M sodium citrate buffer (pH 2.0). Analysis was achieved through cation-exchange chromatography with a Beckman 6300 amino acid analysis instrument using a 120 x 2.5 mm ID column with post-column detection/quantitation by reaction with ninhydrin at 135 °C.

### 3.5 Acetylation of Mattacin

With the knowledge that mattacin contained threonine, it was reasoned that a crystalline product, suitable for x-ray analysis, might be obtained by chemically

modifying nucleophilic residues. To this end, 500  $\mu\text{g}$  of mattacin was treated with 1.0 mL of pyridine/acetic anhydride (1:1) on ice. The mixture was allowed to warm to room temperature, and after 4 h a small aliquot (10  $\mu\text{l}$ ) was removed for mass spectrometric analysis revealing a total of eight acetylations had occurred. Attempts at recrystallizing the octa-acetate of mattacin were unsuccessful under a variety of conditions.

### 3.6 Mass Spectrometry

Samples for MALDI mass analysis were prepared using sinnapinic acid as matrix. Solutions containing the sample peptide were mixed in even part with a stock solution of sinnapinic acid (10 mg/mL) in 60% acetonitrile (0.1% TFA). A thin layer of sinnapinic acid was deposited on the surface of the gold target plate by delivery of a small droplet (0.7  $\mu\text{L}$ ) of a solution containing sinnapinic acid (4 mg/mL) in 50% acetone/50% methanol. After evaporation of the acetone/methanol, a 0.3  $\mu\text{l}$  droplet of the solution containing the sample peptide-matrix mixture was deposited on top of the fresh matrix layer on the plate. The solvent was evaporated at 1 atm prior to analysis. Mass spectra were recorded with a single-stage reflectron, MALDI-TOF mass spectrometer (Applied BioSystems (Foster City, CA) API QSTAR Pulsar with an oMALDI source).<sup>179</sup> Tandem MS/MS was performed using two different instruments. The QSTAR instrument, described above, was of the geometry QqTOF, where MS/MS analysis was achieved through collision-induced dissociation (CID) in the rf-only section of the mass spectrometer ( $Q_2$ ) after mass selection with the  $Q_1$  resolving quadrupole. Fragment ions were detected in the orthogonal time-of-flight section of the mass spectrometer. Ion generation was achieved through MALDI ionization using sinnapinic acid as the matrix.

The QSTAR was equipped with a 20 Hz pulsed nitrogen laser operating at 337 nm. CID MS/MS analysis was completed using argon as the collision gas in Q<sub>2</sub>. Also used in a second MS/MS analysis was a ThermoFinnegan (San Jose, CA) LCQ XP ion trap instrument equipped with a nanospray source. The peptide sample was dissolved in 1:1 methanol:water acidified with 0.2% formic acid and loaded into a PicoTip (New Objective, Woburn, MA) nanospray tip. Static nanospray was achieved by applying ~800 V to the nanospray tip. Ions were introduced to the mass spectrometer, and prior to MS/MS analysis all ions except the parent ion of interest were ejected from the ion trap. MS/MS and MS<sup>3</sup> analysis was completed using resonance excitation with the mass range up to m/z 1200 for the fragment ions.

### 3.7 NMR Spectroscopy

NMR spectra were obtained in 90% H<sub>2</sub>O-10% D<sub>2</sub>O solution at 27 °C and at a peptide concentration of 2 mM. Spectra were acquired on a Varian Inova 600 spectrometer; data matrices of 2048 detected and 512 (1024 for DQF-COSY) indirect data points with 64 (96 for ROESY) scans were recorded and processed using a 90 shifted sine bell window function (unshifted for DQF-COSY). Water signal suppression was achieved by transmitter presaturation. All experiments were performed at pH 2 (H<sub>2</sub>O contained 0.1% TFA); under these conditions, the possibility of peptide aggregation was reduced due to DAB-γ-amino group protonation. The assignment of <sup>1</sup>H resonances was performed using standard two-dimensional DQF-COSY,<sup>180</sup> TOCSY<sup>181</sup> (mixing time 70 ms), and two-dimensional NOE experiments (NOESY<sup>182</sup> and ROESY,<sup>183</sup> mixing times 200 ms). The temperature coefficients of the amide proton chemical shifts were

calculated using a series of one-dimensional experiments performed at four different temperatures in the range 27-42 °C. The two-dimensional transferred NOE (TRNOE) experiment<sup>184,185</sup> with mixing times of 200 ms was recorded for a mixture of mattacin and LPS that corresponded to an 8:1 w/w ratio of both components; these conditions yielded moderately broadened lines in the amide region of the mattacin 1D spectrum. A three-dimensional structure of mattacin was computed based on NOE restraints derived from the TRNOE experiment using a dynamical annealing protocol in CNS 1.1 (© Yale University). Fifty representative structures were calculated based on 62 NOEs. The NOEs were classified as strong, medium, and weak, corresponding to maximum distances of 3.0, 4.0 and 5.0 Å, respectively, based on the volumes of the assigned cross-peaks in the NOESY spectrum.

### 3.8 Stereochemical Analysis of Mattacin

Mattacin (1 mg) was hydrolyzed (1 mL 6 N HCl, 110 °C, 18 h), and the hydrolysate was dried under a nitrogen stream and then derivatized using an Alltech (Deerfield, IL) PFP-IPA (pentafluoropropanamide – isopropyl ester) amino acid derivatization kit (#18093). The dried hydrolysate was treated with 0.2 N HCl (5 min at 110 °C) and dried under an argon stream. To this, 150 µL of acetyl chloride and 500 µL of isopropanol were added, and the mixture was heated at 110 °C for 45 min. After drying with an argon stream, the derivatizing agent, pentafluoropropionic anhydride (1 mL dissolved in 2 mL of CH<sub>2</sub>Cl<sub>2</sub>), was added, and the solution was heated at 115 °C for 15 min, blown dry with argon, and then solubilized in CH<sub>2</sub>Cl<sub>2</sub>. For standards, 10 mg each of D/L threonine, leucine, and α,γ-diaminobutyric acid were subjected to the identical

derivatization sequence. Also, 1 mg of purified polymyxin B was hydrolyzed and treated in the same fashion to serve as standard. All samples were analyzed by GC-MS under identical conditions, using a Heliflex Chirasil-Val, 50 m x 0.25 mm x 0.16 mm column (Alltech #13636), helium as carrier gas (0.6 mL/min), and a temperature gradient beginning at 90 °C (5 min hold) and ramping to 160 °C (3 °C/min) followed by a 12 minute hold.

### 3.9 Isothermal Titration Calorimetry

LPS from *E. coli* strain 055:B5 was obtained from Sigma and polymyxin B sulfate was purchased from Fluka. The polymyxin B was further purified by RP HPLC (using methods identical to those described above for mattacin) and the LPS preparation was used as purchased. Using a molecular weight estimate of 20,000 Da for the LPS monomer<sup>80</sup> a 0.05 mM LPS solution was prepared by dissolving LPS in 50 mM sodium phosphate buffer, pH 6.8, along with equimolar quantities of triethylamine with respect to the anionic groups in the LPS monomer (4 eq.). The solution was vortexed vigorously for 15 min and sonicated for 5 minutes prior to use. Titrations were performed using the OMEGA high-sensitivity microcalorimeter manufactured by MicroCal Inc. (Northampton, MA) as previously described.<sup>186</sup> For measurement of heat exchanges accompanying the binding of polymyxin B or mattacin to LPS, the LPS solution was loaded into the sample cell of the calorimeter (volume = 1.4423 mL) and the reference cell was filled with water containing 0.05% sodium azide. Next, polymyxin B or mattacin, in the same buffer, was placed in a 250 µl syringe at a concentration of 1.25 mM (25-fold higher than that of the LPS). The system was allowed to equilibrate at 20.0



°C and a stable baseline recorded before initiating an automated titration. A titration sequence involved 7.2  $\mu\text{L}$  aliquot injections of polymyxin B or mattacin delivered over 10 s at 5 min intervals into the sample cell. Throughout the titration, the contents of the cell were stirred continuously at 400 rpm.

## **4. Lacticin 3147 and Lantibiotic Peptides**

### **4.1 Bacterial Strains and Culture Conditions**

The producer strain, *Lactococcus lactis* subsp. *lactis* DPC3147 was originally isolated by our collaborators (Hill and Ross) from an Irish kefir grain, and grown at 30°C for 24 hours without aeration in 10 mL Difco M17 broth supplemented with 0.5% (wt/vol) lactose. *L. lactis* subsp. *cremoris* HP, a laboratory strain, was used as a standard sensitive strain and was cultured in Difco M17 broth (supplemented with 0.5% (wt/vol) lactose) for 24 hour at 30 °C without aeration.

### **4.2 Antimicrobial Activity Monitoring During Purification**

Antimicrobial activity was monitored by inhibition of indicator strain growth on agar plates. Plates were prepared by inoculating 200 mL of molten (48°C) Difco M17 Agar (40.0 g/L) with 1.0 mL of a culture of indicator organism *L. lactis* subsp. *cremoris* HP (0.5% inoculum). The molten agar was swirled gently and then dispensed in 20 mL aliquots onto sterile Petri plates, allowed to cool, and stored at 4°C. When performing activity assays, small wells (4.6 mm diameter) were made in the seeded agar plates, and 50 µL aliquots of the solutions to be tested were dispensed into each well. The plates were then incubated at 30°C for 24 hours.

### 4.3 Isolation of Lacticin (from Supernatant)

In 10 mL culture tubes of Difco M17 broth, a pre-culture of *L. lactis* subsp. *lactis* DPC3147 was grown for 24 hours at 30°C. The most practical fermentation volume was a four litre scale. The media contained, per 800 mL; tryptone 2.5 g, yeast extract 5.0 g, 1.5 g D/L- methionine, 50 mg MnSO<sub>4</sub>•4H<sub>2</sub>O, and 125 mg MgSO<sub>4</sub>. Prior to sterilization the media was passed through a column (2.5 x 40 cm) packed with 75 g of Amberlite XAD-16 resin (Aldrich) to remove hydrophobic components that would otherwise interfere with the isolation of the hydrophobic peptide. After dividing the 3.2 litres of clarified media into separate 800 mL volumes it was sterilized (15 min. at 121° C), as were separate solutions of D-glucose (100 g/L) and β-glycerophosphate (190 g/L). The D-glucose and β-glycerophosphate solutions were sterilized separately to prevent caramelization of the media, making the concomitant peptide isolation less problematic. After sterilization of the media, 100 mL of both the glucose and β-glycerophosphate solutions was added to each 800 mL media solution to achieve a final volume of 1 L.

Each 1 L volume of fermentation media was inoculated with a 10 mL *L. lactis* subsp. *lactis* DPC3147 preculture (1% inoculum). After a total growth time of 16 to 24 hours at 30°C without aeration, the peptide isolation was initiated with the addition of 75 mg of DTT to each 1 L fermentation volume. From this point on, all buffers used in the isolation procedure contained 0.1 M DTT to protect the lantibiotic peptides from oxidation.

The cells from the four 1 litre fermentations were removed by centrifugation (20 min., 8000 rpm), and the four litres of supernatant combined. The supernatant was then passed through a column (2.5 x 50 cm) containing 60 g of Amberlite XAD-16 resin at a flow rate of 15 mL/min with the aid of a peristaltic pump. The column was then washed with 30% ethanol (1.0 L). The active peptides were then removed from the Amberlite column by washing with 1.0 L of 70% isopropanol (pH 2 by addition of 1 M HCl). After rotary evaporation of the 70% isopropanol to a volume of ~100 mL, the concentrated bacteriocin solution was loaded onto a disposable column containing 10 gm of C<sub>18</sub> silica (Varian C<sub>18</sub> megabond elut). Prior to sample loading, the C<sub>18</sub> silica was pre-equilibrated with 60 mL of 100% methanol. After loading the sample the column was washed successively with 60 mL of purified (mili-Q system, Millipore, Bedford, Mass.) water, 60 mL of 30% ethanol, and 40 mL of 25% isopropanol. The active peptides were removed from the column by washing with 100 mL of 70% isopropanol (pH 2 by the addition of 1M HCl). The 70% isopropanol fraction was then reduced to a 20 mL volume by rotary evaporation and lyophilized.

The lyophilized sample was then dissolved in 14 mL of 24% isopropanol and the lacticin 3147 A1 and A2 peptides were isolated by reverse phase HPLC using a steel walled column (Vydac, 10 x 250 mm, 5 µm). In the method employed a 1.0 mL injection was applied and a gradient of water and isopropanol (0.1% TFA) was used to separate and isolate each peptide. Gradient: 24% isopropanol for 5 min, then climbing to 44% in 20 min returning to 24% in 0.5 min and remaining at this concentration for an additional 5 min (flow rate 2.25 mL/min., detection at 220 nm). The A1 peptide was isolated as a

single peak ( $R_t=21.4$  min.) and the A2 peptide was isolated as a single, broad peak ( $R_t=27.4$  min.) The active fractions for each peptide were pooled and stored on dry ice until separation was completed.

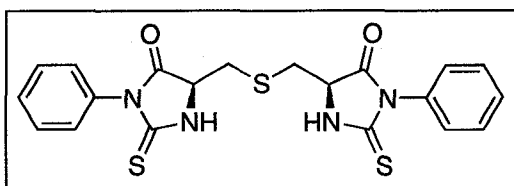
After complete separation, pooling of the active fractions, evaporation of the isopropanol, and lyophilization, approximately 200 to 400  $\mu\text{g}$  of each peptide was recovered from 4 litres of culture. All purified samples were stored under argon at  $-80$  °C to prevent the very rapid oxidation of the peptides.

#### 4.4 Mass Spectrometry

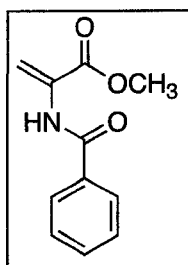
Samples for MALDI mass analysis were prepared using sinnapinic acid as matrix. Solutions containing the sample peptide were mixed in even part with a stock solution of sinnapinic acid (10 mg/mL) in 60% acetonitrile (0.1% TFA). A thin layer of sinnapinic acid was deposited on the surface of the gold target plate by delivery of a small droplet (0.7  $\mu\text{L}$ ) of a solution containing sinnapinic acid (4 mg/mL) in 50% acetone/50% methanol. After evaporation of the acetone/methanol, a 0.3  $\mu\text{L}$  droplet of the solution containing the sample peptide-matrix mixture was deposited on top of the fresh matrix layer on the plate. The solvent was evaporated at 1 atm prior to analysis. Mass spectra were recorded with a single-stage reflectron, MALDI-TOF mass spectrometer (Applied BioSystems (Foster City, CA) API QSTAR Pulsar with an *o*MALDI source).<sup>179</sup>

## 4.5 Experimental Data for Compounds

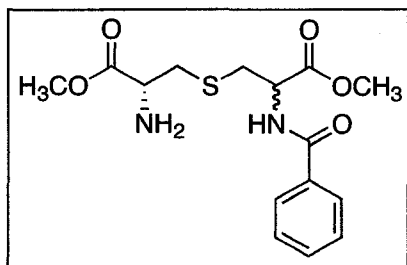
### (D,L)-Lanthionine bis-PTH (57).



D,L-Lanthionine (**55**) (1.0 g, 4.8 mmol) was suspended in 30 mL pyridine/water (1:1) (50 mL). The pH was adjusted to 9.0 by addition of 1.0 M NaOH. While stirring at 40 °C, phenyl isothiocyanate (1.3 mL, 10.6 mmol, 2.2 eq.) was added dropwise. After complete addition of the phenyl isothiocyanate the mixture was extracted with toluene (3 x 25 mL) to remove pyridine and excess phenyl isothiocyanate. The aqueous layer was acidified to pH 3 by addition of 1 M HCl followed by ethyl acetate extraction (3 x 45 mL). After drying over Na<sub>2</sub>SO<sub>4</sub> and removal of solvent by rotary evaporation a white foam remained. This material was then treated with trifluoroacetic acid (15 mL) and stirred under argon at room temperature for 2 hours. The trifluoroacetic acid was removed under vacuum to yield a yellow oil which solidified after addition of water (3 drops). The crude product was then recrystallized from glacial acetic acid to yield the desired compound as white needles. (1.3 g, 60% over 2 steps); mp 213-215 °C; IR (μscope) 3484, 3146, 2991, 1958, 1890, 1748 cm<sup>-1</sup>; <sup>1</sup>H NMR (DMSO-*d*<sub>6</sub>, 600 MHz) δ 7.50–7.41 (m, 6H, ArH), 7.28–7.24 (m, 4H, ArH), 4.80-4.75 (m, 2H, α-H), 3.31 (br s, 2H, NH), 3.19-3.08 (m, 4H, -CH<sub>2</sub>-); <sup>13</sup>C NMR (DMSO-*d*<sub>6</sub>, 125 MHz) δ 182.9 (C=O), 173.0 (CS), 133.2 (Ar-C quaternary), 128.7, 128.6, 128.5 (Ar-CH), 59.7 (α-C), 34.0 (CH<sub>2</sub>); HRMS (ES) Calcd for C<sub>20</sub>H<sub>18</sub>N<sub>4</sub>O<sub>2</sub>S<sub>3</sub>Na 465.04851, found 465.04805 M+Na.

**2-Benzoylaminoacrylic acid Methyl Ester (58).**

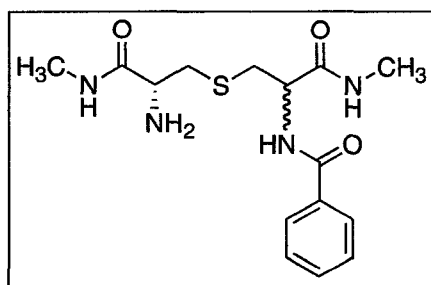
In a 250 mL round bottom flask D/L serine methyl ester (5.0 g, 32 mmol), benzoyl chloride (8.2 mL, 71 mmol), pyridine (8.0 mL, 96 mmol), and DMAP (250 mg, 2.0 mmol) was dissolved in CH<sub>2</sub>Cl<sub>2</sub> (50 mL) and stirred at room temperature for 1 hour. Formation of the dibenzoyl species was deemed complete by TLC after this time (EtOAc/hexane 1:1, R<sub>f</sub> 0.5). The dehydroalanine species was formed directly (1 pot) by dropwise addition of DBU. The elimination was complete in seconds and required a slight excess of DBU (5.3 mL, 35 mmol). The mixture was extracted with saturated NaHCO<sub>3</sub> (2 x 50 mL), water (2 x 50 mL), and brine (2 x 50 mL). The organic phase was dried over Na<sub>2</sub>SO<sub>4</sub> and evaporated to yield the crude product. Purification by flash column chromatography (SiO<sub>2</sub>, EtOAc/hexane, 1:10, R<sub>f</sub> 0.70) yielded the title compound as a yellow oil. (4.6 g, 70% over 2 steps); IR (CDCl<sub>3</sub> cast) 3408, 2954, 1721, 1679, 1637, 1601 cm<sup>-1</sup>; <sup>1</sup>H NMR (CDCl<sub>3</sub>, 300 MHz) δ 8.50 (br s, 1H, NH), 7.80 (m, 2H, ArH), 7.54–7.38 (m, 3H, ArH), 6.78 (s, 1H, olefin CH), 5.98 (s, 1H, olefin CH), 3.84 (s, 3H, OCH<sub>3</sub>); <sup>13</sup>C NMR (CDCl<sub>3</sub>, 125 MHz) δ 165.8 (CO), 164.8 (NCO), 134.4 (Ar-C quaternary), 132.1 (Ar-CH), 131.1 (olefin-C quaternary), 128.9, 127.0 (Ar-CH), 109.0 (olefin-CH<sub>2</sub>), 53.2 (OCH<sub>3</sub>); HRMS (EI) Calcd for C<sub>11</sub>H<sub>11</sub>NO<sub>3</sub> 205.07390, found 205.07372 M<sup>+</sup>.

**(2L)-Amino-(6D,L)-(benzoylamino)lanthionine Dimethyl Ester (59).**

In a 250 mL round bottom flask D/L serine methyl ester (5.0 g, 32 mmol), benzoyl chloride (8.2 mL, 71 mmol), pyridine (8.0 mL, 96 mmol), and DMAP (250 mg, 2.0

mmol) were dissolved in  $\text{CH}_2\text{Cl}_2$  (50 mL) and stirred at room temperature for 1 hour. Formation of the dibenzoyl species was deemed complete by TLC after this time. The dehydroalanine species was formed directly (1 pot) by dropwise addition of DBU. The rapid elimination was complete in seconds and required a slight excess of DBU (5.3 mL, 35 mmol). To the same reaction flask was next added L-cysteine methyl ester hydrochloride (5.6 g, 32 mmol) and DBU (5.3 mL, 35 mmol). After stirring at room temperature under argon for 1 hour, the mixture was extracted with saturated  $\text{NaHCO}_3$  (2 x 50 mL), water (2 x 50 mL), and brine (2 x 50 mL). The organic phase was dried over  $\text{Na}_2\text{SO}_4$  and evaporated to yield the product as an oil with no need for further purification (pure by  $^1\text{H}$  NMR spectroscopy). (7.6 g, 70% over 3 steps); IR ( $\text{CH}_2\text{Cl}_2$  cast) 3305, 2952, 1739, 1648, 1602, 1579  $\text{cm}^{-1}$ ;  $^1\text{H}$  NMR ( $\text{DMSO}-d_6$ , 600 MHz)  $\delta$  8.86 (m, 1H,  $-\text{NH}$ ), 7.86–7.82 (m, 2H, ArH), 7.58–7.44 (m, 3H, ArH), 4.69–4.58 (m, 1H, amide  $\alpha\text{-H}$ ), 3.68–3.60 (m, 7H, 2 x  $\text{OCH}_3$  and free amino  $\alpha\text{-H}$ ), 3.50–3.20 (br s, 2H,  $\text{NH}_2$ ), 3.10–2.72 (m, 4H,  $-\text{CH}_2-$ );  $^{13}\text{C}$  NMR ( $\text{DMSO}-d_6$ , 125 MHz)  $\delta$  174.2 ( $\text{CO}_2$ ), 171.1 ( $\text{CO}_2$ ), 166.3 ( $\text{NCO}$ ), 133.5 (Ar-C quaternary), 131.4, 128.2, 127.3 (Ar-CH), 54.4 ( $\alpha\text{-C}$ ), 52.8 ( $\alpha\text{-C}$ ), 52.0 ( $\text{OCH}_3$ ), 51.5 ( $\text{OCH}_3$ ), 36.5 ( $\text{CH}_2$ ), 32.9 ( $\text{CH}_2$ ); HRMS (ES) Calcd for  $\text{C}_{15}\text{H}_{21}\text{N}_2\text{O}_5\text{S}$  341.11657, found 341.11677 M+H.

**(2L)-Amino-(6D,L)-(benzoylamino)lanthionine Bis-methylamide (60).**

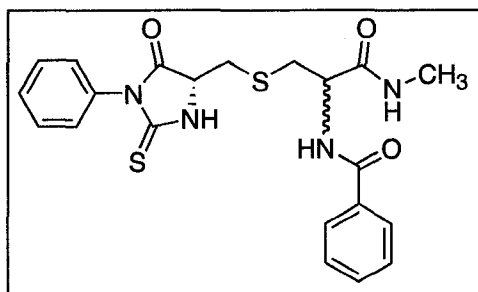


In a 100 mL round bottom flask D/L,L lanthionine dimethylester monobenzamide (**59**) (1.0 g, 2.9 mmol) was dissolved in a 40% aqueous solution of methylamine (20 mL). After thirty minutes at room



temperature conversion to the dimethyl amide was complete. The excess methyl amine and water were removed by rotary evaporation and the residue was dissolved in water (5.0 mL) and lyophilized to yield a glass. (980 mg, quantitative); IR (CHCl<sub>3</sub> cast) 3296, 2065, 3002, 1648, 1535, 1490 cm<sup>-1</sup>; <sup>1</sup>H NMR (DMSO-*d*<sub>6</sub>, 600 MHz) δ 8.86 (m, 1H, -NH), 8.13 (m, 1H, -NH), 7.86–7.82 (m, 3H, -NH and ArH), 7.58–7.42 (m, 3H, ArH), 4.62–4.52 (m, 1H, amide α-H), 3.50–3.20 (br m, 1H, free amino-NH<sub>2</sub>), 3.00–2.65 (m, 4H, -CH<sub>2</sub>-), 2.57–2.62 (m, 6H, 2 x NCH<sub>3</sub>); <sup>13</sup>C NMR (DMSO-*d*<sub>6</sub>, 125 MHz) δ 173.7 (NCO), 170.5 (NCO), 166.2 (NCO), 133.9 (Ar-C quaternary), 131.2, 128.0, 127.4 (Ar-CH), 54.5 (α-C), 53.2 (α-C), 37.4 (CH<sub>2</sub>), 33.8 (CH<sub>2</sub>), 25.6 (NCH<sub>3</sub>), 25.3 (NCH<sub>3</sub>); HRMS (ES) Calcd for C<sub>15</sub>H<sub>23</sub>N<sub>4</sub>O<sub>3</sub>S 339.14854, found 339.14849 M+H.

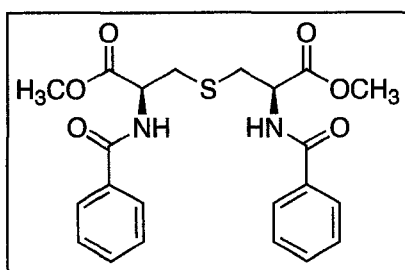
**(2L)-PTH-(6D,L)-(benzoylamino)lanthionine Mono-methylamide (61).**



In a 100 mL round bottom flask D/L,L lanthionine dimethylamide monobenzamide (**60**) (500 mg, 1.5 mmol) was dissolved in a 9 mL mixture of methanol, water, and triethylamine (7:1:1). While stirring at 40 °C, phenyl isothiocyanate (205 μL, 1.7 mmol) was added dropwise. After complete addition of the phenyl isothiocyanate and stirring for 1 hour, the solvent was removed *in vacuo* and the intermediate was treated directly with trifluoroacetic acid (5 mL) at room temperature to induce cyclization to the PTH. After 1 hour the excess TFA was removed by rotary evaporation and the TFA-methylamine adduct was removed from the desired product by filtering through silica (100% EtOAc). (496 mg, 74%); IR (CHCl<sub>3</sub> cast) 3305, 2925,

1765, 1642, 1532, 1493  $\text{cm}^{-1}$ ;  $^1\text{H}$  NMR (DMSO- $d_6$ , 600 MHz)  $\delta$  8.70-8.50 (m, 2H, ArH), 8.00 (m, 1H, -NH), 7.90-7.82 (m, 2H, ArH), 7.65-6.90 (m, 8H, 2NH and 6ArH), 5.05 (m, 1H, PTH  $\alpha$ -H), 4.55 (m, 1H, amide  $\alpha$ -H), 3.26-2.75 (m, 4H, -CH $_2$ -), 2.57-2.62 (m, 3H, NCH $_3$ );  $^{13}\text{C}$  NMR (DMSO- $d_6$ , 125 MHz)  $\delta$  180.2 (PTH NCO), 171.8 (PTH NCS), 170.3 (NCO), 166.2 (NCO), 138.9 (Ar-C quaternary), 138.8 (Ar-C quaternary), 131.2, 128.5, 128.4, 127.4, 124.2, 122.8 (Ar-CH), 56.3 ( $\alpha$ -C), 53.2 ( $\alpha$ -C), 34.3 (CH $_2$ ), 33.7 (CH $_2$ ), 25.6 (NCH $_3$ ); HRMS (ES) Calcd for  $\text{C}_{21}\text{H}_{23}\text{N}_4\text{O}_3\text{S}_2$  443.12061, found 443.12099 M+H.

**(2D,6L)-Bis-(benzoylamino)lanthionine Dimethyl Ester (62).**



In a 50 mL Erlenmeyer flask NaOH (0.77 g, 19.2 mmol) was dissolved in 20 mL of water. D,L-lanthionine (**55**) (2.0 g, 9.6 mmol) was then added to the basic solution and cooled to 0 °C in an ice bath. While stirring, benzoyl chloride (2.5 mL, 21.1 mmol) and aqueous NaOH (0.77 g in 5 mL H $_2$ O) were sequentially added so as to maintain a pH > 7.0. After warming to room temperature, the mixture was basified to pH 10 with 1 M NaOH and extracted with EtOAc (2 x 50 mL) to remove excess benzoyl chloride. The aqueous layer was then acidified to pH 2 by addition of concentrated HCl followed by ethyl acetate extraction (3 x 50 mL). After drying over Na $_2$ SO $_4$  and removal of solvent by rotary evaporation a white foam remains. This material is then dissolved in ethanol and treated with an excess of diazomethane. Diazomethane was freshly prepared using an Aldrich Diazald kit. Briefly, a Diazald solution in ether (5.0 g in 45 mL) was added dropwise to a reaction vessel containing

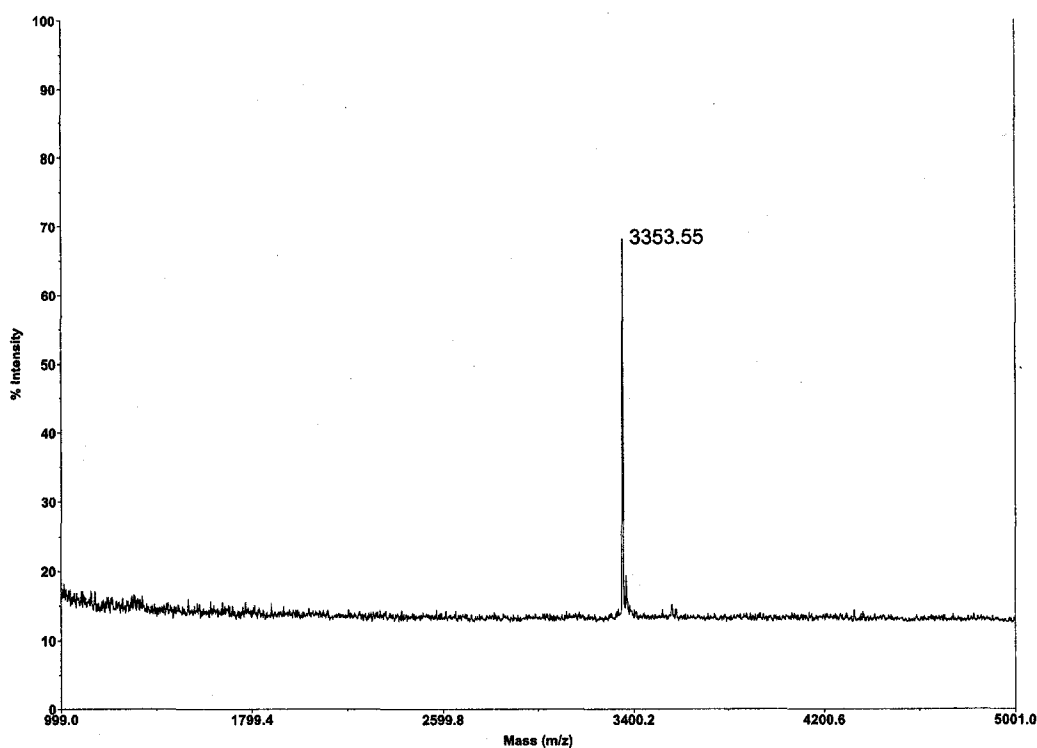
KOH (5 g) dissolved in water (8 mL) and ethanol (10 mL). Using a cold finger (dry ice-acetone) diazomethane was condensed into the ethanol solution containing the bis-benzoylated lanthionine species. Diazomethane addition was deemed complete when bubbling of N<sub>2</sub> was no longer observed and the yellow colour remained. Excess diazomethane was consumed by addition of glacial acetic acid. Solvent was removed by rotary evaporation, and the residue partitioned between 5% NaHCO<sub>3</sub> (50 mL) and CH<sub>2</sub>Cl<sub>2</sub> (2 x 50 mL). The combined CH<sub>2</sub>Cl<sub>2</sub> layers were dried over Na<sub>2</sub>SO<sub>4</sub>, and solvent was removed *in vacuo* to yield a white solid shown to be the desired product in good purity. (3.2 g, 79% over 2 steps); mp 155–157 °C; IR (μscope) 3238, 3052, 2949, 1738, 1637, 1600 cm<sup>-1</sup>; <sup>1</sup>H NMR (CDCl<sub>3</sub>, 300 MHz) δ 7.84–7.78 (m, 4H, ArH), 7.54–7.36 (m, 6H, ArH), 7.05 (br d, 2H, NH, *J* = 7.2 Hz), 4.99 (dt, 2H, α-H, *J* = 5.1, 7.2 Hz), 3.79 (s, 6H, 2 x OCH<sub>3</sub>), 3.21 (dd, 2H, -CH<sub>2</sub>-, *J* = 4.6, 13.9 Hz), 3.09 (dd, 2H, -CH<sub>2</sub>-, *J* = 5.4, 13.9 Hz); <sup>13</sup>C NMR (CDCl<sub>3</sub>, 75 MHz) δ 171.1 (C=O), 167.2 (NCO), 133.5 (Ar-C quaternary), 132.0, 128.7, 127.2 (Ar-CH), 52.9 (α-C), 52.5 (OCH<sub>3</sub>), 35.1 (CH<sub>2</sub>); HRMS (EI) Calcd for C<sub>22</sub>H<sub>24</sub>N<sub>2</sub>O<sub>6</sub>S 444.13550, found 444.13482 M<sup>+</sup>.

### Isolation of Nisin (53).

Nisin is commercially available (Sigma) as a 2.5% preparation with the majority of contaminant comprised of sodium chloride and other small peptides. An efficient purification of nisin involved suspending 500 mg of the commercial material in 10 mL of 35% acetonitrile (0.1% TFA) and sonicating for 15 minutes. The insoluble material was then removed by centrifugation and the supernatant used directly in a final HPLC purification. Nisin was isolated by reverse phase HPLC using a steel walled column

(Vydac, 10 x 250 mm, 5  $\mu$ m). In the method employed, a 1.0 mL injection was applied and a gradient of water and acetonitrile (0.1% TFA) was used to separate and isolate the peptide. Gradient; 15% acetonitrile for 5 min, then climbing to 50% in 20 min returning to 15% in 0.5 min and remaining at this concentration for an additional 5 min (flow rate 3.5 mL/min., detection at 220 nm). Nisin was isolated as a single peak ( $R_t=15.5$  min.) and its identity confirmed by MALDI mass spectrometry (Figure 43).

**Figure 43.** MALDI mass spectrum of nisin



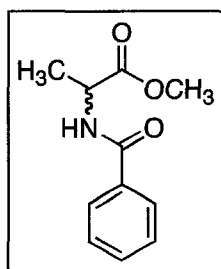
Multi milligram quantities of pure nisin were thus obtained within a day with an efficiency of recovery near 50%.

### General Procedure for Ni<sub>2</sub>B Desulfurization/Reduction of Model Compounds 58, 62

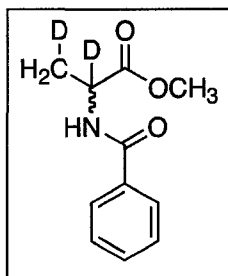
This procedure is representative of the model studies performed using the dehydroalanine and lanthionine analogues (**58** and **62**) and was generally performed on a 1.0 – 5.0 mmol scale.

The protected lanthionine or dehydroalanine species and nickel chloride (10 equivalents) were dissolved in a methanol/THF (3:1) mixture and sealed from atmosphere. While stirring at 0°C NaBH<sub>4</sub> (30 equivalents) was added in portions over 15 minutes with rapid resealing of the reaction vessel between additions. A black precipitate (Ni<sub>2</sub>B) forms immediately with the evolution of hydrogen gas. After complete addition of NaBH<sub>4</sub> the mixture was stirred for an additional 20 minutes. Ni<sub>2</sub>B was removed by centrifugation, and following solvent evaporation, the alanine analogue was purified by flash column chromatography (SiO<sub>2</sub>, EtOAc/hexane, 1:1) with isolated yields of 32 – 85%.

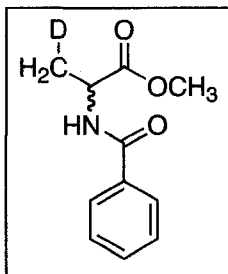
#### (D,L)-Alanine Methyl Ester Benzamide (**63**).



(77% from **62** and 85% from **58**); IR (CDCl<sub>3</sub> cast) 3320, 3061, 2993, 2952, 1744, 1641 cm<sup>-1</sup>; <sup>1</sup>H NMR (CDCl<sub>3</sub>, 300 MHz) δ 7.80 (m, 2H, ArH), 7.54–7.38 (m, 3H, ArH), 6.70 (br s, 1H, NH), 4.80 (qn, 1H, α-CH, *J* = 7.2 Hz), 3.82 (s, 3H, OCH<sub>3</sub>), 1.51 (d, 3H, -CH<sub>3</sub>, *J* = 7.1 Hz); <sup>13</sup>C NMR (CDCl<sub>3</sub>, 125 MHz) δ 173.8 (C=O), 166.8 (NCO), 134.0 (Ar-C quaternary), 131.8, 128.6, 127.1 (Ar-CH), 52.6 (OCH<sub>3</sub>), 48.5 (α-CH), 18.7 (CH<sub>3</sub>); HRMS (EI) Calcd for C<sub>11</sub>H<sub>13</sub>NO<sub>3</sub> 207.08954, found 207.08953 M<sup>+</sup>.

**$\alpha,\beta$ -Dideutero-(D,L)-alanine Methyl Ester Benzamide (64)**

(80% from **58** unoptimized); IR (CDCl<sub>3</sub> cast) 3319, 2952, 1743, 1640, 1603, 1580 cm<sup>-1</sup>; <sup>1</sup>H NMR (CDCl<sub>3</sub>, 300 MHz)  $\delta$  7.80 (m, 2H, ArH), 7.54–7.38 (m, 3H, ArH), 6.70 (br s, 1H, NH), 3.78 (s, 3H, OCH<sub>3</sub>), 1.48 (br s, 2H, -CH<sub>2</sub>-D); <sup>13</sup>C NMR (CDCl<sub>3</sub>, 125 MHz)  $\delta$  173.8 (CO), 166.9 (NCO), 134.5 (Ar-C quaternary), 132.0, 128.9, 127.3 (Ar-CH), 52.7 (OCH<sub>3</sub>), 48.5 (t,  $\alpha$ -CD,  $J$  = 21.4 Hz), 18.7 (t, CH<sub>2</sub>D,  $J$  = 20.1 Hz); HRMS (EI) Calcd for C<sub>11</sub>H<sub>11</sub>NO<sub>3</sub>D<sub>2</sub> 209.10210, found 209.10183 M<sup>+</sup>.

 **$\beta$ -Deutero-(D,L)-alanine Methyl Ester Benzamide (65).**

(32% from **62** unoptimized); IR (CDCl<sub>3</sub> cast) 3320, 3061, 2952, 1742, 1641, 1603 cm<sup>-1</sup>; <sup>1</sup>H NMR (CDCl<sub>3</sub>, 300 MHz)  $\delta$  7.80 (m, 2H, ArH), 7.54–7.38 (m, 3H, ArH), 6.70 (br s, 1H, NH), 4.80 (q, 1H,  $\alpha$ -CH,  $J$  = 7.2 Hz), 3.78 (s, 3H, OCH<sub>3</sub>), 1.50 (m, 2H, -CH<sub>2</sub>-D); <sup>13</sup>C NMR (CDCl<sub>3</sub>, 125 MHz)  $\delta$  173.8 (CO), 166.8 (NCO), 134.0 (Ar-C quaternary), 131.8, 128.6, 127.1 (Ar-CH), 52.6 (OCH<sub>3</sub>), 48.5 ( $\alpha$ -CH), 18.7 (t, CH<sub>2</sub>D,  $J$  = 20.1 Hz); HRMS (EI) Calcd for C<sub>11</sub>H<sub>12</sub>NO<sub>3</sub>D 208.09583, found 208.09574 M<sup>+</sup>.

**4.6 Lacticin A2 N-terminal Deblocking**

Unlike the other lantibiotics to be desulfurized and reduced, the lacticin A2 peptide has its N-terminus blocked by what is assumed to be an  $\alpha$ -keto amide moiety. It was therefore necessary to chemically remove this group prior to treatment with nickel boride. This was accomplished via the method of Dixon and coworkers.<sup>187,188</sup> Briefly;

purified A2 peptide (100  $\mu\text{g}$ , 0.04  $\mu\text{mol}$ ) was dissolved in 3.5 mL of a strong acetic acid/sodium acetate buffer (4.0 M, pH 4.8) containing 1,2-diaminobenzene at a concentration of 40 mM (3.5 mL corresponds to 0.14 mmol of 1,2-diaminobenzene, a 3500 fold excess relative to the peptide). The mixture was stirred at 38  $^{\circ}\text{C}$  for 12 hours, after which MALDI-TOF mass analysis reveals the desired, deblocked species as the major product. The peptide was then isolated by reverse phase HPLC using a steel walled column (Vydac, 10 x 250 mm, 5  $\mu\text{m}$ ). A method employing a 1.0 mL injection loop was used with a gradient of water and isopropanol (0.1% TFA). Gradient; 24% isopropanol for 5 min, then climbing to 44% in 20 min returning to 24% in 0.5 min and remaining at this concentration for an additional 5 min (flow rate 2.25 mL/min., detection at 220 nm). The desired peptide was isolated as a single broad peak ( $R_t=23.0$  min).

#### **4.7 General Procedure for $\text{Ni}_2\text{B}$ Desulfurization/Reduction of Lantibiotic Peptides**

This procedure is representative of the desulfurization and reduction experiments performed using nisin (**53**) and the lacticin peptides.

The lantibiotic peptide (0.5 mg) and nickel chloride (1 mg) were dissolved/suspended in 2.0 mL of methanol/ $\text{H}_2\text{O}$  (1:1) This mixture was then transferred via pipette into a screw-cap flask containing  $\text{NaBH}_4$  (1.0 mg) with rapid resealing of the reaction vial. A black precipitate ( $\text{Ni}_2\text{B}$ ) forms immediately with the evolution of hydrogen gas. The mixture was then stirred for 1 hour at 50  $^{\circ}\text{C}$ .  $\text{Ni}_2\text{B}$  was removed by centrifugation. After removing and retaining the supernatant, fresh MeOH/ $\text{H}_2\text{O}$  (2.0 mL) was added to the  $\text{Ni}_2\text{B}$  precipitate, the mixture sonicated, and re-centrifuged to recover

any residual peptide. After combining the supernatants, the methanol was removed by rotary evaporation and the aqueous solution, containing the modified peptide, was submitted for Edman degradation analysis.

#### **4.8 General Procedure for Deuterium Labeling $N_2B$ Desulfurization/Reduction of Lantibiotic Peptides**

The procedure is identical to that described in the previous section with substitution of  $NaBD_4$  for  $NaBH_4$  and the use of  $CD_3OD/D_2O$  in place of  $MeOH/H_2O$ .

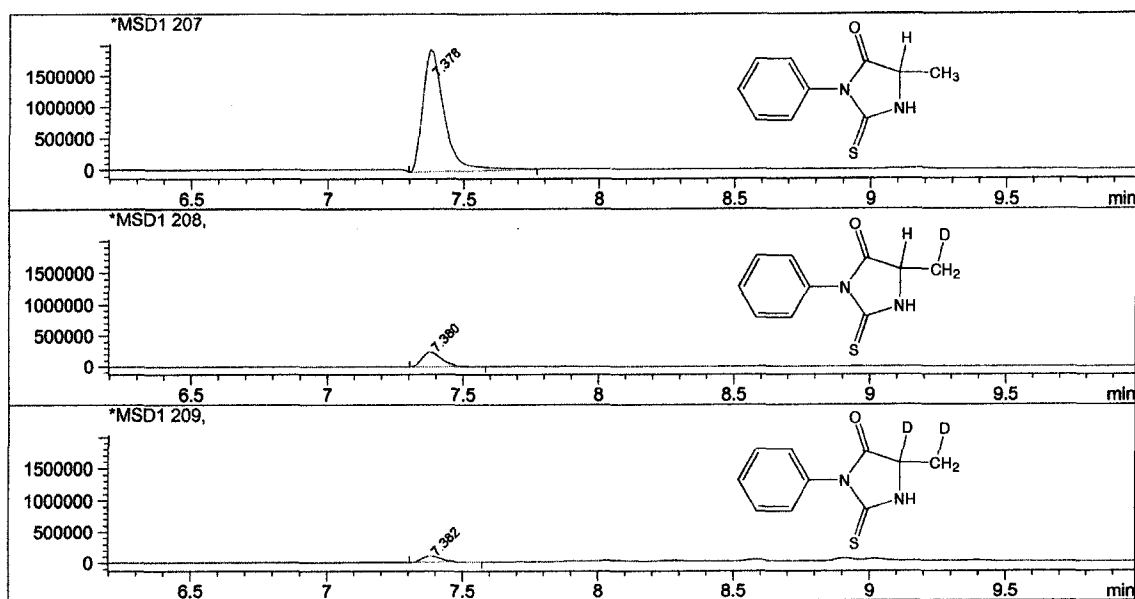
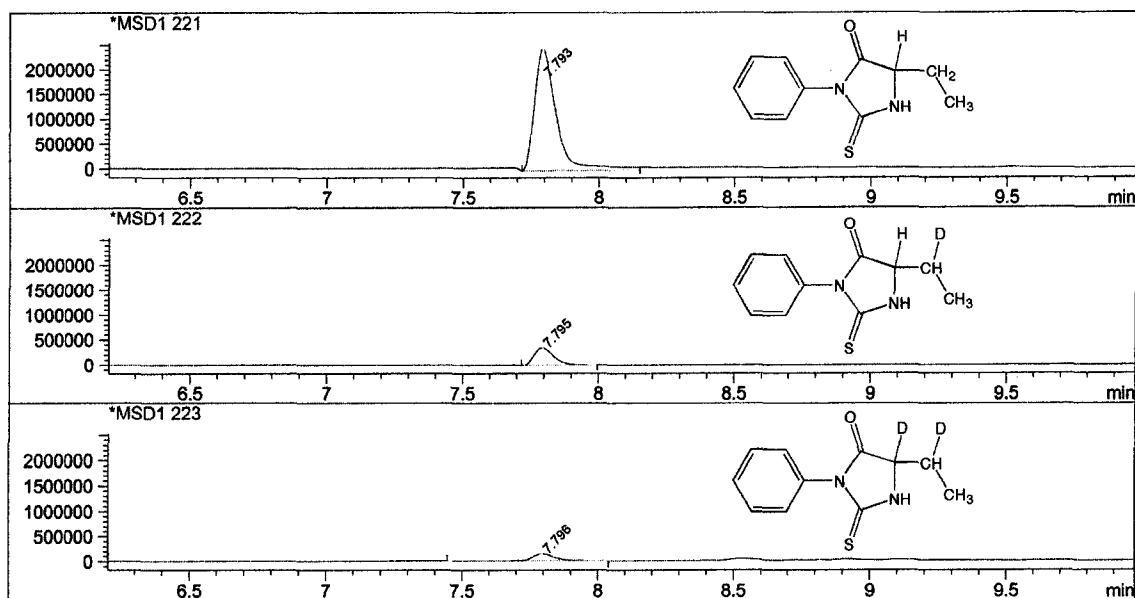
#### **4.9 Peptide Sequencing (Automated Edman Degradation)**

Peptide sequencing was performed using a Hewlett Packard G1000A protein sequencer coupled to a Hewlett Packard series II 1090 HPLC instrument for online PTH identification. Hewlett Packard routine 3.0 was utilized in the automated Edman chemistry involving phenyl isothiocyanate derivitization and TFA cleavage. HPLC characterization of the PTHs made use of a steel-wall  $C_{18}$  analytical column (Agilent, Hypersil  $C_{18}$  2.1 x 250 mm 5  $\mu$ m) at 40 °C. The method employed a 2-component gradient, component "A" (15% acetonitrile, 0.1% TFA) and component "B" (31% isopropanol, 0.1% TFA). Gradient; 100% "A" changing to 100% "B" over 16 minutes (flow rate 300  $\mu$ L/min, detection at 269 nm). PTH alanine was isolated as a single peak ( $R_t=10.7$  min.) as was PTH aminobutyric acid ( $R_t=12.9$  min.).



#### 4.10 LCMS Characterization of PTH Amino Acids from Edman Degradation

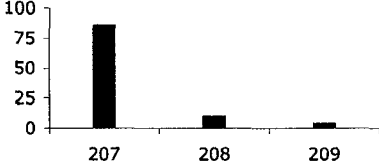
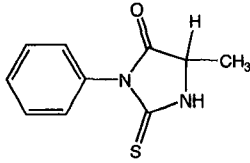
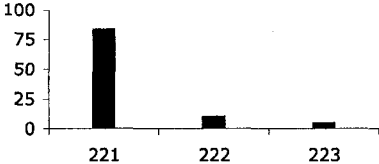
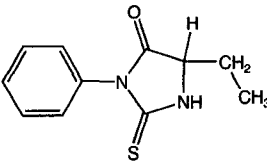
For each cycle of the Edman degradation generating a PTH derivative incorporating an unknown amount of deuterium, a manual collection of the PTH species was performed (a reliable and practical automated system could not be achieved). Deuterium incorporation was quantified using a 1100MSD single quadrupole instrument from Agilent Technologies (formerly Hewlett-Packard). This low-resolution ESI system was equipped with an HPLC interface and variable wavelength detector for LCMS analysis. Standards of PTH alanine and PTH amino-butyric acid were used in establishing an appropriate HPLC method using a steel walled column (Phenomenex Luna, 2.1 x 50 mm, 5  $\mu$ m, at 50°C). In the method employed, a 5  $\mu$ l injection was applied and a gradient of water and methanol (0.1% TFA) was used to isolate each PTH. Gradient; 10% methanol climbing to 95% in 5 min remaining at this concentration for an additional 5 min (flow rate 0.25 mL/min). Detection of the PTH was accomplished by mass spectrometry providing an extracted ion chromatogram (EIC) for the species of interest. Figures 42a and 42b display the EICs for the standards PTH alanine and PTH aminobutyric acid species, respectively.

**Figure 42a.** Extracted ion chromatogram for PTH-alanine standard**Figure 42b.** Extracted ion chromatogram for PTH-aminobutyric acid standard

The PTHs collected from the Edman sequencing were subjected to the same analysis and their deuterium incorporation values determined. Tables 9-12 illustrate the percentages of

non, mono, and di-deuterated PTH species in the two PTH standards and with respect to the residue number in the sequences of nisin, and lacticin A1 and A2.

**Table 9.** Mass analysis of standard PTH alanine and aminobutyric acid

PTH	Mass Analysis (% Abundance of mass ion indicated)	Structure (see Figures 41a, b)								
Ala	 <table border="1" data-bbox="634 606 1015 769"> <caption>Mass Spectrum Data for PTH-Ala</caption> <thead> <tr> <th>m/z</th> <th>Relative Abundance (%)</th> </tr> </thead> <tbody> <tr> <td>207</td> <td>100</td> </tr> <tr> <td>208</td> <td>~10</td> </tr> <tr> <td>209</td> <td>~5</td> </tr> </tbody> </table>	m/z	Relative Abundance (%)	207	100	208	~10	209	~5	
m/z	Relative Abundance (%)									
207	100									
208	~10									
209	~5									
Abu	 <table border="1" data-bbox="634 798 1015 962"> <caption>Mass Spectrum Data for PTH-Abu</caption> <thead> <tr> <th>m/z</th> <th>Relative Abundance (%)</th> </tr> </thead> <tbody> <tr> <td>221</td> <td>100</td> </tr> <tr> <td>222</td> <td>~10</td> </tr> <tr> <td>223</td> <td>~5</td> </tr> </tbody> </table>	m/z	Relative Abundance (%)	221	100	222	~10	223	~5	
m/z	Relative Abundance (%)									
221	100									
222	~10									
223	~5									

**Table 10.** Mass analysis of PTH residues derived from nisin treated with D<sub>2</sub>/Ni<sub>2</sub>B

Residue Number	Mass Analysis (% Abundance of mass ion indicated)	Structure Suggested (see Figures 41a, b)								
2	<table border="1"> <tr><th>Mass Ion</th><th>Abundance (%)</th></tr> <tr><td>221</td><td>10</td></tr> <tr><td>222</td><td>40</td></tr> <tr><td>223</td><td>50</td></tr> </table>	Mass Ion	Abundance (%)	221	10	222	40	223	50	
Mass Ion	Abundance (%)									
221	10									
222	40									
223	50									
3	<table border="1"> <tr><th>Mass Ion</th><th>Abundance (%)</th></tr> <tr><td>207</td><td>40</td></tr> <tr><td>208</td><td>45</td></tr> <tr><td>209</td><td>10</td></tr> </table>	Mass Ion	Abundance (%)	207	40	208	45	209	10	
Mass Ion	Abundance (%)									
207	40									
208	45									
209	10									
5	<table border="1"> <tr><th>Mass Ion</th><th>Abundance (%)</th></tr> <tr><td>207</td><td>10</td></tr> <tr><td>208</td><td>50</td></tr> <tr><td>209</td><td>40</td></tr> </table>	Mass Ion	Abundance (%)	207	10	208	50	209	40	
Mass Ion	Abundance (%)									
207	10									
208	50									
209	40									
7	<table border="1"> <tr><th>Mass Ion</th><th>Abundance (%)</th></tr> <tr><td>207</td><td>40</td></tr> <tr><td>208</td><td>45</td></tr> <tr><td>209</td><td>10</td></tr> </table>	Mass Ion	Abundance (%)	207	40	208	45	209	10	
Mass Ion	Abundance (%)									
207	40									
208	45									
209	10									
8	<table border="1"> <tr><th>Mass Ion</th><th>Abundance (%)</th></tr> <tr><td>221</td><td>40</td></tr> <tr><td>222</td><td>40</td></tr> <tr><td>223</td><td>10</td></tr> </table>	Mass Ion	Abundance (%)	221	40	222	40	223	10	
Mass Ion	Abundance (%)									
221	40									
222	40									
223	10									
11	<table border="1"> <tr><th>Mass Ion</th><th>Abundance (%)</th></tr> <tr><td>207</td><td>50</td></tr> <tr><td>208</td><td>40</td></tr> <tr><td>209</td><td>10</td></tr> </table>	Mass Ion	Abundance (%)	207	50	208	40	209	10	
Mass Ion	Abundance (%)									
207	50									
208	40									
209	10									
13	<table border="1"> <tr><th>Mass Ion</th><th>Abundance (%)</th></tr> <tr><td>221</td><td>40</td></tr> <tr><td>222</td><td>40</td></tr> <tr><td>223</td><td>10</td></tr> </table>	Mass Ion	Abundance (%)	221	40	222	40	223	10	
Mass Ion	Abundance (%)									
221	40									
222	40									
223	10									
19	<table border="1"> <tr><th>Mass Ion</th><th>Abundance (%)</th></tr> <tr><td>207</td><td>60</td></tr> <tr><td>208</td><td>30</td></tr> <tr><td>209</td><td>10</td></tr> </table>	Mass Ion	Abundance (%)	207	60	208	30	209	10	
Mass Ion	Abundance (%)									
207	60									
208	30									
209	10									

**Table 11.** Mass analysis of PTH residues derived from A1 peptide treated with D<sub>2</sub>/Ni<sub>2</sub>B

Residue Number	Mass Analysis (% Abundance of mass ion indicated)	Structure Suggested (see Figures 41a, b)								
2	<table border="1"> <tr><th>m/z</th><td>207</td><td>208</td><td>209</td></tr> <tr><th>Abundance (%)</th><td>~10</td><td>100</td><td>~15</td></tr> </table>	m/z	207	208	209	Abundance (%)	~10	100	~15	
m/z	207	208	209							
Abundance (%)	~10	100	~15							
3	<table border="1"> <tr><th>m/z</th><td>221</td><td>222</td><td>223</td></tr> <tr><th>Abundance (%)</th><td>0</td><td>100</td><td>~40</td></tr> </table>	m/z	221	222	223	Abundance (%)	0	100	~40	
m/z	221	222	223							
Abundance (%)	0	100	~40							
5	<table border="1"> <tr><th>m/z</th><td>221</td><td>222</td><td>223</td></tr> <tr><th>Abundance (%)</th><td>0</td><td>100</td><td>~40</td></tr> </table>	m/z	221	222	223	Abundance (%)	0	100	~40	
m/z	221	222	223							
Abundance (%)	0	100	~40							
7	<table border="1"> <tr><th>m/z</th><td>207</td><td>208</td><td>209</td></tr> <tr><th>Abundance (%)</th><td>100</td><td>~15</td><td>~5</td></tr> </table>	m/z	207	208	209	Abundance (%)	100	~15	~5	
m/z	207	208	209							
Abundance (%)	100	~15	~5							
9	<table border="1"> <tr><th>m/z</th><td>207</td><td>208</td><td>209</td></tr> <tr><th>Abundance (%)</th><td>~40</td><td>100</td><td>~10</td></tr> </table>	m/z	207	208	209	Abundance (%)	~40	100	~10	
m/z	207	208	209							
Abundance (%)	~40	100	~10							
20	<table border="1"> <tr><th>m/z</th><td>221</td><td>222</td><td>223</td></tr> <tr><th>Abundance (%)</th><td>~5</td><td>100</td><td>~40</td></tr> </table>	m/z	221	222	223	Abundance (%)	~5	100	~40	
m/z	221	222	223							
Abundance (%)	~5	100	~40							
22	<table border="1"> <tr><th>m/z</th><td>221</td><td>222</td><td>223</td></tr> <tr><th>Abundance (%)</th><td>~5</td><td>100</td><td>~40</td></tr> </table>	m/z	221	222	223	Abundance (%)	~5	100	~40	
m/z	221	222	223							
Abundance (%)	~5	100	~40							

*Dashed bars represent uncertain data.*

**Table 12.** Mass analysis of PTH residues derived from A2 peptide treated with D<sub>2</sub>/Ni<sub>2</sub>B

Residue Number	Mass Analysis (% Abundance of mass ion indicated)	Structure Suggested (see Figures 41a, b)
5		
9		
12		
16		
22		
26		

*Dashed bars represent uncertain data.*

### **Lacticin 3147 Overproducer**

The overproducing strain, *Lactococcus lactis* subsp. *lactis* MG1363 pMRC01 pMOM02 was prepared by our collaborators (Hill and Ross) and contained the original lacticin producing plasmid, pMRC01. The second plasmid, pOM02, is a pCI372 derivative that possesses the lacticin genes. The overproducing strain, like the wild type organism was grown at 30°C for 24 hours without aeration in 10 mL Difco M17 broth supplemented with 0.5% (wt/vol) lactose.

### **Enhanced Isolation of Lacticin (from Cells)**

In 10 mL culture tubes of Difco M17 broth, a pre-culture of *Lactococcus lactis* subsp. *lactis* MG1363 was grown for 24 hours at 30°C. The most practical fermentation volume (yielding enough of the lacticin peptides) was a four litre scale. The media was prepared, pre-purified, sterilized, and inoculated using the protocol described earlier for the isolation of the peptide from the supernatant.

After a total growth time of 16 to 24 hours at 30°C without aeration, 50 g of ammonium sulfate and 75 mg of DTT was added to each 1 L fermentation. From this point on, all buffers used in the isolation procedure contained 0.1 M DTT to protect the lantibiotic peptides from oxidation. The cells from the four litre fermentation were collected by centrifugation (20 min., 8000 rpm), combined, and re-suspended in 250 mL of 70% isopropanol (adjusted to pH 2 by addition of 1M HCl). After stirring for 3 hours at 4 °C the cell debris was removed by centrifugation (20 min., 8000 rpm) and the supernatant reduced to a volume of 60 mL by rotary evaporation. The concentrated

bacteriocin solution was next loaded onto a disposable column containing 10 g of C<sub>18</sub> silica (Varian C<sub>18</sub> megabond elut). Prior to sample loading, the C<sub>18</sub> silica was pre-equilibrated with 60 mL of 100% methanol. After loading the sample the column was washed successively with 60 mL of purified (milli-Q system, Millipore, Bedford, Mass.) water, 60 mL of 30% ethanol, and 40 mL of 25% isopropanol. The active peptides were removed from the column by washing with 100 mL of 70% isopropanol (pH 2 by the addition of 1M HCl). The 70% isopropanol fraction was then reduced to a 20 mL volume by rotary evaporation and lyophilized. The HPLC column and method used in the final purification were identical to those used when the peptides were isolated from the fermentation supernatant.

After complete separation, pooling of the active fractions, evaporation of the isopropanol, and lyophilization, approximately 2.0 to 4.0 mg of each peptide was recovered from 4 litres of culture. All purified samples were stored under argon at -80 °C to prevent the very rapid oxidation of the peptides.

#### **4.13 NMR Spectroscopy**

NMR spectra were acquired on a Varian Inova 600 spectrometer; data matrices of 2048 detected and 1024 indirect data points with 64 scans were recorded and processed using a 90 shifted sine bell window function (unshifted for DQF-COSY). Solvent signal suppression was achieved by transmitter presaturation.



Samples of the A1 peptide were prepared in either in 90% H<sub>2</sub>O-10% D<sub>2</sub>O (for amide analysis) or 100% D<sub>2</sub>O at 27 °C and at a peptide concentration of 2 mM. All experiments with the A1 peptide were performed at pH 2 (H<sub>2</sub>O contained 0.1% TFA); under these conditions, the solubility of the peptide was greatly improved likely due to reduced peptide aggregation via protonation of cationic side chains. Samples of the more hydrophobic A2 peptide were prepared in either in 100% CD<sub>3</sub>OH (for amide analysis) or 100% CD<sub>3</sub>OD at 27 °C and at a peptide concentration of 2 mM.

The assignment of <sup>1</sup>H resonances was performed using standard two-dimensional DQF-COSY,<sup>180</sup> TOCSY<sup>181</sup> (mixing time 75 ms), and two-dimensional NOE experiments (NOESY<sup>182</sup> mixing times 200 ms).

## References

---

1. Chenault, H. K.; Dahmer, J.; Whitesides, G. M. *J. Am. Chem. Soc.* **1989**, *111*, 6354-64.
2. Fu, S. C. J.; Birnbaum, S. M. *J. Am. Chem. Soc.* **1953**, *75*, 918-920.
3. Williams, R. M. In *Organic Chemistry Series, Volume 7: Synthesis of Optically Active-Amino Acids*; Baldwin, J. E., Magnus, P. D., Eds.; Pergamon Press: Oxford, 1989.
4. Williams, R. M.; Sinclair, P. J.; Zhai, D.; Chen, D. *J. Am. Chem. Soc.* **1988**, *110*, 1547.
5. Aoyagi, Y.; Jain, R. P.; Williams, R. M. *J. Am. Chem. Soc.* **2001**, *123*, 3472.
6. Schollkopf, U.; Groth, U.; Deng, C. *Angew. Chem., Int. Ed. Engl.* **1981**, *20*, 798.
7. Schollkopf, U. *Tetrahedron* **1983**, *39*, 2085.
8. Evangelopoulos, A. E. *Chemical and Biological Aspects of Vitamin B6 Catalysis*; A. R. Liss: New York, 1984.
9. Dolphin, D., Poulson, R., Avramovic, O. Eds. *Vitamin B6 Pyridoxal Phosphate, Chemical, Biochemical, and Medical Aspects*; Wiley-Interscience: New York, 1986; Parts A and B.
10. John, R. A. *Biochim. Biophys. Acta* **1995**, *1248*, 81-96.
11. Metzler, D. E.; Snell, E. E. *J. Biol. Chem.* **1952b**, *198*, 353-361.
12. Metzler, D. E.; Ikawa, M.; Snell, E. E. *J. Am. Chem. Soc.* **1954**, *76*, 648-652.
13. Christen, P.; Metzler, D. E. *Transaminases*; John Wiley & Sons: New York, 1985.
14. Davis, F. A.; Slegeir, W. A. R.; Evans, S.; Schwartz, A.; Goff, D. L.; Palmer, R. *J. Org. Chem.* **1973**, *38*, 2809-2813.
15. Gordon, E. M.; Pluscec, J. *J. Org. Chem.* **1979**, *44*, 1218-1221.
16. Cornforth, J. W. in *Heterocyclic Compounds* (Elderfield, R. C.; Ed.), Wiley, New York, Vol. 5, 1957, pp. 336-377.

- 
17. Filler, R. in *Advances in Heterocyclic Chemistry* (Katritzky, A. R.; Ed.), Academic Press, New York, Vol. 4, 1965, pp. 75-103.
18. Leung, D.; Abbenante, G.; Fairlie, D. P.; *J. Med. Chem.* **2000**, *43*, 305-341.
19. Patick, A. K.; Potts, K. E. *Clin. Microbiol. Rev.* **1998**, *11*, 614-627.
20. Hill, R. D.; Vederas, J. C. *J. Org. Chem.* **1999**, *64*, 9538-9546.
21. Lall, M. S.; Karvellas, C.; Vederas, J. C. *Org. Lett.* **1999**, *1*, 803-806.
22. Malcolm, B. A.; Lowe, C.; Shechosky, S.; Mckay, R. T.; Yang, C. C.; Shah, V. J.; Simon, R. J.; Vederas, J. C.; Santi, D. V. *Biochemistry* **1995**, *34*, 8172-8179.
23. Bergmann, E. M.; James, M. N. G. In *Proteases as Targets for Therapy*; Von der Helm, K., Korant, B. Eds.; Springer: Heidelberg, 1999.
24. Malcolm, B. A. *Protein Sci.* **1995**, *4*, 1439-1445 and references therein.
25. Jewell, D. A.; Swietnicki, W.; Dunn, B. N.; Malcolm, B. A. *Biochemistry* **1992**, *31*, 7862-7869.
26. Webber, S. E.; Okano, K.; Little, T. L.; Reich, S. H.; Xin, Y.; Fuhrman, S. A.; Matthews, D. A.; Love, R. A.; Hendrickson, T. F.; Patick, A. K.; Meador III, J. W.; Ferre, R. A.; Brown, E. L.; Ford, C. E.; Binford, S. L.; Worland, S. T. *J. Med. Chem.* **1998**, *41*, 2786-2805.
27. Morris, T. S.; Frommann, S.; Shechosky, S.; Lowe, C.; Lall, M. S.; Gauss-Müller, V.; Purcell, R. H.; Emerson, S. U.; Vederas, J. C.; Malcolm, B. A. *Bioorg. Med. Chem.* **1997**, *5*, 797-807.
28. Huang, Y.; Malcolm B. A.; Vederas, J. C. *Bioorg. Med. Chem.* **1999**, *7*, 607-619.
29. McKendrick, J. E.; Frommann, S.; Luo, C.; Semchuk, P.; Vederas, J. C.; Malcolm, B. A. *Int. J. Mass Spectrometry* **1998**, *176*, 113-124.

- 
30. Lall, M. S.; Ramtohul, Y. K.; James, M. N. G.; Vederas, J. C. *J. Org. Chem.* **2002**, *67*, 1536-1547.
  31. Ramtohul, Y. K.; James, M. N. G.; Vederas, J. C.; *J. Org. Chem.* **2002**, *67*, 3169-3178.
  32. Liu, G.; Cogan, D. A.; Owens, T. D.; Tang, T. P.; Ellman, J. A. *J. Org. Chem.* **1999**, *64*, 1278-1284.
  33. Davis, F. A.; Friedman, A. J.; Kluger, E. W. *J. Am. Chem. Soc.* **1974**, *96*, 5000-5001.
  34. Davis, F. A.; Kluger, E. W. *J. Am. Chem. Soc.* **1976**, *98*, 302-303.
  35. Verdaguer, X.; Lange, U. E. W.; Buchwald, S. L. *Angew. Chem., Int. Ed.* **1998**, *37*, 1103-1107.
  36. Kobayashi, S.; Ishitani, H. *Chem. Rev.* **1999**, *99*, 1069-1094.
  37. King, J. A.; McMillan, F. H. *J. Am. Chem. Soc.* **1950**, *72*, 833-836.
  38. Ramtohul, Y. K.; Martin, N. I.; Silkin, L.; James, M. N. G.; Vederas, J. C. *J. Chem. Soc. Chem. Commun.* **2001**, 2740-2741.
  39. Filler, R.; Piasek, E. J. *J. Org. Chem.* **1963**, *28*, 221-223.
  40. Stolle, R.; Wolf, F. *Chem. Ber.* **1913**, *46*, 2248-2251.
  41. Mukaiyama, T.; Nagata, T.; Yorozu, K.; Yamada, T. *Angew. Chem. Int. Ed.* **1995**, *34*, 2145.
  42. Verdaguer, X.; Lange, U. E. W.; Reding, M. T.; Buchwald, S. L. *J. Am. Chem. Soc.* **1996**, *118*, 6784.
  43. Itsuno, S.; Ito, K.; Hirao, A.; Nakahama, S. *J. Org. Chem.* **1984**, *49*, 555-557.
  44. Corey, E. J.; Bakshi, R. K.; Shibata, S. *J. Am. Chem. Soc.* **1987**, *109*, 5551-5553.
  45. Hajipour, A. R.; Hantehzadeh, M. *J. Org. Chem.* **1999**, *64*, 8475-8478.

- 
46. Chan, P. C. M.; Chong, J. M. *J. Org. Chem.* **1988**, *53*, 5584-5586.
47. Burk, M. J. *Acc. Chem. Res.* **2000**, *33*, 363-372.
48. Noyori, R.; Ohkuma, T.; Kitamura, M.; Takaya, H.; Sayo, N.; Kumobayashi, H.; Akutagawa, S. *J. Am. Chem. Soc.* **1987**, *109*, 5856-5858.
49. Evans, D. A.; Chapman, K. T.; Carreira, E. M. *J. Am. Chem. Soc.* **1988**, *110*, 3560-3578.
50. D'Angeli, F.; Di Bello, C.; Filira, F. *J. Org. Chem.* **1971**, *36*, 1818-1820.
51. Speckamp, N. W.; Moolenaar, M. J. *Tetrahedron* **2000**, *56*, 3817-3856.
52. (a) Kaneda, A.; Sudo, R. *Bull. Chem. Soc. Jpn.*, **1970**, *43*, 2159-2161. (b) Knunyants, I. L.; Kil'disheva, O. V.; Krasuskaya, M. P.; Lin'kova, M. G.; Shokina, V. V.; Benevolenskaya, Z. V.; Rasteikene, L. P. *Bull. Acad. Sci. USSR, Div. Chem. Sci.*, (Engl. Transl.) **1959**, 1702-1710.
53. Ramtohul, Y. K.; Martin, N. I.; Silkin, L.; James, M.; Vederas, J. C. *J. Chem. Soc. Perkin Trans. 1* **2002**, 1351-1359.
54. van Belkum M. J.; Worobo, R. W.; Stiles, M. E. *Mol. Microbiol.* **1997**, *2*, 1293-1301.
55. Wang, Y.; Henz, M. E.; Fregeau Gallagher, N. L.; Chai, S.; Yan, L. Z.; Stiles, M. E.; Wishart, D. S.; Vederas, J. C. *Biochemistry* **1999**, *38*, 15438-15447.
56. Garneau, S.; Martin, N. I.; and Vederas, J. C. *Biochimie* **2002**, *84*, 577-592.
57. Zheng, G.; Yan, L. Z.; Vederas, J. C.; Zuber, P. *J. Bacteriol.* **1999**, *181*, 7346-7355.
58. Twomey, D.; Ross, R. P.; Ryan, M.; Meaney, B.; Hill, C. *Antonie van Leeuwenhoek* **2002**, *82*, 165-185.
59. Klaenhammer T. R. *Biochimie* **1988**, *70*, 337-349.
60. Tagg, J. R.; Dajani, A. S.; Wannamaker, L. W. *Bacteriol. Rev.* **1976**, *40*, 722-756.

- 
61. Marahiel, M. A.; Stachelhaus, T.; Mootz, H. D. *Chem. Rev.* **1997**, *97*, 2651-2673.
62. Doekel, S.; Marahiel, M. A. *Metab. Eng.* **2001**, *6*, 64-77.
63. Du, L.; Shen, B. *Chem. Biol.* **1999**, *6*, 507-517.
64. Kleinkauf, H.; von Dohren, H. *Eur. J. Biochem.* **1990**, *192*, 1-15.
65. Kleinkauf, H.; von Dohren, H. *Crit. Rev. Biochem.* **1988**, *8*, 1-32.
66. Nissen-Meyer, J.; Nes, I. F. *Arch. Microbiol.* **1997**, *167*, 67-77.
67. Riley, R. A.; Wertz, J. E. *Annu. Rev. Microbiol.* **2002**, *56*, 117-137.
68. Sahl, H.-G.; Bierbaum, G. *Annu. Rev. Microbiol.* **1998**, *52*, 41-79.
69. Ainsworth, G. C.; Brown, A. M.; Brownlee, G. *Nature* **1947**, *160*, 263-264.
70. Komura, S.; Kurahashi, K. *J. Biochem.* **1985**, *97*, 1409-1417.
71. Storm, D. R.; Rosenthal, K. S.; Swanson P. E. *Ann. Rev. Biochem.* **1977**, *46*, 723-763.
72. Tsubery, H.; Ofek, I.; Cohen, S.; Fridkin, M. *J. Med. Chem.* **2000**, *43*, 3085-3092.
73. Rietschel, E. T.; Brade, L.; Holst, O.; Kulshin, V. A.; Lindner, B.; Moran, A. P.; Schade, U. F.; Zaehring, U.; Brade, H. in *Cellular and molecular aspects of endotoxin reactions*, **1990**, Nowotny, A., Spitzer, J. J., Ziegler, E. J., Eds., pp. 15-32, Elsevier Science Publishers B. V., Amsterdam.
74. Koch, P.J.; Frank, J.; Schuler, J.; Kahle, C.; Bradaczek, H. *Colloid Interface Sci.* **1999**, *213*, 557-564.
75. Silaev, A. B.; Maevskaya, S. N.; Trifonova, Z. P.; Yulikova, E. P. *Zh. Obshch. Khim.* **1975**, *45*, 2331-2337. *Chem. Abstr.* 84:106040n.
76. Okhanov, V. V.; Dubovskii, P. V.; Trakhanova, M. N.; Bairamashvili, D. I. *Antibiot. Med. Biotekhnol.* **1987**, *32*, 738-743. *Chem. Abstr.* 108:51535.

- 
77. Trakhanova, M. N.; Zinchenko, A. A.; Okhanov, V. V.; Dubovskii, P. V. *Antibiot. Khimioter.* **1989**, *34*, 20-24. *Chem. Abstr.* 110:189234.
78. Okhanov, V. V.; Dubovskii, P. V.; Miroshnikov, A. I. *Bioorg. Khim.* **1991**, *17*, 1689-1693. *Chem. Abstr.* 116:59981.
79. Pristovsek, P.; Kidric, J. *J. Med. Chem.* **1999**, *42*, 4604-4613.
80. Srimal, S.; Surolia, N.; Balasubramanian, S.; Surolia, A. *Biochem. J.* **1996**, *315*, 679-686.
81. **MicroCal Origin**; 5.0 (1991-1997); MicroCal Software, Inc.: Northampton, MA.
82. Yin, N.; Marshall, R. L.; Matheson, S.; Savage, P. B. *J. Am. Chem. Soc.* **2003**, *125*, 2426-2435.
83. Martin, N. I.; Hu, H.; Moake, M. M.; Churey, J. J.; Whittal, R.; Worobo, R. W.; Vederas, J. C. *J. Biol. Chem.* **2003**, *278*, 13124 - 13132.
84. van Belkum M. J.; Stiles M. E. *Nat. Prod. Rep.* **2000**, *17*, 323-335.
85. Medical Economics Company. Top 200 Drugs by Retail Sales in 2000  
[http://me.pdr.net/be\\_core/content/journals/d/data/2001/0319/dsrtop20003b.html](http://me.pdr.net/be_core/content/journals/d/data/2001/0319/dsrtop20003b.html)  
(accessed Aug 2003)
86. van Heijenoort, J. *Nat. Prod. Rep.* **2001**, *18*, 503-519.
87. Bugg, T. D. H.; Walsh, C. T. *Nat. Prod. Rep.* **2001**, *18*, 503-519.
88. Levy, S. B. In *Antimicrobial resistance, a global perspective in Antimicrobial resistance, a crisis in Health Care*; Jungkind, D. L.; Mortensen, J. E.; Fraimow, H. S.; Calendra, G. B., Eds.; Plenum Press: New York, 1995.
89. Davies, J. *Nature* **1996**, *383*, 219-220.
90. Levy, S. B. *Sci. Am.* **1998**, *278*, 46-53.

- 
91. Ghuysen, J. M. In *Topics in Antibiotic Chemistry*; Sammes, P. G., Ed.; Ellis Horwood Ltd.: Chichester, U.K., 1980; Vol. 5.
  92. Fontana, R.; Valisena, S.; Cornaglia, G. *J. Chemotherapy* **1996**, *8*, 23-30.
  93. Nicolaou, K. C.; Boddy, C. N. C.; Bräse, S.; Winssinger, N. *Angew. Chem. Int. Ed.* **1999**, *38*, 2096-2152.
  94. Williams, D. H.; Bardsley, B. *Angew. Chem. Int. Ed.* **1999**, *38*, 1172-1193.
  95. Shinabarger, D. *Expert Opin. Invest. Drugs* **1999**, *8*, 1195-1202.
  96. Bahavnani, S. M.; Ballow, C. H. *Curr. Opin. Microbiol.* **2000**, *3*, 528-534.
  97. Senior, K. *Lancet* **2000**, *355*, 1523.
  98. Diekoma, D. J.; Jones, R. N. *Drugs* **2000**, *59*, 7-16.
  99. Maxwell, A. *Biochem. Soc. Trans.* **1999**, *27*, 48-53.
  100. Chu, D. T. W. *Med. Res. Rev.* **1999**, *19*, 497-520.
  101. Bergogne-Bérézin, E. *Presse Medicale* **2000**, *29*, 2028-2032.
  102. Severinov, K.; Mustaev, A.; Severinov, E.; Kozlov, M.; Darst, S. A.; Goldfarb, A. J. *Biol. Chem.* **1995**, *270*, 29428-29432.
  103. Anthony, D. D.; Zeszotek, E.; Goldthwait, D. A. *Proc. Natl. Acad. Sci. USA* **1966**, *56*, 1026-1033.
  104. Chopra, I.; Brennan, P. J. *Tubercle and Lung Disease* **1997**, *78*, 89-98.
  105. Gratia, A. *C. R. Soc. Biol.* **1925**, *93* 1040.
  106. Hansen, J. N.; Banerjee, S.; Buchman, L. W. *J. Food Safety* **1989**, *10*, 119-130.
  107. Guder, A.; Wiedemann, I.; Sahl, H.-G. *Biopolymers* **2000**, *55*, 62-73.
  108. Schnell, N.; Entian, K.-D.; Schneider, U.; Götz, F.; Zähner, H.; Kellner, R.; Jung, G. *Nature* **1998**, *333*, 276-278.



- 
109. Jung, G., Sahl, H.-G. Eds. *Nisin and Novel Lantibiotics*; ESCOM Science Publishers B. V.: Leiden, 1991.
110. Nel, H. A.; Bauer, G. M.; Wolfaardt, G. M.; Dicks, L. M. T. *Am. J. Enol. Vitic.* **2002**, *53*, 191–196.
111. Mota-Meira, M.; Lapointe, G.; Lacroix, C.; Lavoie, M. C. *Antimicrob. Agents Chemother.* **2000**, *44*, 24-29.
112. Delves-Broughton, J.; Blackburn, P.; Evans, R. J.; Hugenholtz, J. *Antonie van Leeuwenhoek* **1996**, *69*, 193-202.
113. Booth, M. C.; Bogie, C. P.; Sahl, H.-G.; Siezen, R. J.; Hatter, K. L.; Gilmore, M. S. *Mol. Microbiol.* **1996**, *21*, 1175-1184.
114. Ryan, M.; Rea, M. C.; Hill, C.; Ross, R. P. *Appl. Environ. Microbiol.* **1996**, *62*, 612-619.
115. Kaletta C.; Entian, K.-D.; Kellner R.; Jung G.; Reis M.; Sahl H.-G. *Arch. Microbiol.* **1989**, *152*, 16-19.
116. Higgins C.F.; *Annu. Rev. Cell Biol.* **1992**, *8*, 67-113.
117. Booth M.C.; Bogie C.P.; Sahl H.-G.; Siezen R.J.; Hatter K.L.; Gilmore M.S. *Molec. Microbiol.* **1996**, *21*, 1175-1184.
118. Ingram L.C. *Biochim. Biophys. Acta* **1969**, *184*, 216-219.
119. Bierbaum G.; Götz F.; Peschel A.; Kupke T.; van de Kamp M.; Sahl H.-G. *Antonie van Leeuwenhoek* **1996**, *69*, 119-127.
120. Skaugen ,M.; Nissen-Meyer, J.; Jung, G.; Stevanovic, S.; Sletten, K.; Abildgaard, C.I.M.; Nes, I.F. *J. Biol. Chem.* **1994**, *269*, 27183-27185.

- 
121. Kellner, R.; Jung, G.; Sahl, H.-G. In *Nisin and Novel Lantibiotics*; Jung, G.; Sahl H.-G., Eds.; ESCOM Science Publishers B. V.: Leiden, 1991; 141-158.
122. Kupke, T.; Kempter, C.; Jung, G.; Götz, F. *J. Biol. Chem.* **1995**, *270*, 11282-89
123. Minami, Y.; Yoshida, K-I.; Azuma, R.; Urakawa, A.; Kawauchi, T. *Tetrahedron Lett.* **1994**, *35*, 8001-8004.
124. Nes, I.G.; Holo, H. *Biopolymers* **2000**, *55*, 50-61.
125. Jack, R. W.; Tagg, J. R.; Ray, B. *Microbiol. Rev.* **1995**, *59*, 171-200.
126. Palmer, D. E.; Mierke, D. F.; Pattaroni, C.; Goodman, M.; Wakamiya, T.; Fukase, K.; Kitazawa, M.; Fujita, H.; Shiba, T. *Biopolymers* **1989**, *28*, 397-408.
127. Benz, R.; Jung, G.; Sahl, H.-G. In *Nisin and Novel Lantibiotics*; Jung, G.; Sahl H.-G., Eds.; ESCOM Science Publishers B. V.: Leiden, 1991; 359-372.
128. Bruno, M. E. C.; Montville, T. J.; *Appl. Environ. Microbiol.* **1993**, *59*, 3003-3010.
129. Garcia-Garcera, M. J.; Elfrink, M. G. L.; Driessen, A. J. M.; Konings, W. N. *Eur. J. Biochem.* **1993**, *212*, 417-422.
130. Demel, R. A.; Peelen, T.; Siezen, R. J; de Kruiff, B.; Kuipers, O. P. *Eur. J. Biochem.* **1996**, *235*, 267-274.
131. Wang, Y. J.; Henz, M. E.; Fregeau-Gallagher, N. L.; Chai, S. Y.; Gibbs, A. C.; Yan, L. Z.; Stiles , M. E.; Wishart, D. S.; Vederas, J.C. *Biochemistry* **1999**, *38*, 15438-15447.
132. Fregeau-Gallagher, N. L.; Sailer, M.; Niemczura, W. P.; Nakashima, T. T.; Stiles, M. E.; Vederas, J. C. *Biochemistry* **1997**, *36*, 15062-15072.
133. Moll, G. N.; Roberts, G. C. K.; Konings, W. N.; Driessen, A. J. M. *Antonie van Leeuwenhoek* **1996**, *69*, 185-191.

- 
134. Boheim, G.; Hanke, W.; Jung, G. *Biophys. Struct. Mech.* **1983**, *9*, 181-191.
135. Ludtke, S. J.; He, K.; Heller, W. T.; Harroun, T. A.; Yang, L.; Huang, H. W. *Biochemistry* **1996**, *35*, 13723-13728.
136. Abee, T.; *FEMS Microbiol. Lett.* **1995**, *129*, 1-10.
137. Wiedemann, I.; Breukink, E.; van Kraaij, C.; Kuipers, O. P.; Bierbaum, G.; de Kruiff, B.; Sahl, H.-G. *J. Biol. Chem.* **2001**, *276*, 1772-1779.
138. Breukink, E.; Wiedemann, I.; van Kraaij, C.; Kuipers, O. P.; Sahl, H.-G.; de Kruiff, B. *Science* **1999**, *286*, 2361-2364.
139. Yan, L. Z.; Gibbs, A. C.; Stiles, M. E.; Wishart, D. S.; Vederas, J. C. *J. Med. Chem.* **2000**, *43*, 4579-4581.
140. Héchard, Y.; Pelletier, C.; Cenatiempo, Y.; Frère, J. *Microbiology* **2001**, *147*, 1575-1580.
141. McAuliffe, O.; Ryan, M. P.; Ross, R. P.; Hill, C.; Breeuwer, P.; Abee, T. *Appl. Environ. Microbiol.* **1998**, *64*, 439-445.
142. Ryan, M. P.; Meaney, W. J.; Ross, R. P.; Hill, C. *Appl. Environ. Microbiol.* **1998**, *64*, 2287-2290.
143. Ryan, M. P.; Flynn, J.; Hill, C.; Ross, R. P.; Meaney, W. J. *J. Dairy Sci.* **1999**, *82*, 2108-2114.
144. Ryan, M. P.; Rea, M. C.; Hill, C.; Ross, R. P. *Appl. Environ. Microbiol.* **1996**, *62*, 612-619.
145. McAuliffe, O.; Hill, C.; Ross, R. P. *J. Appl. Microbiol.* **1999**, *86*, 251-256.

- 
146. Ross, R. P. Assessment and Control of Foodborne Pathogens in Ireland.  
<http://www.teagasc.ie/research/reports/dairyproduction/4541/eopr-4541.htm>  
(accessed Aug 2003)
147. Kettenring, J. K.; Malabarba, A.; Vékey, K.; Cavalleri, B. *J. Antibiot.* **1990**, *43*, 1082-1088.
148. Kogler, H.; Bauch, M.; Fehlhaber, H-W.; Griesinger, C.; Schubert, W.; Teetz, V. In *Nisin and Novel Lantibiotics*; Jung, G.; Sahl, H.-G., Eds.; ESCOM Science Publishers B. V.: Leiden, 1991; 159-70.
149. Lian, L-Y.; Chan, W. C.; Morley, S. D.; Roberts, G. K. C.; Bycroft, B. W.; Jackson, D. *Biochem. J.* **1991**, *283*, 413-420.
150. Prash, T.; Naumann, T.; Markert, R. L. M.; Sattler, M.; Schubert, W. *Eur. J. Biochem.* **1997**, *244*, 501-512.
151. Van de Kamp, M.; van den Hooven, H. W.; Konings, R. N. H.; Hilbers, C. W.; van de Ven, F. J. M. *Eur. J. Biochem.* **1995**, *230*, 587-600.
152. Van de Ven, F. J. M.; van den Hooven, H. W.; Konings, R. N. H.; Hilbers, C. W. *Eur. J. Biochem.* **1991**, *202*, 1181-1188.
153. Zimmermann, N.; Jung, G. *Eur. J. Biochem.* **1997**, *246*, 809-819.
154. Zimmermann, N.; Metzger, J. W.; Jung, G. *Eur. J. Biochem.* **1995**, *228*, 786-797.
155. Gross, E.; Morell, J. L. *J. Am. Chem. Soc.* **1967**, *89*, 2791-2792.
156. Gross, E.; Morell, J. L. *J. Am. Chem. Soc.* **1970**, *92*, 2919-2920.
157. Gross, E.; Morell, J. L. *J. Am. Chem. Soc.* **1971**, *93*, 4634-4635.
158. Morell, J.; L.; Gross, E. *J. Am. Chem. Soc.* **1973**, *95*, 6480-6481.

- 
159. Meyer, H. E.; Heber, M.; Eisermann, B.; Korte, H.; Metzger, J. W.; Jung, G. *Anal Biochem.* **1994**, *223*, 185-190.
160. Anfiteatro, D. Dom's Kefir in-site. <http://users.chariot.net.au/~dna/kefirpage.html> (accessed Aug 2003).
161. Micheli, L.; Uccelletti, D.; Palleschi, C.; Crescenzi, V. *Appl. Microbiol. Biotechnol.* **1999**, *53*, 69-74.
162. Ryan, M. P.; Jack, R. W.; Josten, M.; Sahl, H.-G.; Jung, G.; Ross, R. P.; Hill, C. J. *Biol. Chem.* **1999**, *274*, 37544-37550.
163. Edman, P. *Acta Chem. Scand.* **1950**, *4*, 283-293.
164. Dougherty, B. A.; Hill, C.; Weidman, J. F.; Richardson, D. R.; Venter, J. C., Ross, R. P. *Mol. Microbiol.* **1998**, *29*, 1029-1038.
165. Back, T. G.; Yang, K.; Krouse, R. H. *J. Org. Chem.* **1992**, *57*, 1986-1990.
166. Jung, M.; Elsohly, H. N.; Croon, E. M.; McPhail, D. R.; McPhail, A. T. *J. Org. Chem.* **1986**, *51*, 5417-5419.
167. Back, T. G.; Baron, D. L.; Yang, K. *J. Org. Chem.* **1993**, *58*, 2407-2413.
168. Schneider, T. R.; Karcher, J.; Pohl, E.; Lubini, P.; Sheldrick, G. M. *Acta Crystallogr. Sect. D Biol. Crystallogr.* **2000**, *56*, 705-713.
169. Breukink, E.; van Heusden, H. E.; Vollmerhaus, P. J.; Swiezewska, E.; Brunner, L.; Walker, S.; Heck, A. J. R.; de Kruijff, B. *J. Biol. Chem.* **2003**, *278*, 19898-19903.
170. Hsu, S.-T.; Breukink, E.; de Kruijff, B.; Kaptein, R.; Bonvin, A. M. J. J.; van Nuland, N. A. J. *Biochemistry* **2002**, *41*, 7670-7676.
171. van Heusden, H. E.; de Kruijff, B.; Breukink, E. *Biochemistry* **2002**, *41*, 12171-12178.

- 
172. Hsu, S-T. D.; Breukink, E.; Bierbaum, G.; Sahl, H.-G.; de Kruijff, B.; Kaptein, R.; van Nuland, N. A. J.; Bonvin, A. M. J. *J. Biol. Chem.* **2003**, *278*, 13110-13117.
173. Perrin, D. D.; Armarego, W. L. F.; Perrin, D. R. *Purification of Laboratory Chemicals*; 2<sup>nd</sup> ed.; Pergamon Press: New York, 1980.
174. Vogel, A. *Vogel's Textbook of Practical Organic Chemistry*; 4<sup>th</sup> ed.; J. Wiley & Sons Inc.: New York, 1978.
175. Still, W. C.; Kahn, M.; Mitra, A. *J. Org. Chem.* **1978**, *43*, 2923-2925.
176. Martichonok, V.; Whitesides, G. M. *J. Org. Chem.* **1996**, *61*, 1702 - 1706;
177. Iwakura, Y.; Toda, F.; Kosugi, M.; Torii, Y. *J. Org. Chem.* **1971**, *36*, 3990-3992.
178. Servi, S. *J. Org. Chem.* **1985**, *50*, 5865-5867.
179. Baldwin, M. A.; Medzihradzky, K. F.; Lock, C. M.; Settineri, T. A.; Burlingame, A. L. *Anal. Chem.* **2001**, *73*, 1707-1720.
180. Piantini, U.; Sorensen, O. W.; Ernst, R. R. *J. Am. Chem. Soc.* **1982**, *104*, 6800-6801.
181. Braunschweiler, L.; Ernst, R. R. *J. Magn. Reson.* **1983**, *53*, 521-528.
182. Jeneer, J.; Meier, B. H.; Bachman, P.; Ernst, R. R. *J. Chem. Phys.* **1979**, *71*, 4546-4553.
183. Bothner-By, A. A.; Stephens, R. L.; Lee, J.; Warren, C. D.; Jeanloz, R. W. *J. Am. Chem. Soc.* **1984**, *106*, 811-813.
184. Clore, G. M.; Gronenborn, A. M. *J. Magn. Reson.* **1982**, *48*, 402-417.
185. Gronenborn, A. M.; Clore, G. M.; *J. Mol. Biol.* **1982**, *157*, 155-160.
186. Wiseman, T.; Williston, S.; Brandts, J. F.; Lin, L. N. *Anal. Biochem.* **1989**, *179*, 131-137.

- 
187. Sunde, M.; Sparkes, M. J.; Dixon, H. B. F. *Biochim. Biophys. Acta* **1998**, *1388*, 45-52.
188. Stevens, J.; Dixon, H. B. F. *Biochim. Biophys. Acta* **1995**, *1252*, 195–202.